

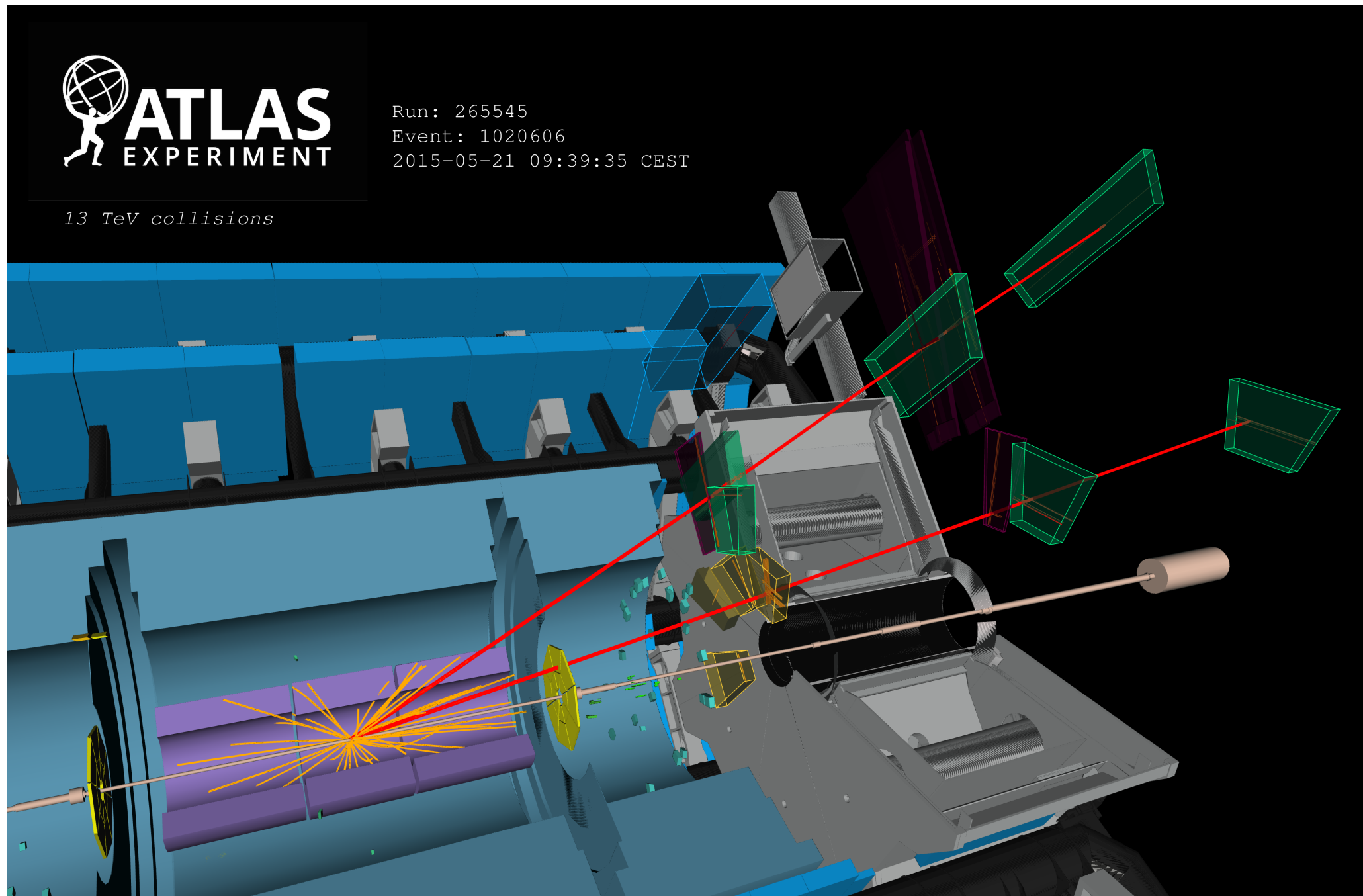
# ATLAS results on heavy flavour production and its relation to quark matter

Marisilvia Donadelli  
on behalf of the ATLAS  
Collaboration

Strangeness in Quark Matter 2015

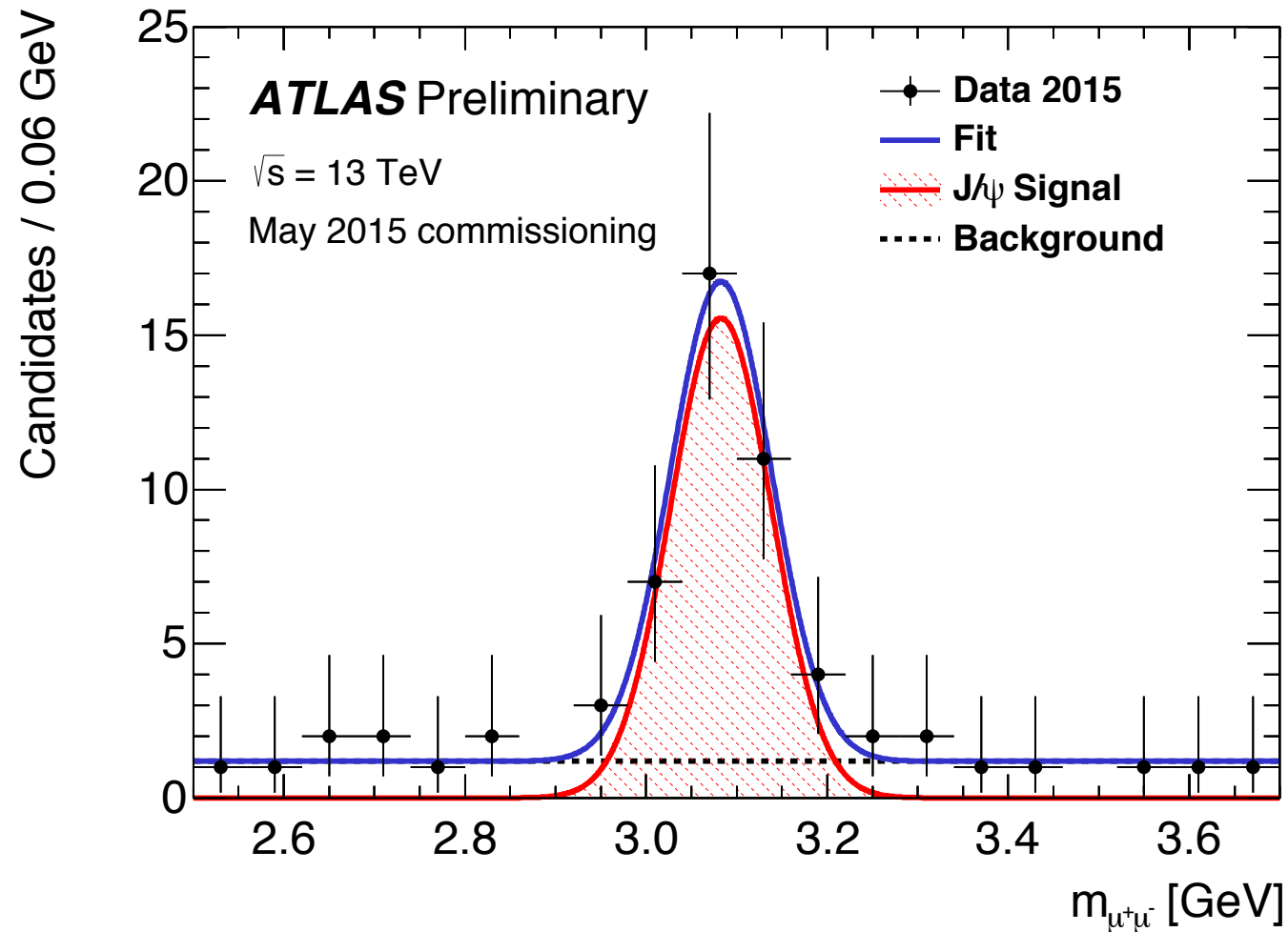


# Wetting our appetite...

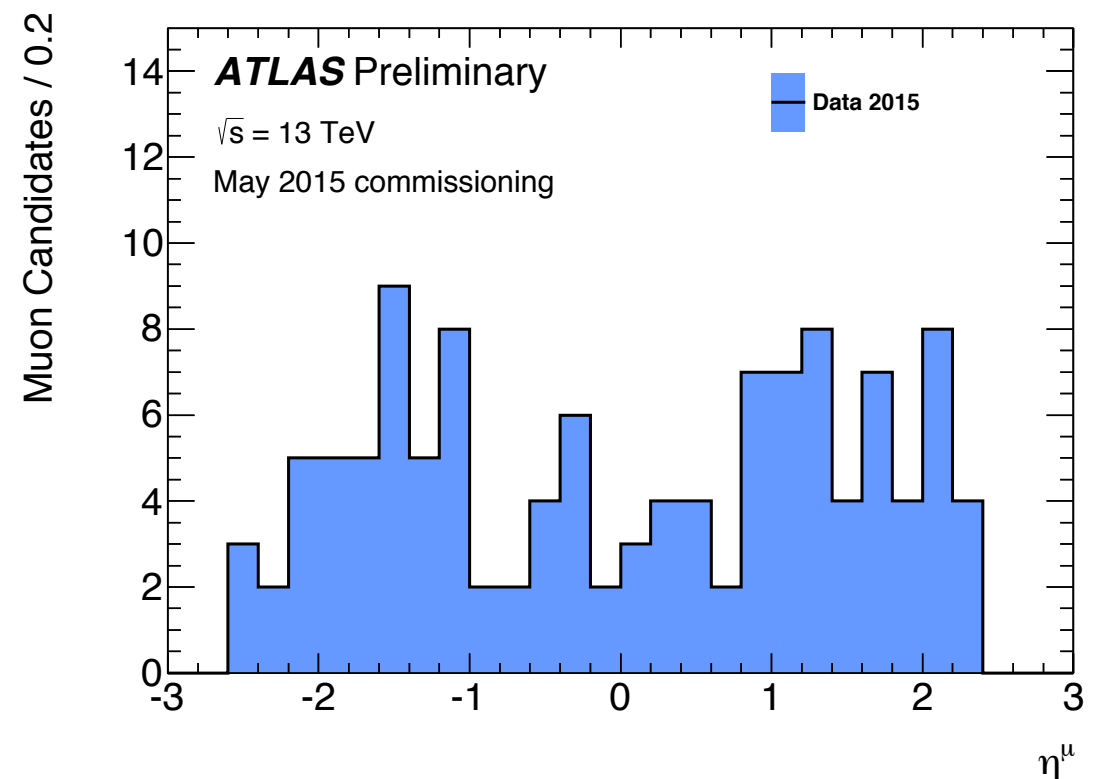
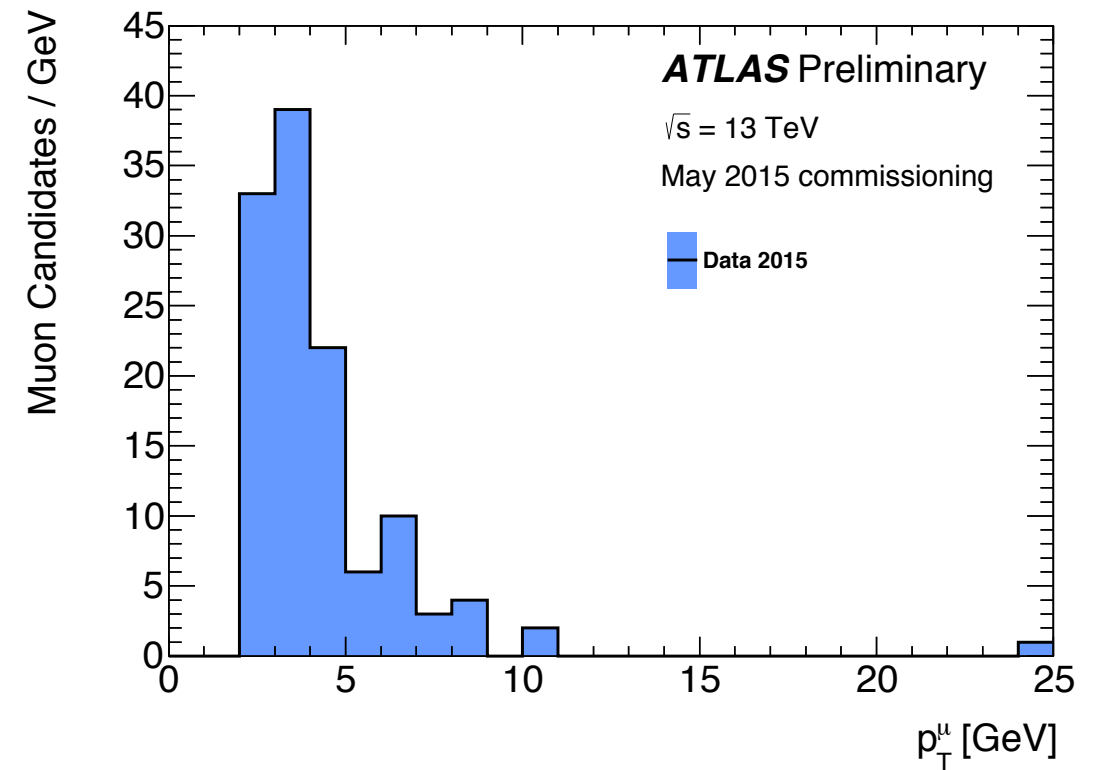


Display of a  $J/\Psi$  candidate event from proton-proton collisions recorded by ATLAS on 21 May 2015, with LHC stable beams at a collision energy of 13 TeV. The red lines show the paths of two muons through the detector, with transverse momenta of 5.6 and 8.2 GeV. The green and yellow bars indicate energy deposits in the liquid argon and scintillating-tile calorimeters. Charged particle tracks reconstructed from hits in the inner tracking detector are shown as orange arcs, curving in the solenoidal magnetic field. The reconstructed dimuon invariant mass is 3.12 GeV.

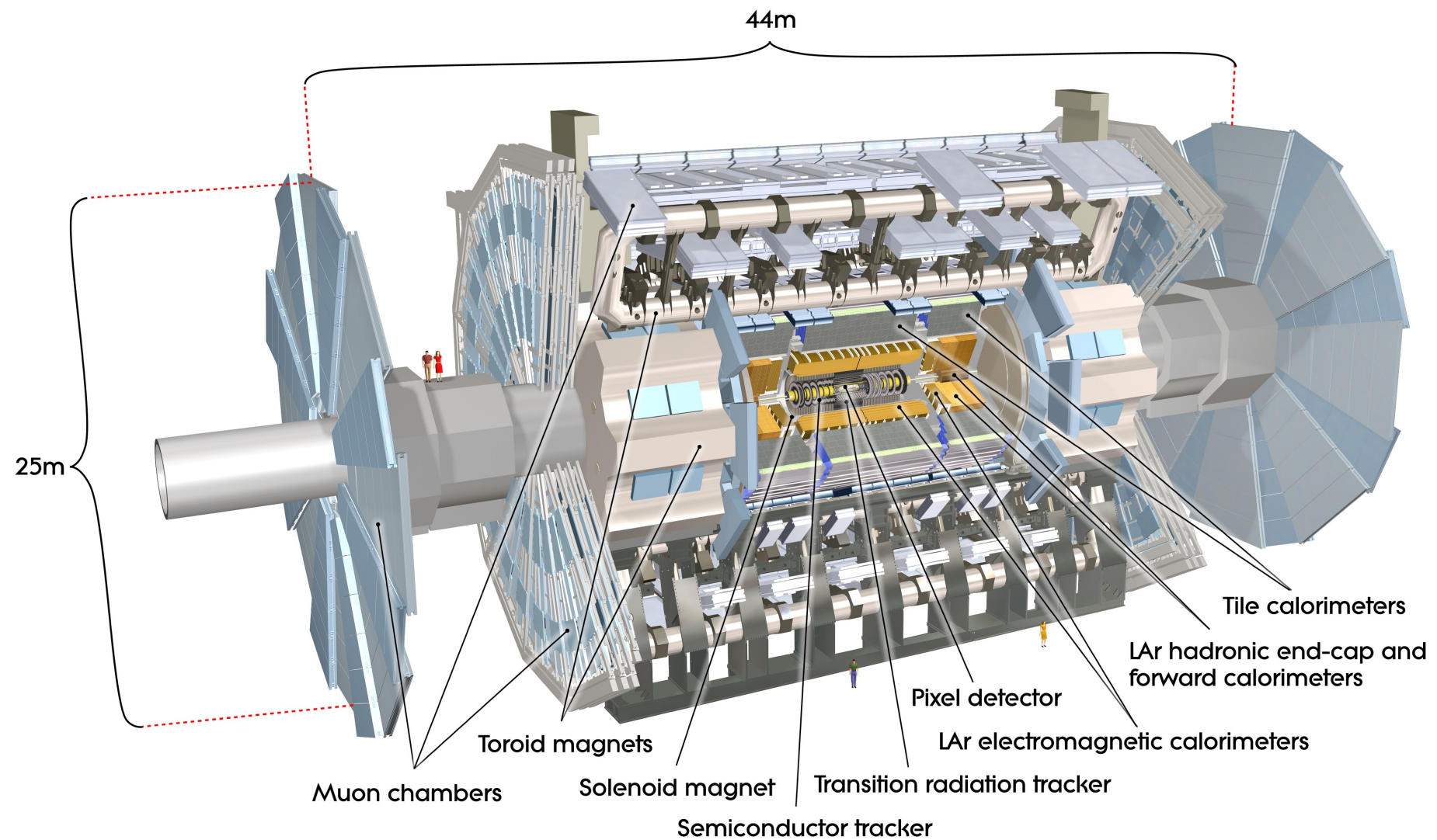
# $J/\psi \rightarrow \mu^+\mu^-$ candidates in pp collisions @ 13 TeV pp collisions



Data taken during "quiet beams" delivered as part of the LHC beam commissioning period in May 2015



# ATLAS Detector



Inner Detector – Tracking  $|\eta| < 2.5$

Calorimetry –  $|\eta| < 4.9$

Muon Spectrometer -  $|\eta| < 2.7$



13 TeV collisions

## Why p+Pb collisions?

Suppression of quarkonium yields in nucleus-nucleus collisions is one key feature of the **hot** quark-gluon plasma (QGP), but the baseline should be determined from **Cold Nuclear Matter (CNM)** effects.

## Several Phenomenological interpretations proposed to explain suppression in p+A, d+A:

- nuclear absorption;
- modifications of parton distribution functions in nuclei (shadowing),
- gluon saturation;
- induced medium energy loss.

## Why pp collisions?

Tests of QCD calculations at the perturbative / non-perturbative boundary.

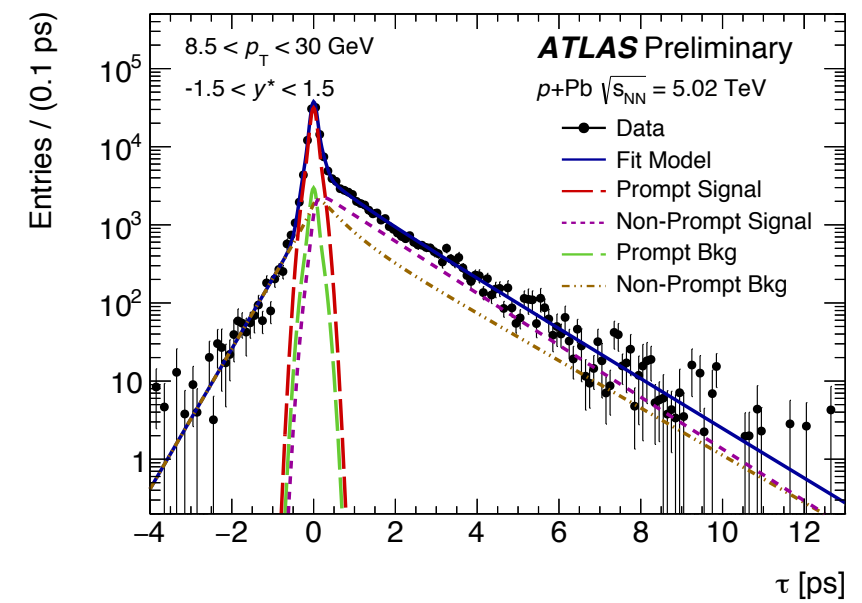
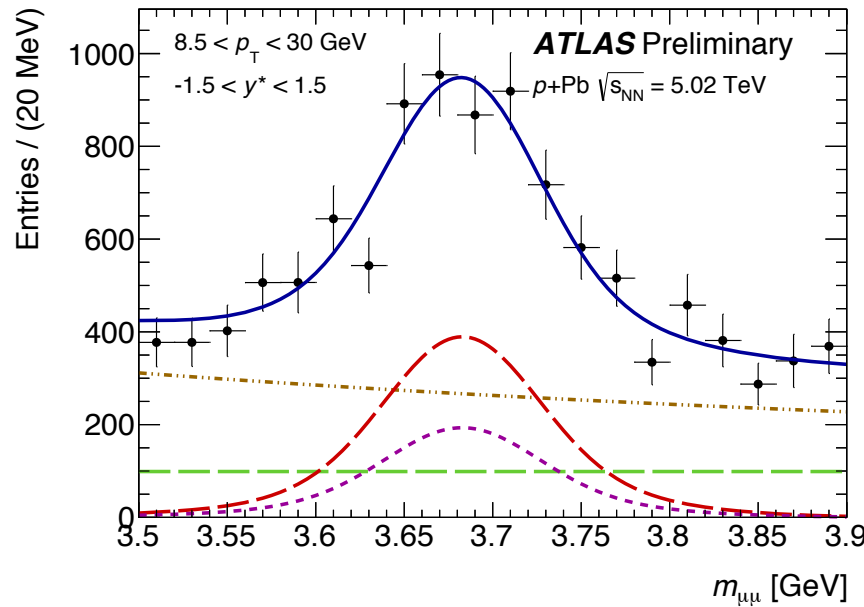
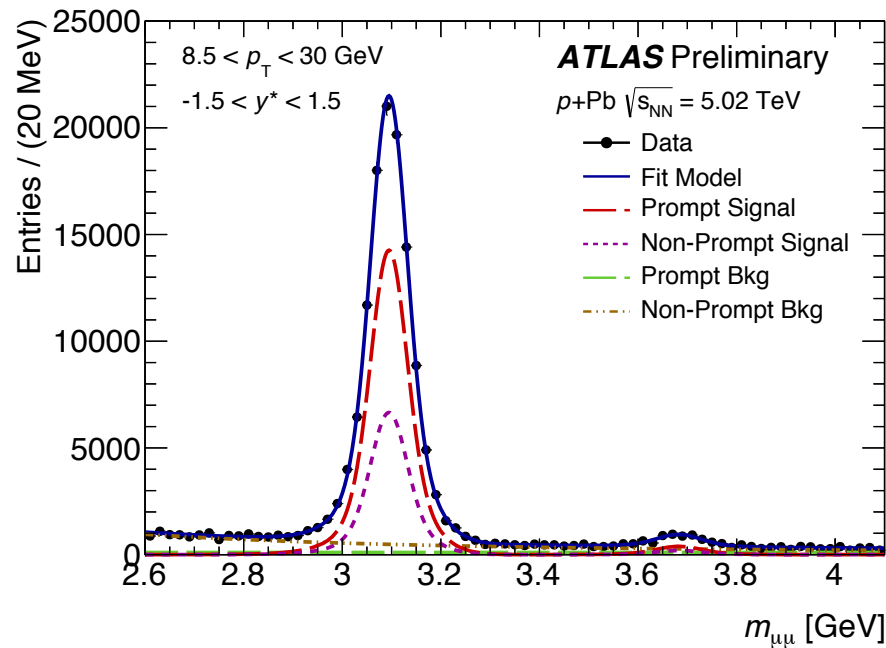
Standard candles for Heavy Ions, B-meson production, backgrounds to SM/BSM processes.

Test multiple parton scattering effects, parton density functions.

Search for rare decays and probes of new physics.

# $\psi(2S)$ and $J/\psi$ @ 5.02 TeV p+Pb and @ 2.76 TeV pp

p+Pb



i	Type	Source	$f_i(m)$	$h_i(\tau)$
1	$J/\psi$ S	P	$\omega_i CB_1(m) + (1 - \omega_i)G_1(m)$	$\delta(\tau)$
2	$J/\psi$ S	NP	$\omega_i CB_1(m) + (1 - \omega_i)G_1(m)$	$E_1(\tau)$
3	$\psi(2S)$ S	P	$\omega_i CB_2(m) + (1 - \omega_i)G_2(m)$	$\delta(\tau)$
4	$\psi(2S)$ S	NP	$\omega_i CB_2(m) + (1 - \omega_i)G_2(m)$	$E_2(\tau)$
5	Bkg	P	flat	$\delta(\tau)$
6	Bkg	NP	$E_3(m)$	$E_4(\tau)$
7	Bkg	NP	$E_5(m)$	$E_6( \tau )$

CB: Crystal Ball function

G: Gaussian

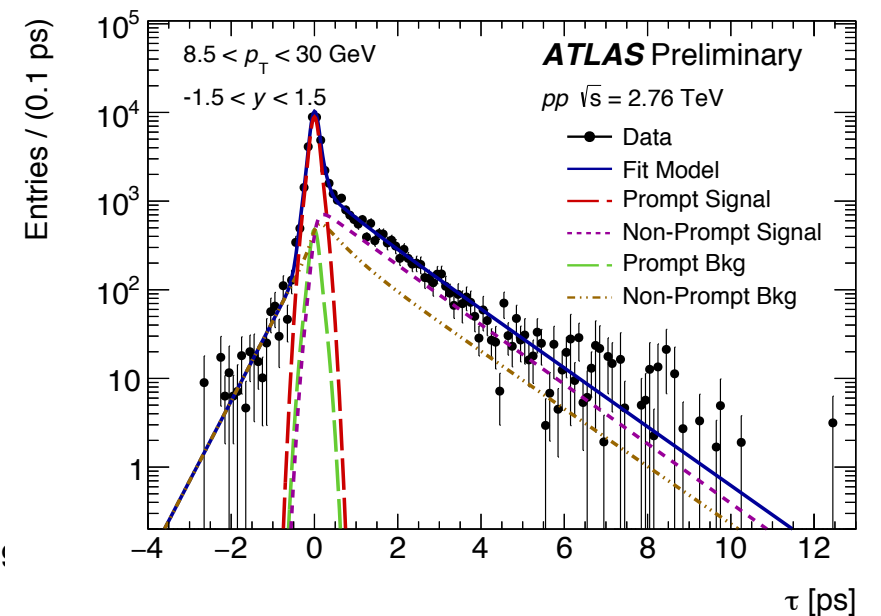
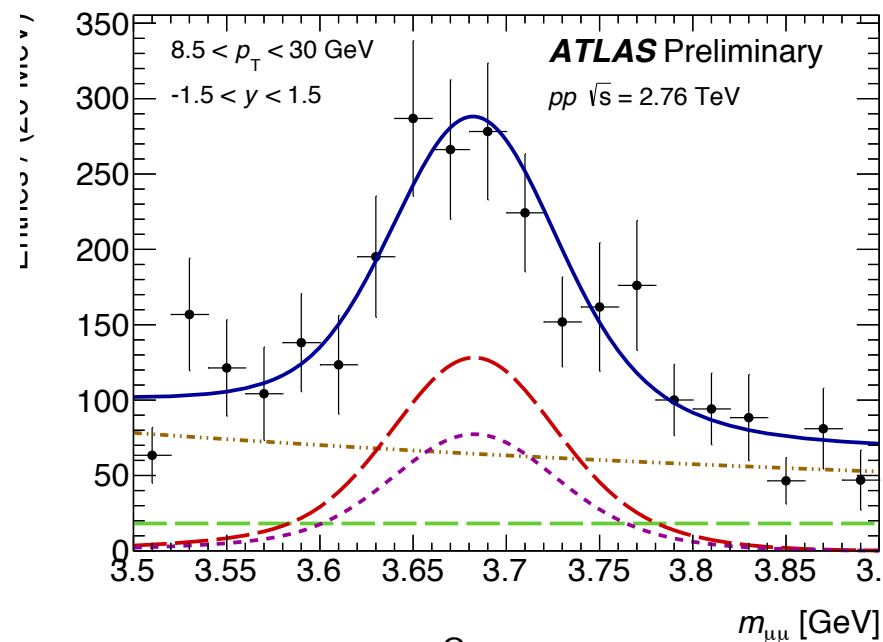
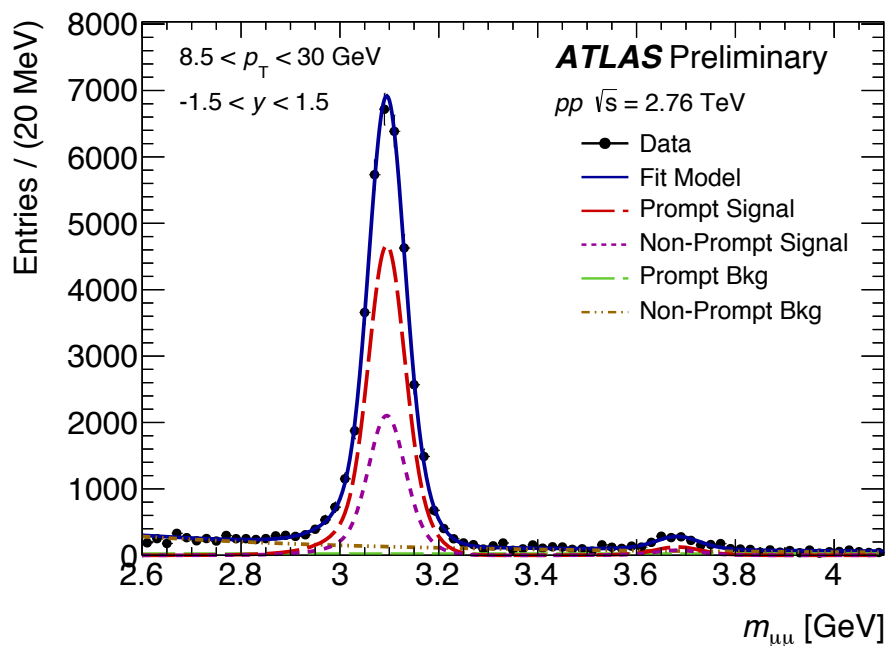
$E(\tau)$  - single sided exponential;

$E(|\tau|)$  - double sided exponential

$\delta$ : delta function

$\omega$ : fraction of CB function  
in the signal

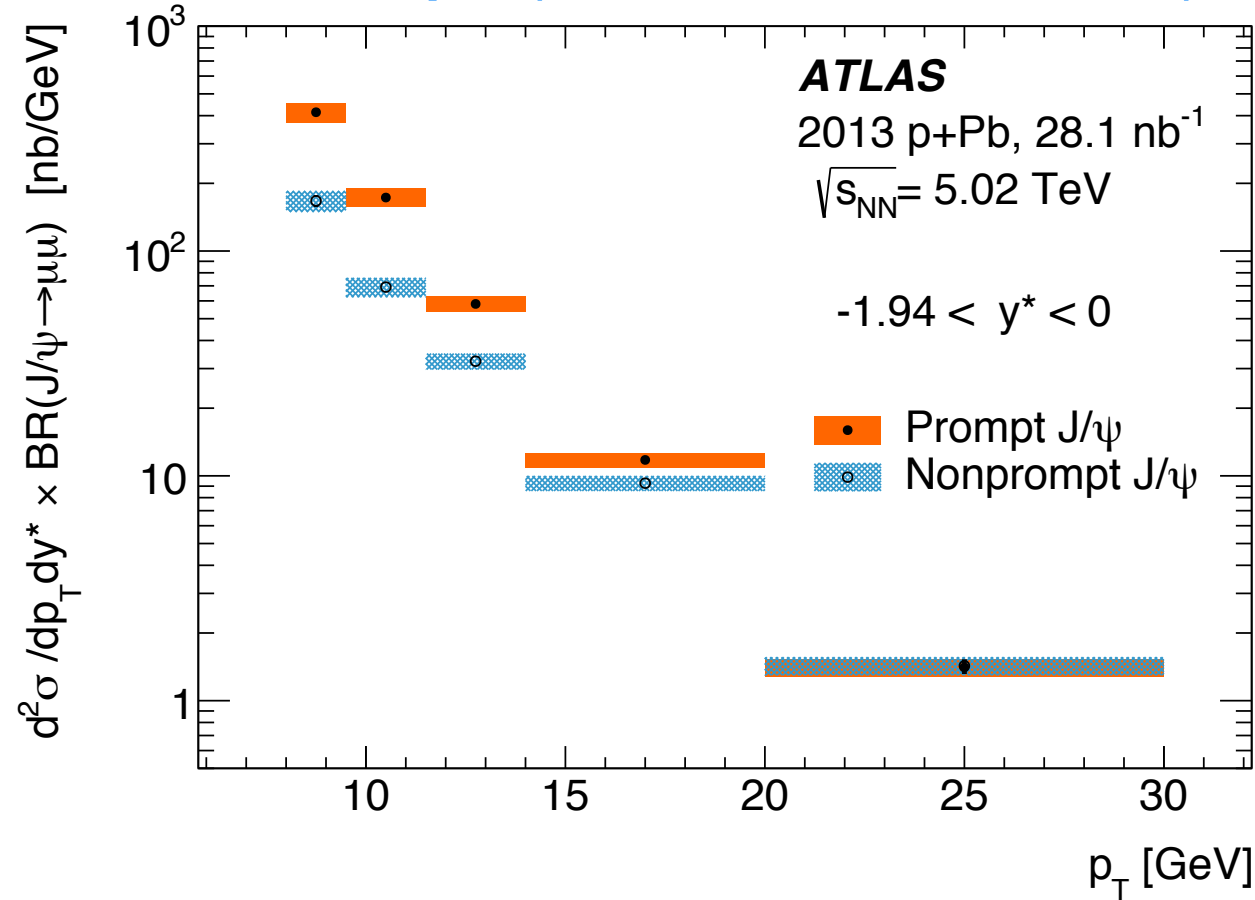
pp



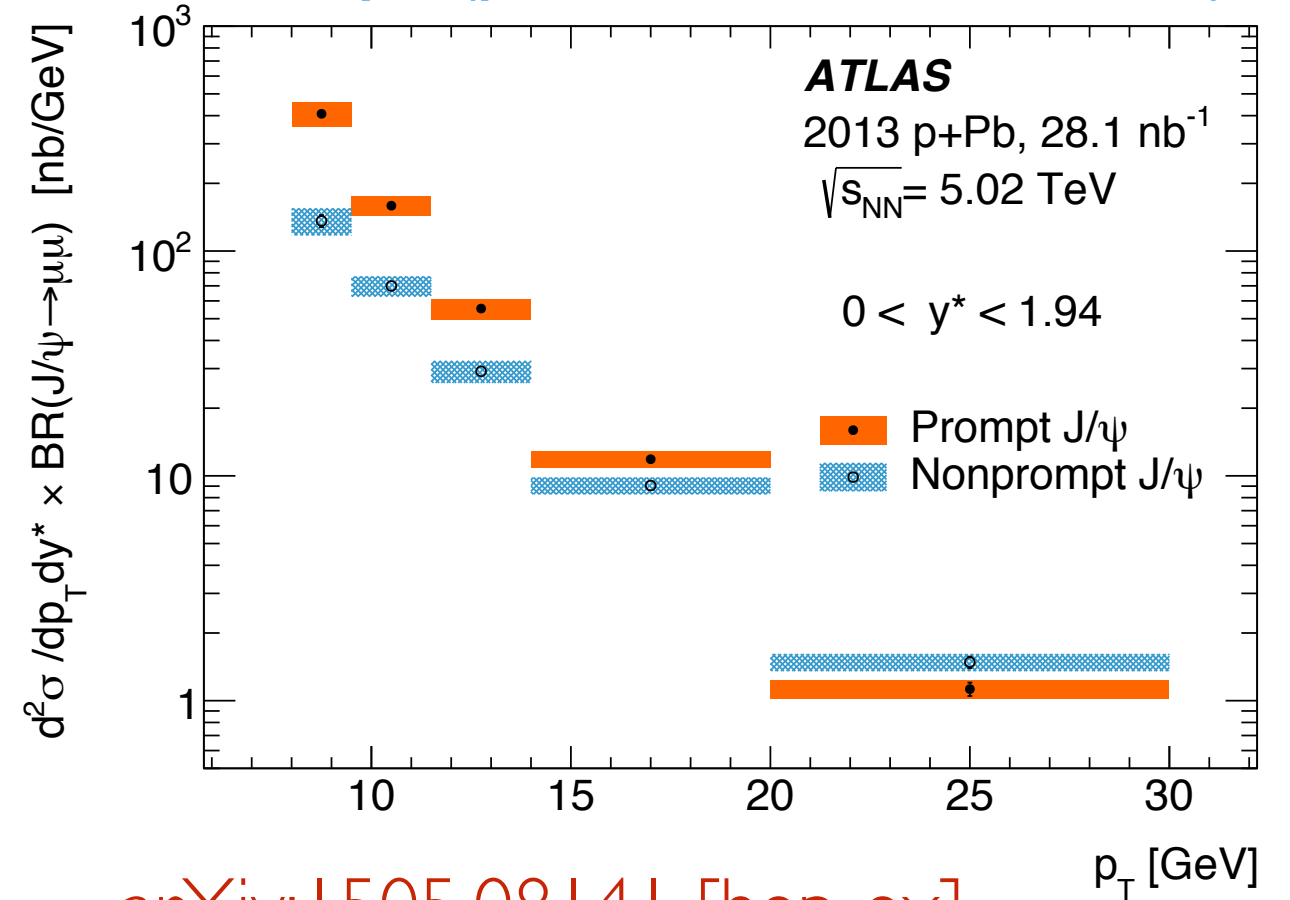
[ATLAS-CONF-2015-023](#)

# Double differential cross sections for **prompt** and **non-prompt** $J/\psi$ @ 5.02 TeV p+Pb

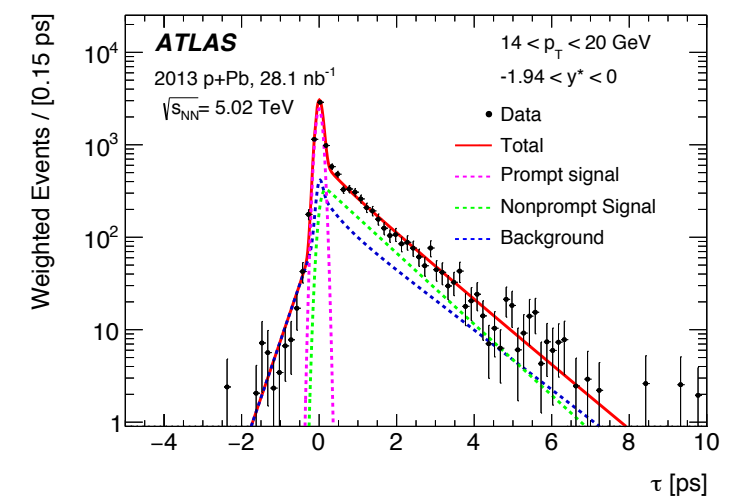
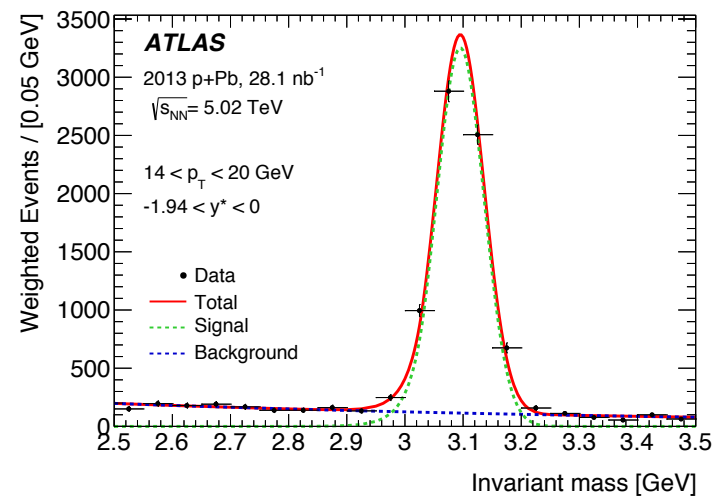
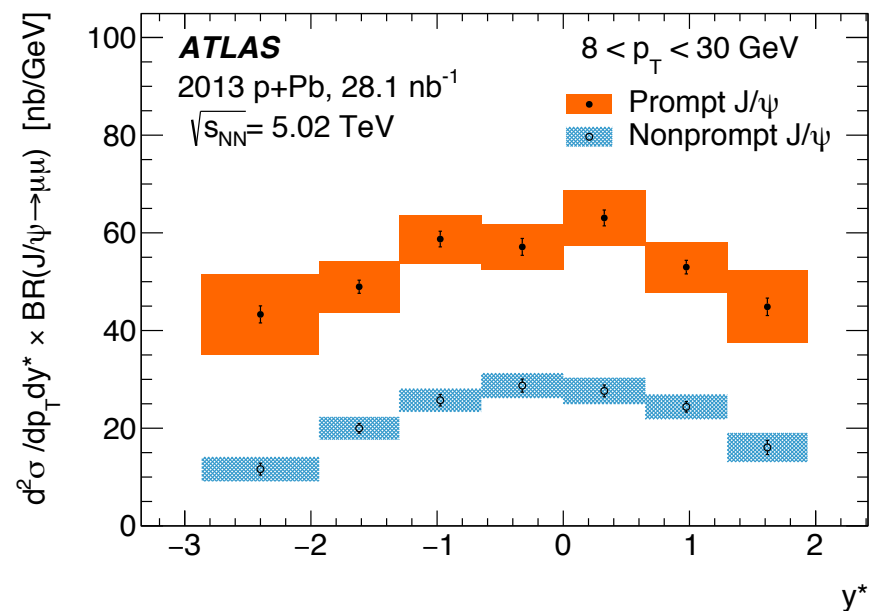
backward  $y^*$  (lead beam direction)



forward  $y^*$  (proton beam direction)

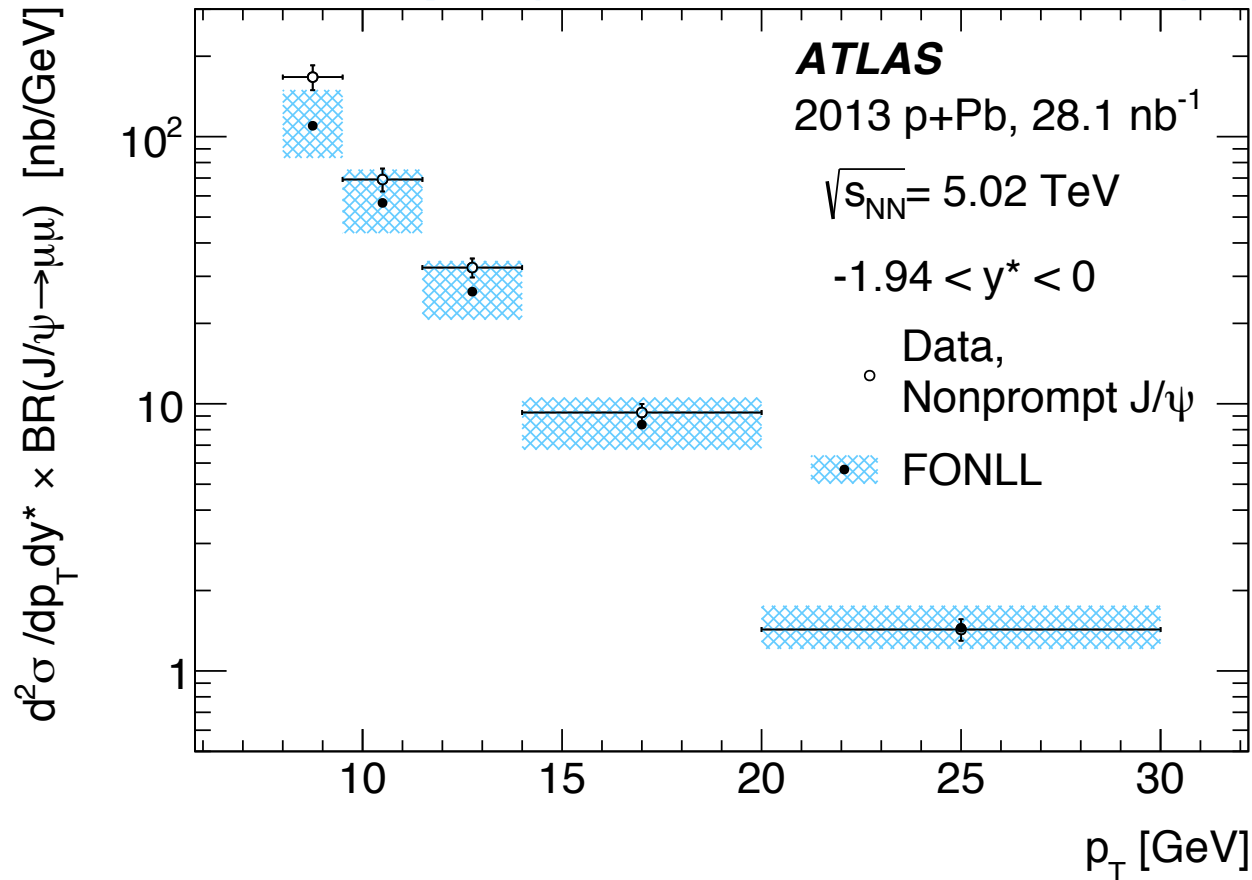


[arXiv:1505.08141 \[hep-ex\]](https://arxiv.org/abs/1505.08141)

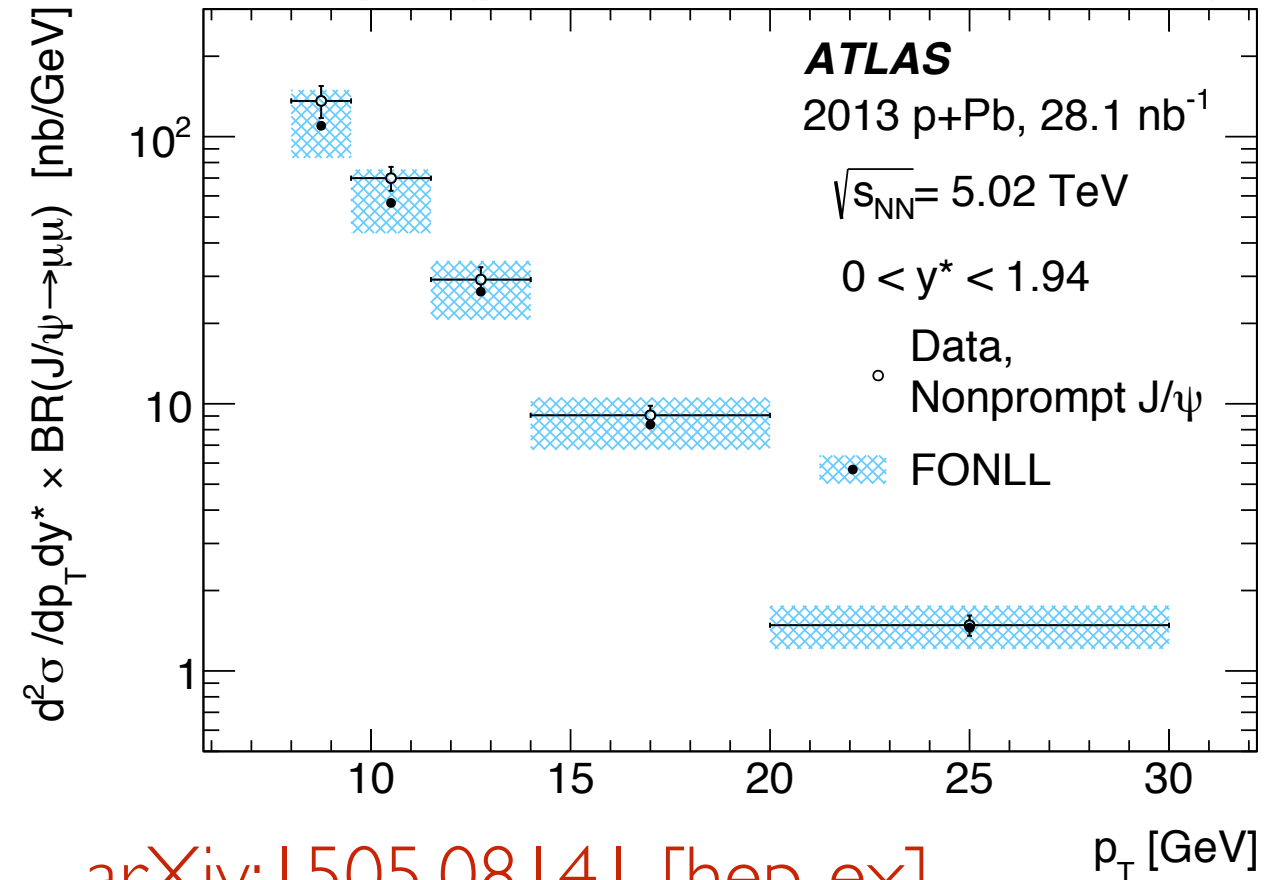


# Double differential cross sections for non-prompt $J/\psi$ @ 5.02 TeV p+Pb

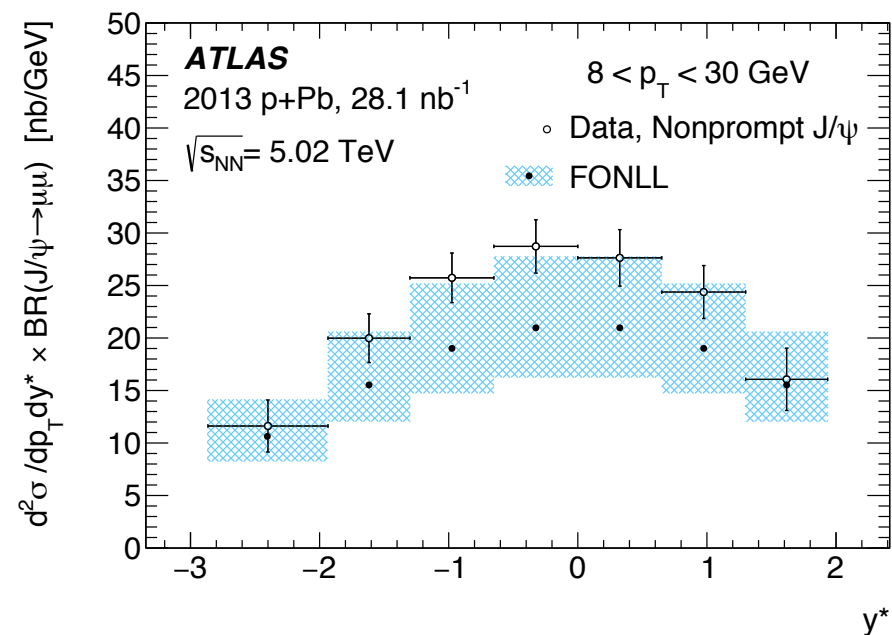
backward  $y^*$  (lead beam direction)



forward  $y^*$  (proton beam direction)



[arXiv:1505.08141 \[hep-ex\]](https://arxiv.org/abs/1505.08141)



Comparison with a FONLL calculation for pp collisions scaled by the number of nucleons in the Pb ion.

Shaded boxes: theoretical uncertainties on the FONLL predictions, which are strongly correlated between bins.

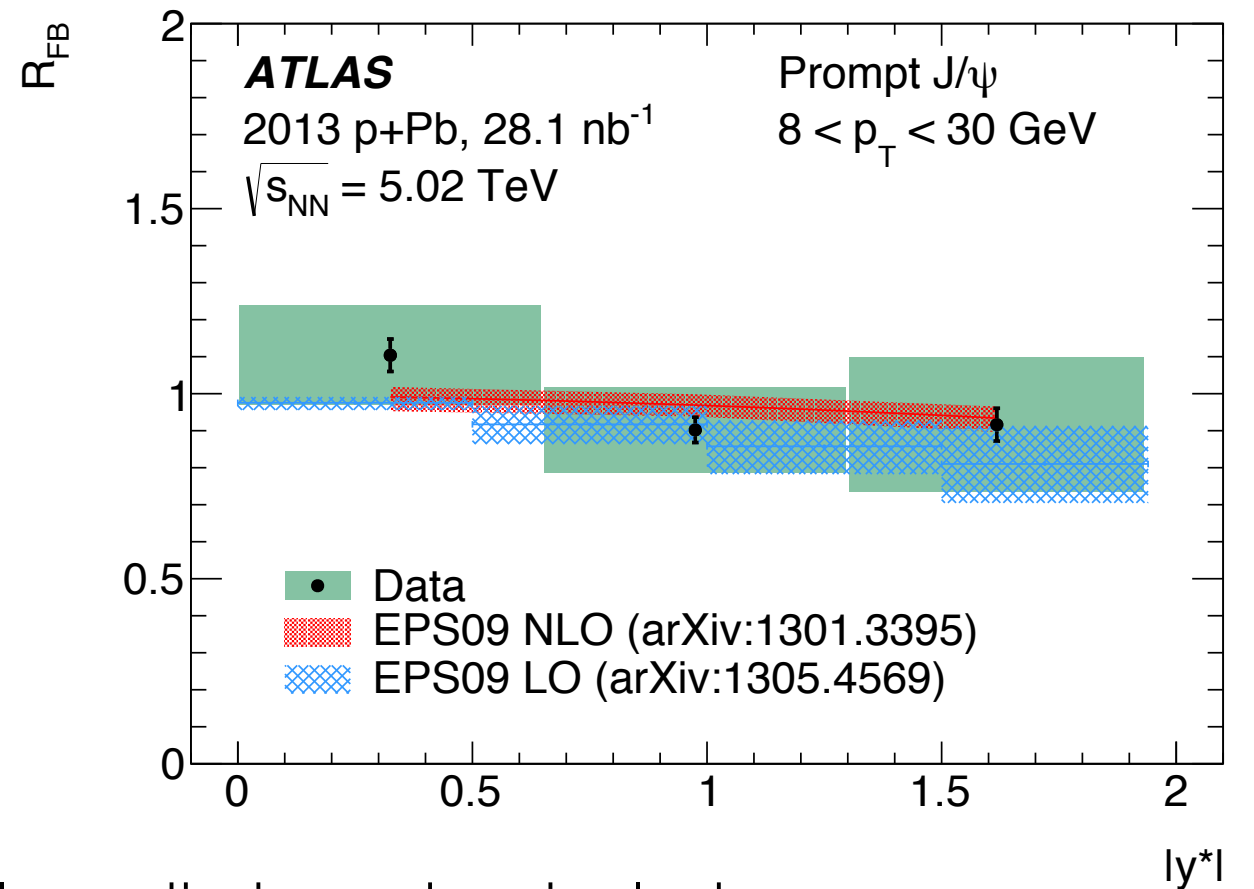
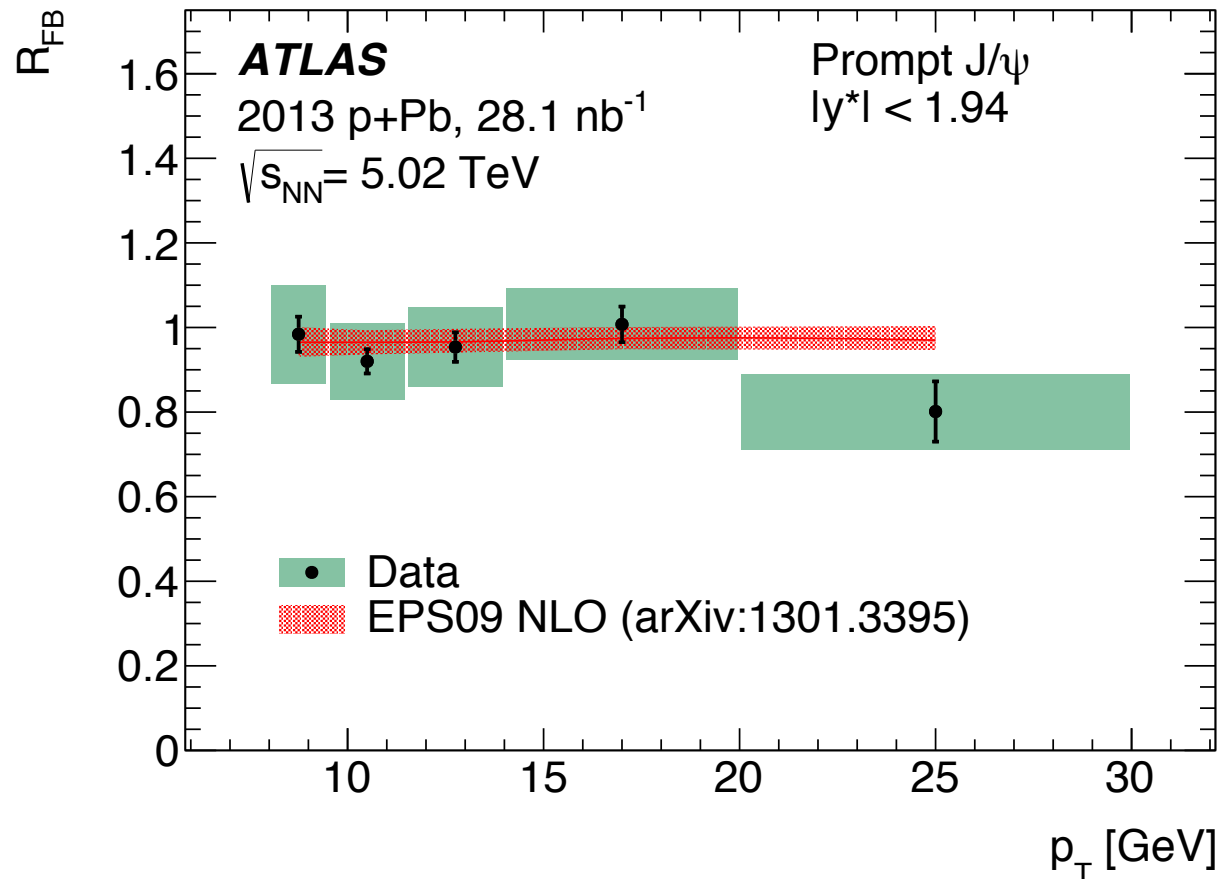


# Forward-backward ratios of $J/\psi$ @ 5.02 TeV p+Pb

$$R_{\text{FB}}(p_{\text{T}}, y^*) \equiv \frac{d^2\sigma(p_{\text{T}}, y^* > 0)/dp_{\text{T}}dy^*}{d^2\sigma(p_{\text{T}}, y^* < 0)/dp_{\text{T}}dy^*}$$

[arXiv:1505.08141 \[hep-ex\]](https://arxiv.org/abs/1505.08141)

## Prompt component



Data agrees with theoretical predictions that include shadowing effects based on EPS09 nPDF

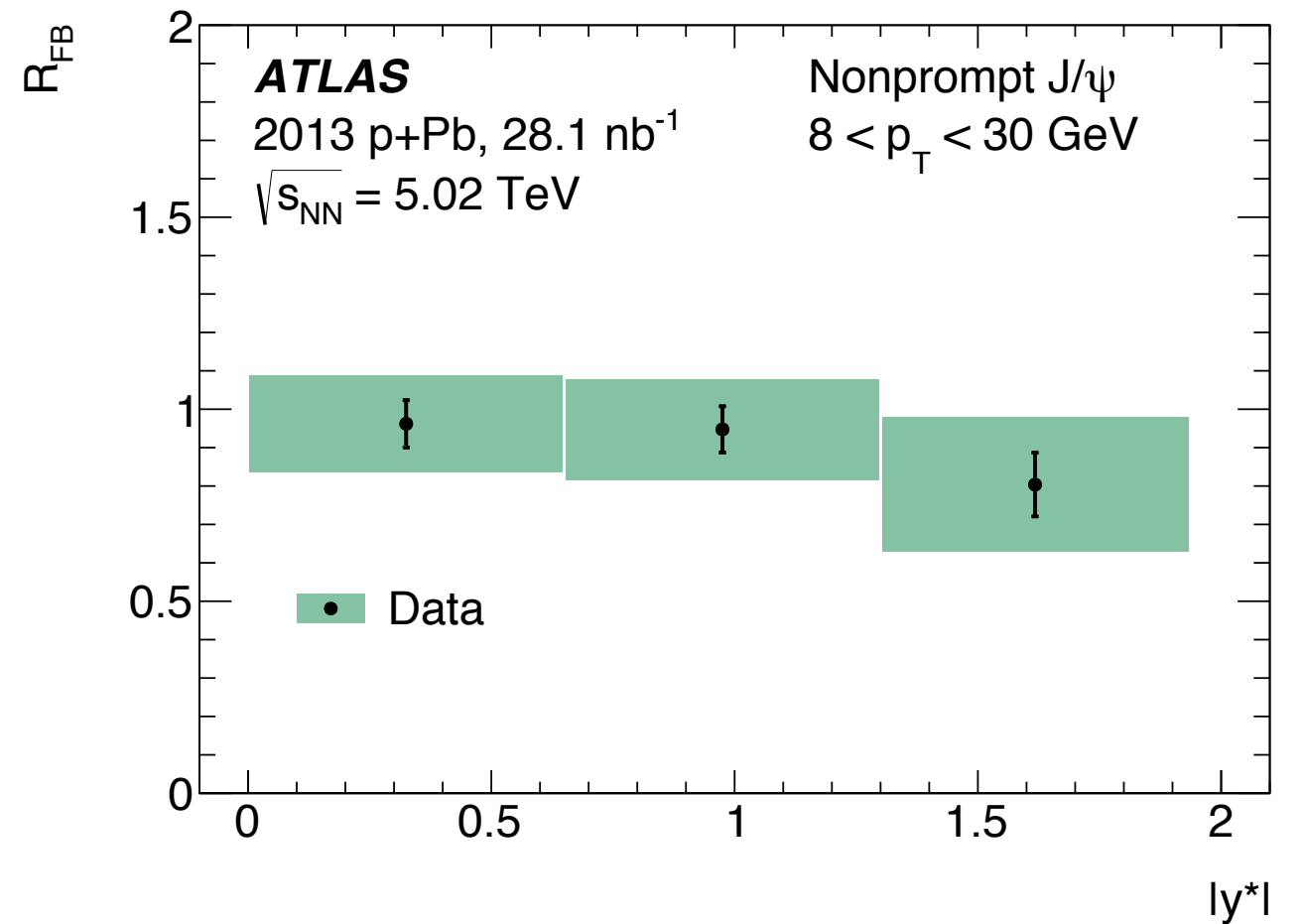
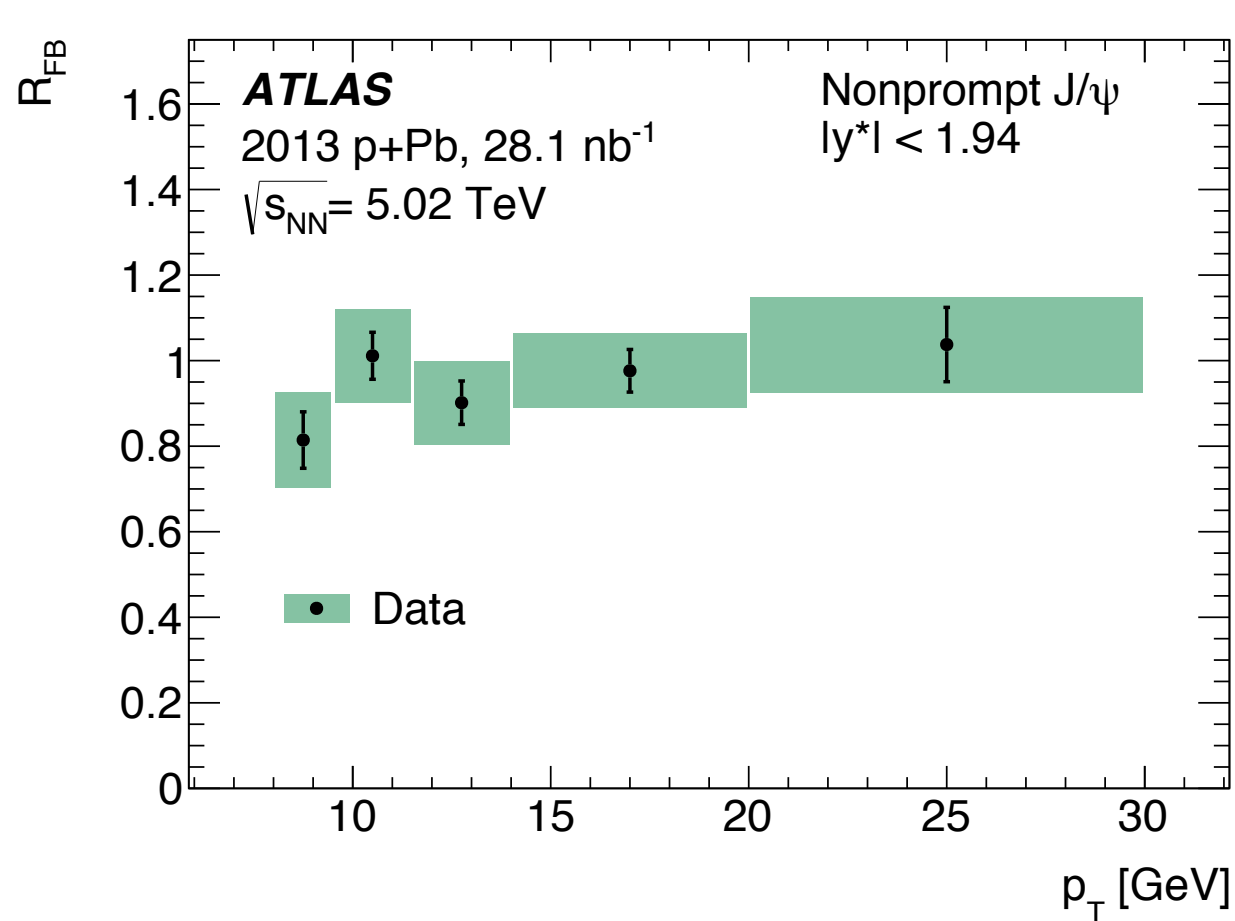
ALICE inclusive  $J/\psi$ :  $R_{\text{FB}} \sim 0.6$ ,  $y^* \sim 3-3.5$ ,  $p_{\text{T}} < 15$  GeV

LHCb results:  $\sim 0.75$  for  $y = 2.8$  for prompt  $J/\psi$   $p_{\text{T}} < 15$  GeV

# Forward-backward ratios of $J/\psi$ @ 5.02 TeV p+Pb

## Non-prompt component

[arXiv:1505.08141 \[hep-ex\]](https://arxiv.org/abs/1505.08141)



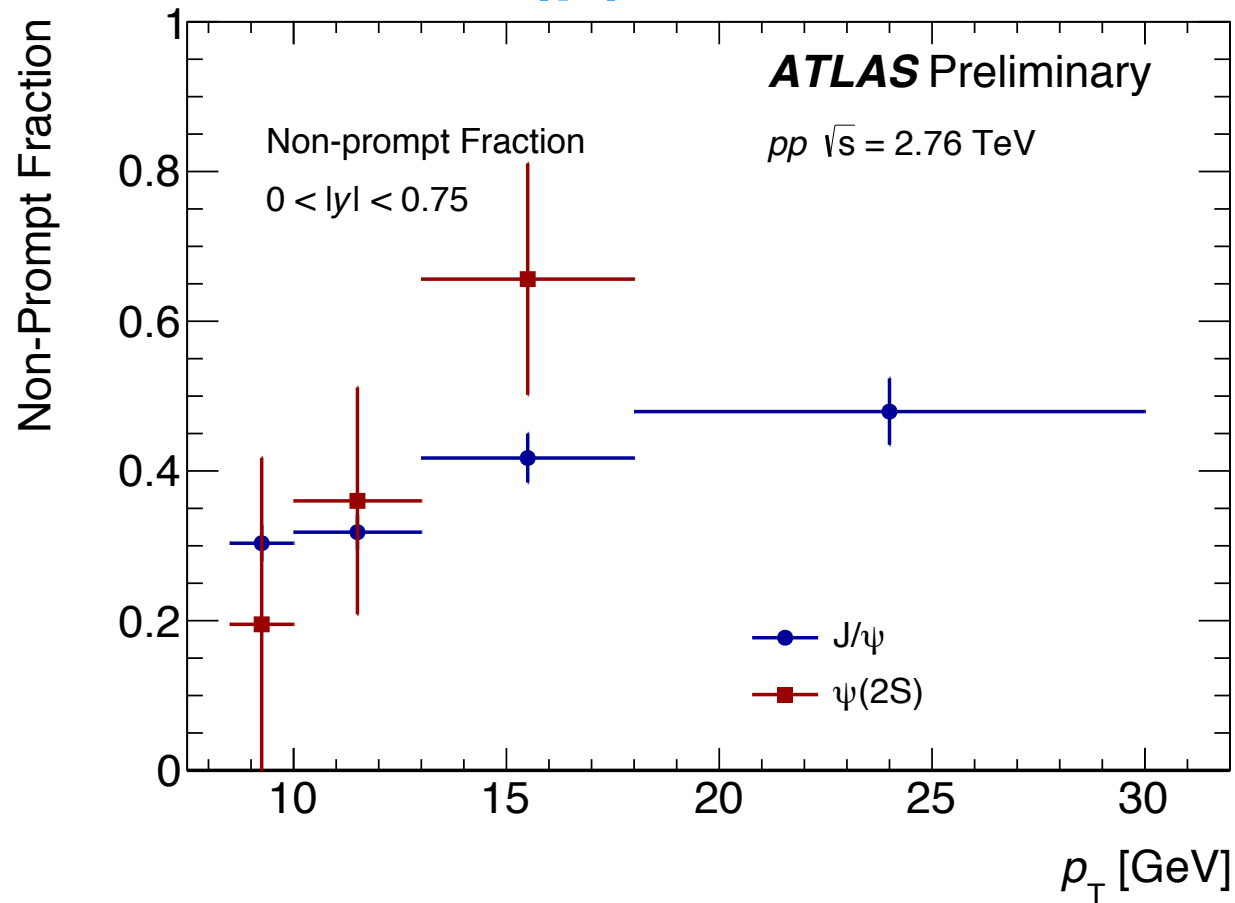
LHCb non-prompt  $J/\psi$ :  $\sim 0.9$ ,  $p_T < 15$  GeV

# Non-prompt J/ $\psi$ and $\psi(2S)$ @ 2.76 TeV pp

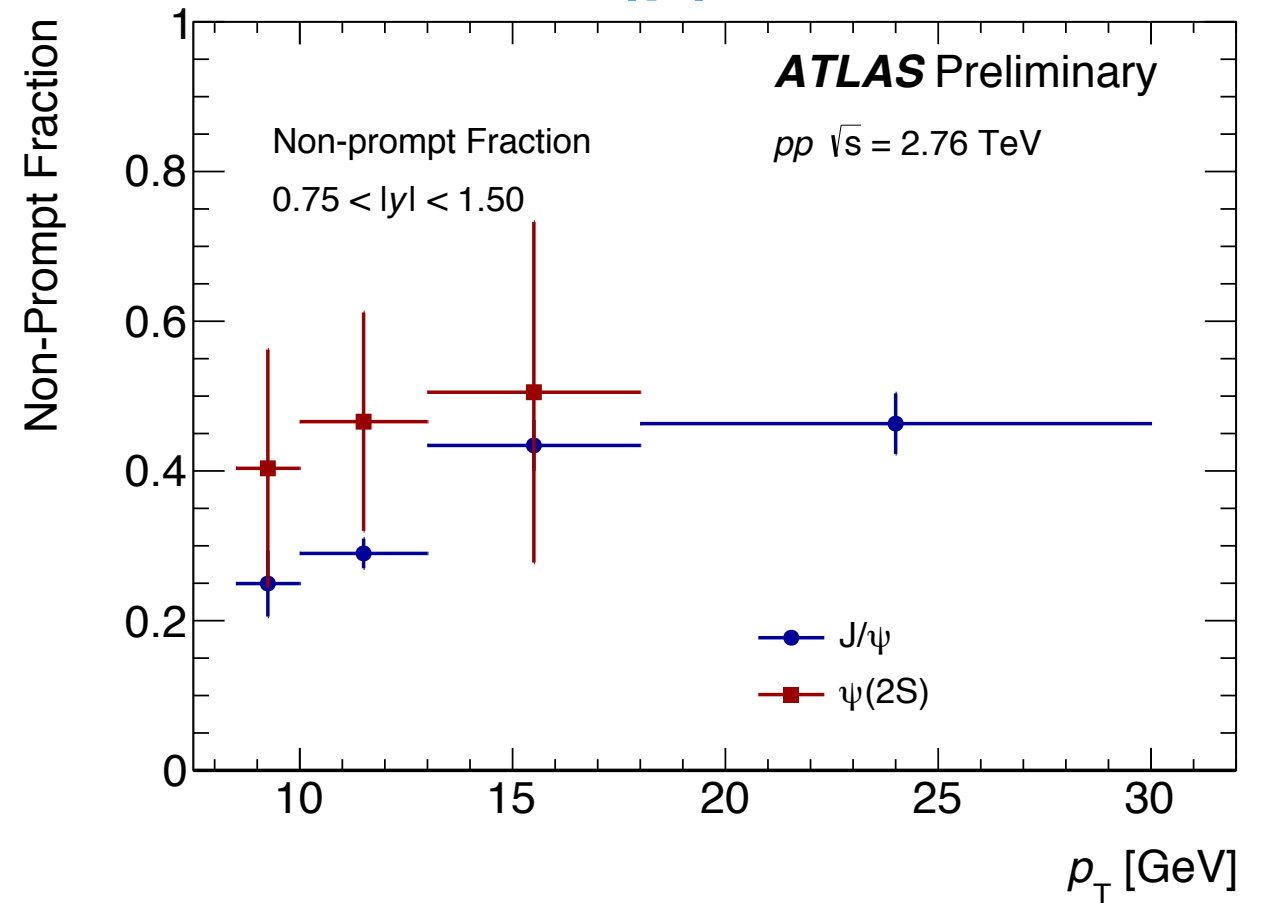
$$f_{NP}^{\psi} = \frac{N_{\psi}^{\text{np, corr}}}{N_{\psi}^{\text{np, corr}} + N_{\psi}^{\text{p, corr}}}$$

[ATLAS-CONF-2015-023](#)

$0 < |y| < 0.75$



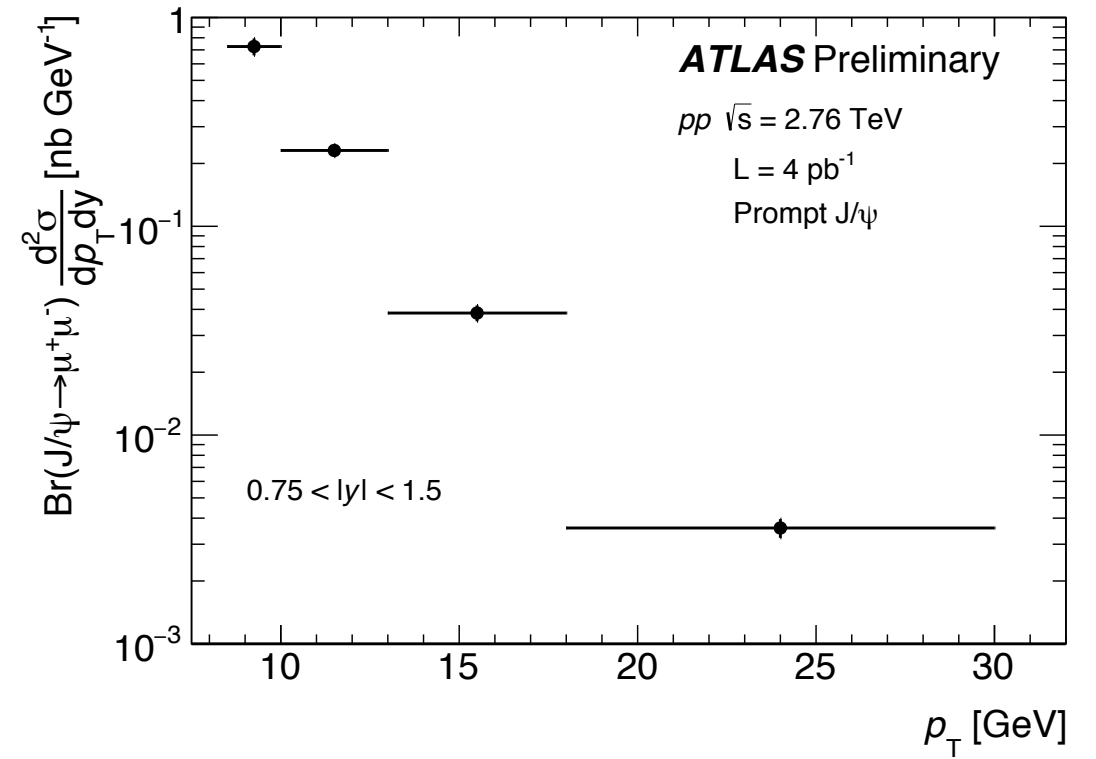
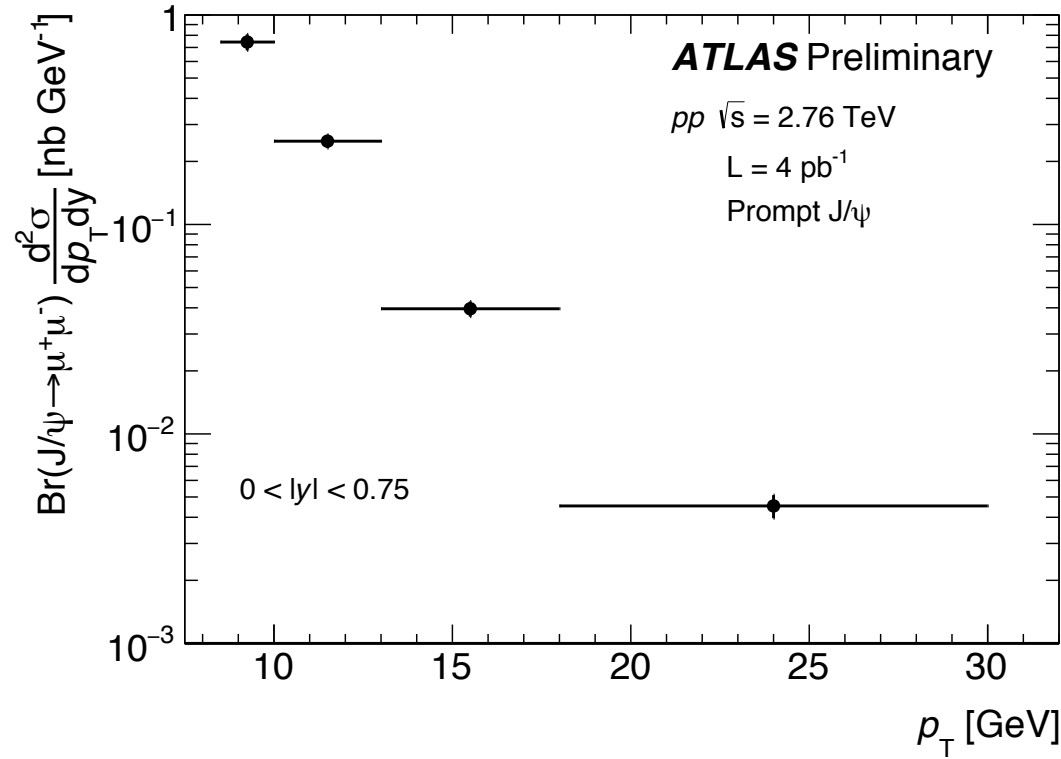
$0.75 < |y| < 1.5$



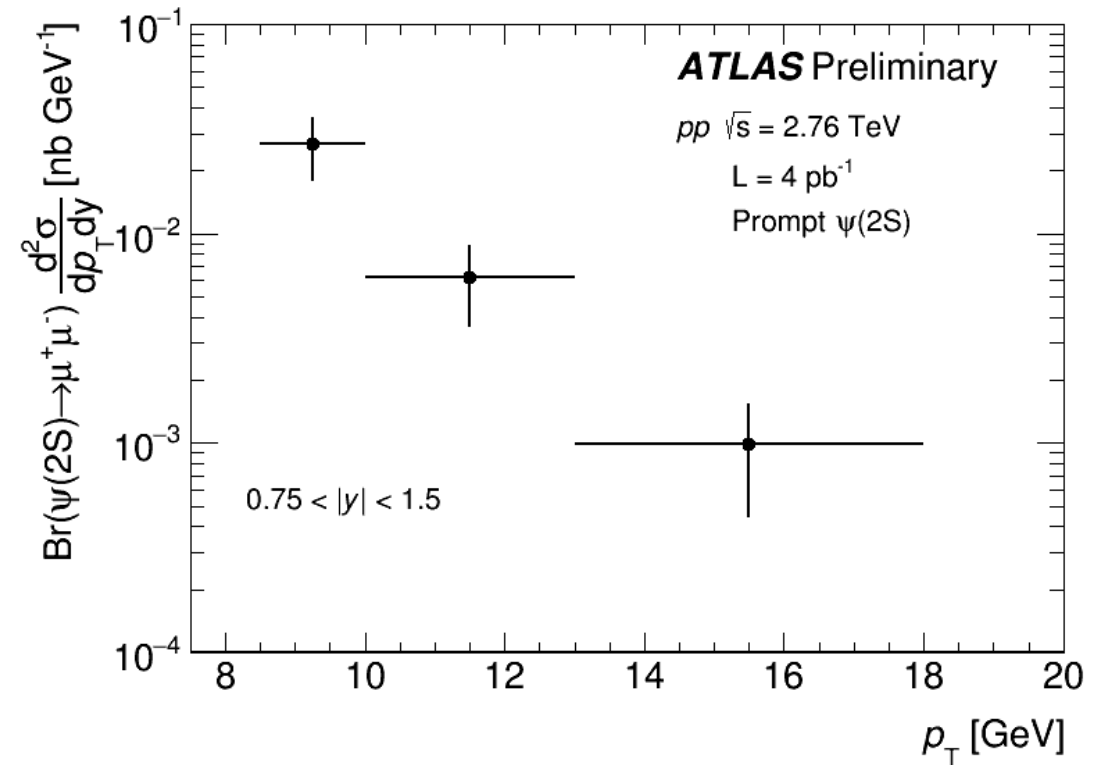
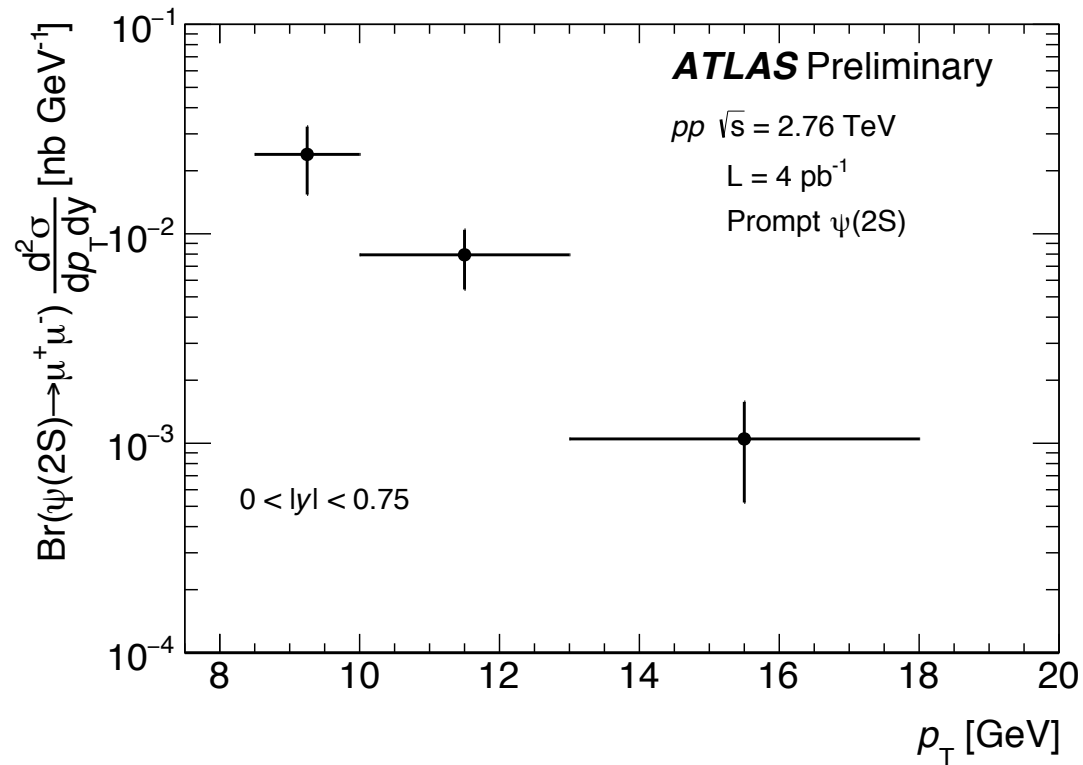
# Double differential cross sections for prompt J/ψ and ψ(2S) @ 2.76 TeV pp

0 < |y| < 0.75 [ATLAS-CONF-2015-023](#) 0.75 < |y| < 1.5

J/ψ



ψ(2S)

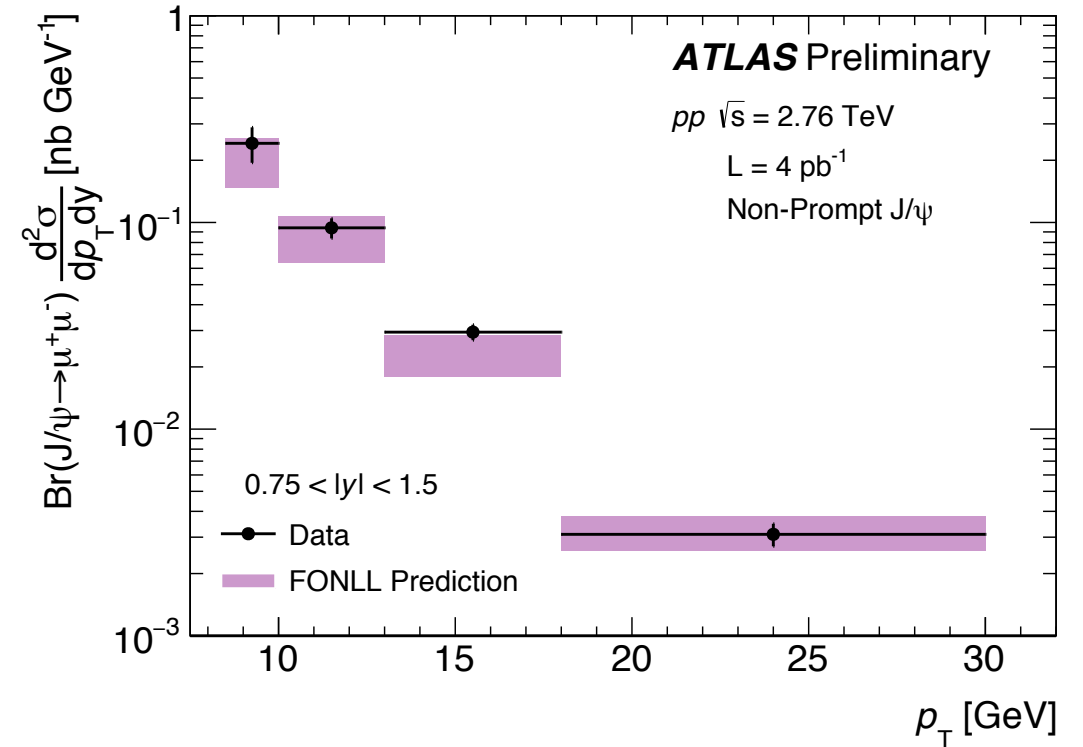
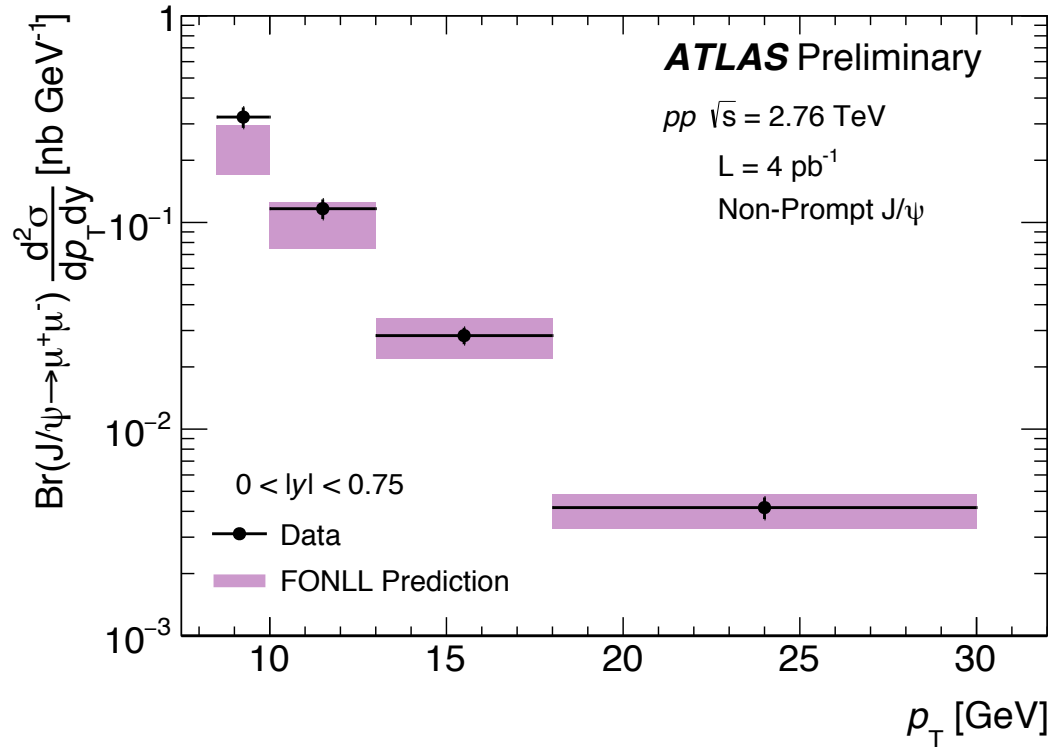




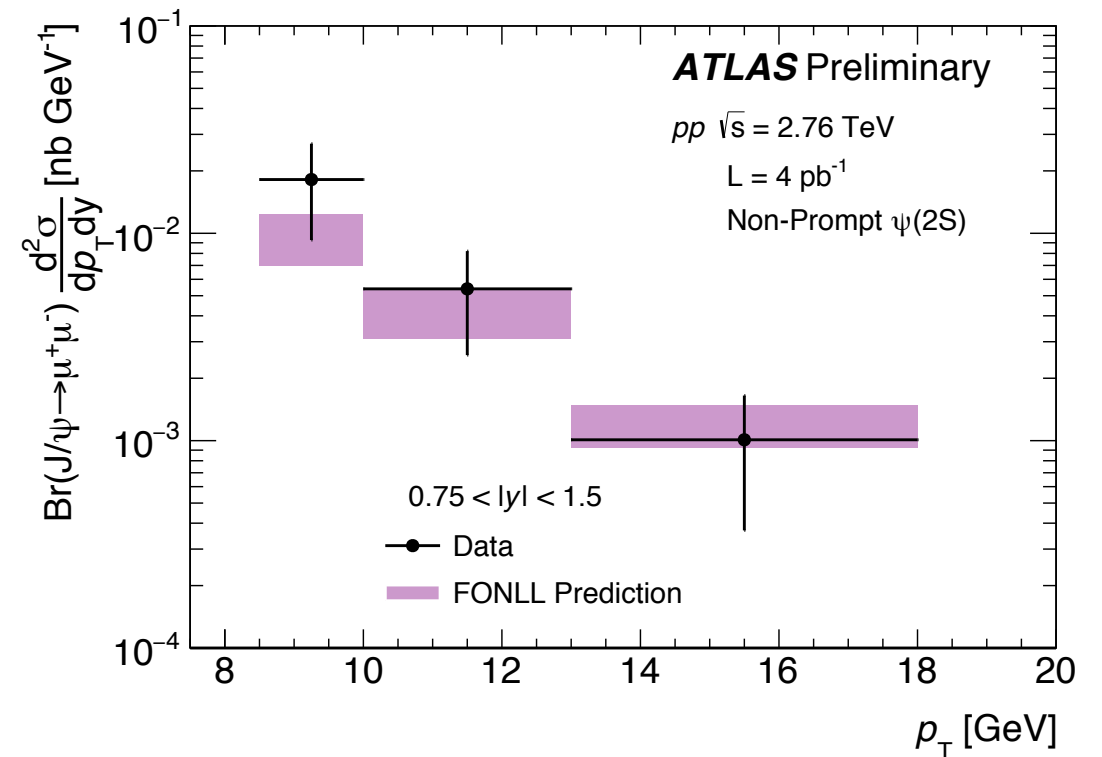
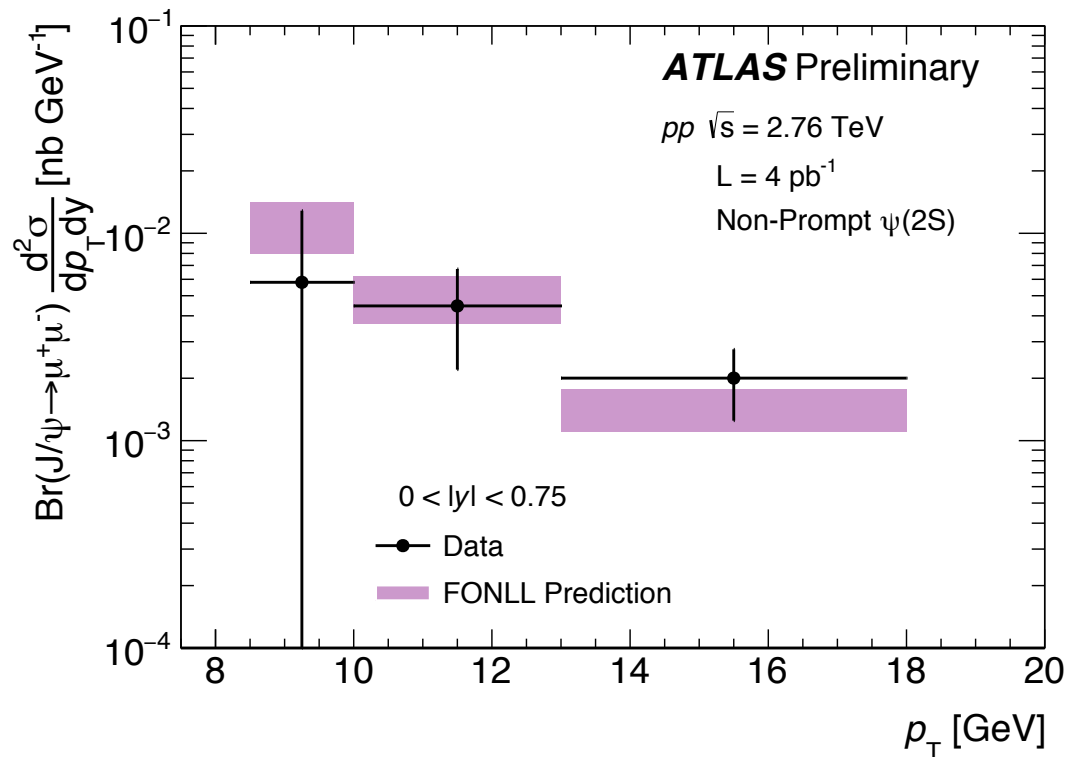
# Double differential cross sections for **non-prompt** J/ψ and ψ(2S) @ 2.76 TeV pp

**0 < |y| < 0.75** [ATLAS-CONF-2015-023](#) **0.75 < |y| < 1.5**

J/ψ



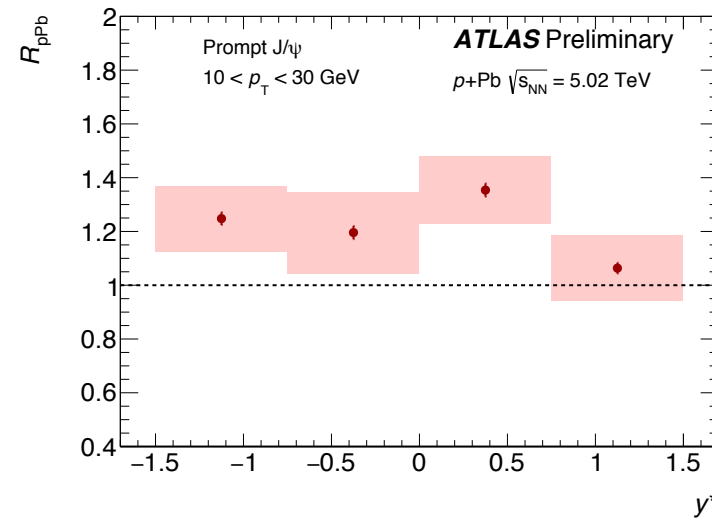
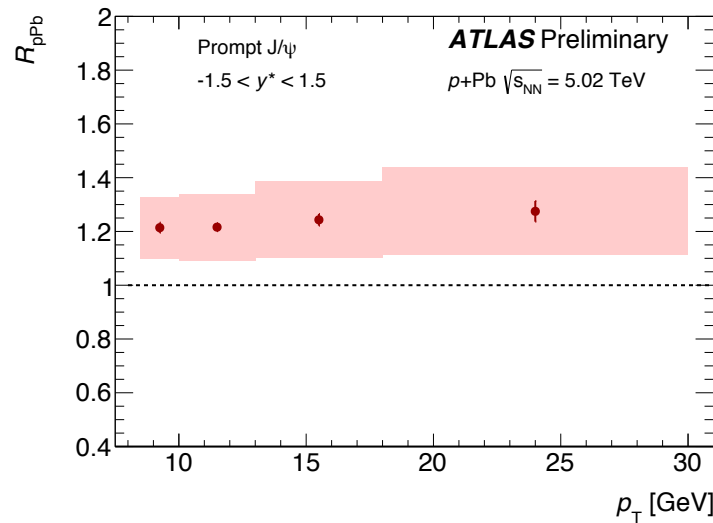
ψ(2S)



# Nuclear modification factor $J/\psi$ and $\psi(2S)$ @ 5.02 TeV $p+Pb$

ATLAS-CONF-2015-023

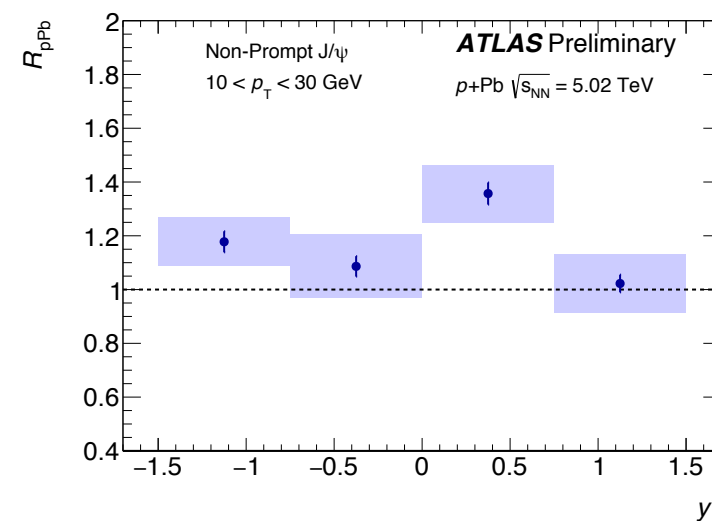
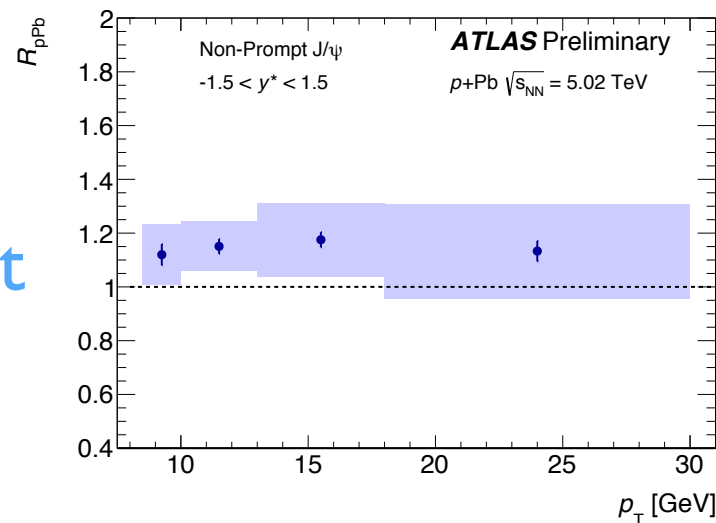
prompt  
 $J/\psi$



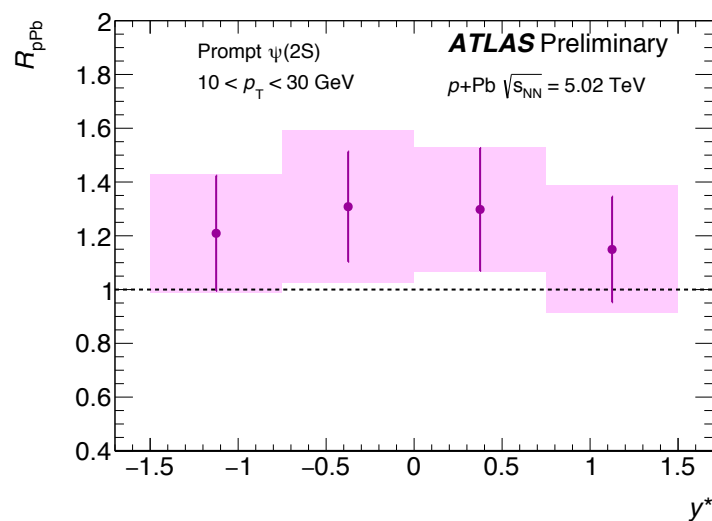
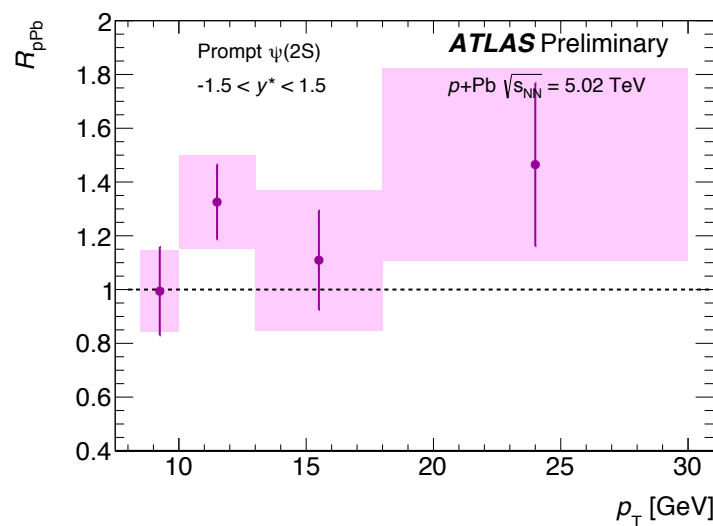
$R_{pPb} \times p_T, y^*$

$$R_{pPb} = \frac{1}{A^{Pb}} \frac{d^2\sigma_{\psi}^{p+Pb} / dy^* dp_T}{d^2\sigma_{\psi}^{pp} / dy dp_T}$$

non-prompt  
 $J/\psi$



prompt  
 $\psi(2S)$

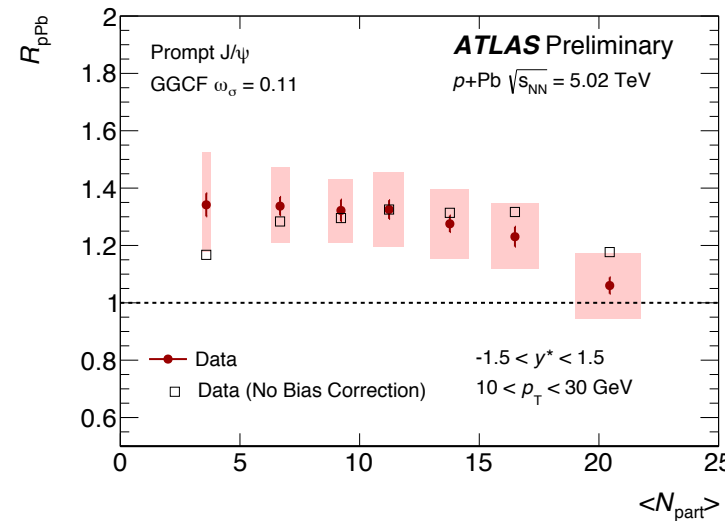
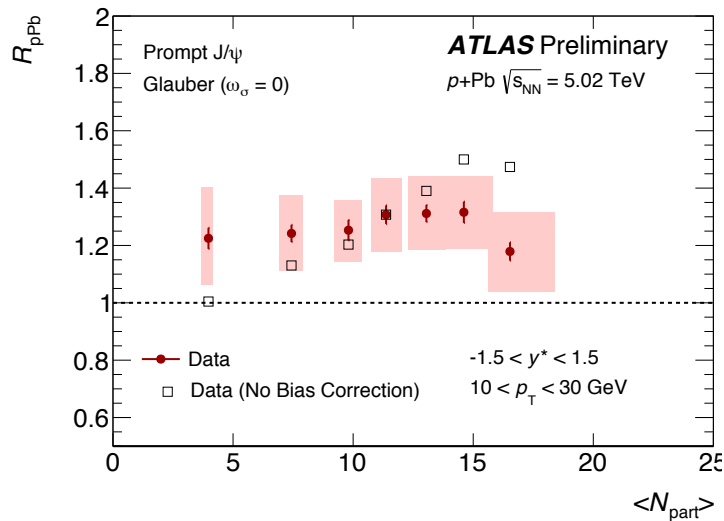


# Nuclear modification factor $J/\psi$ and $\psi(2S)$ @ 5.02 TeV p+Pb

ATLAS-CONF-2015-023

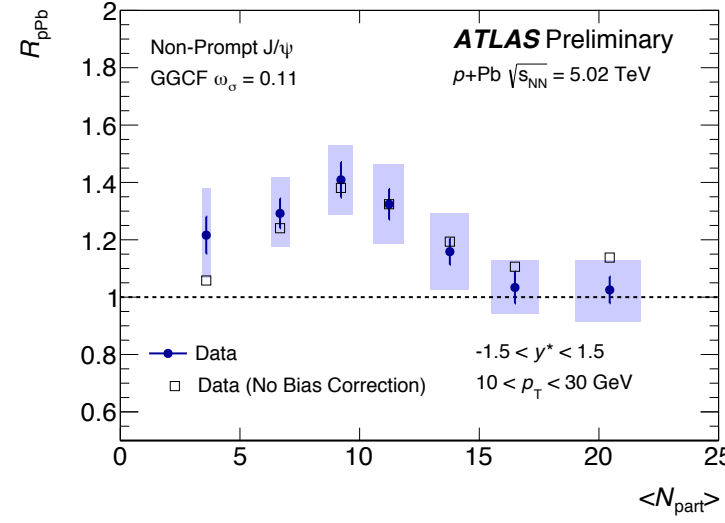
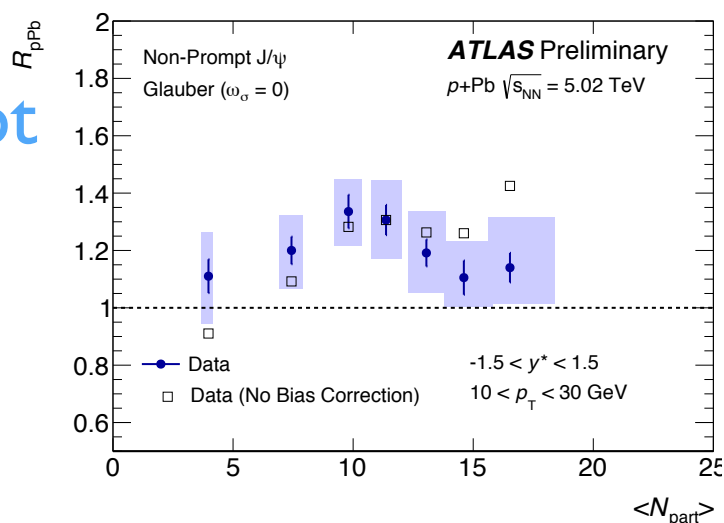
$$R_{pPb} = \frac{1}{\langle T_{pPb} \rangle_{\text{cent}}} \frac{1/N_{\text{evt}} d^2 N_{\psi}^{p+Pb} / dy^* dp_T}{d^2 \sigma_{\psi}^{pp} / dy dp_T} \Big|_{\text{cent}}$$

prompt  
 $J/\psi$   
 $R_{pPb} > 1$



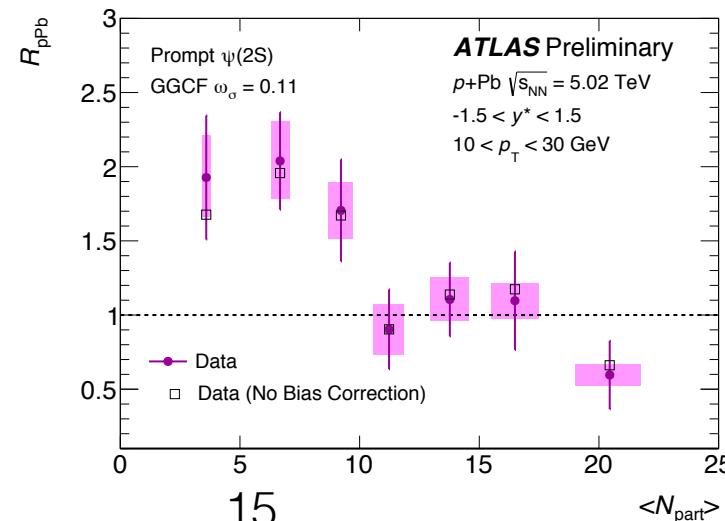
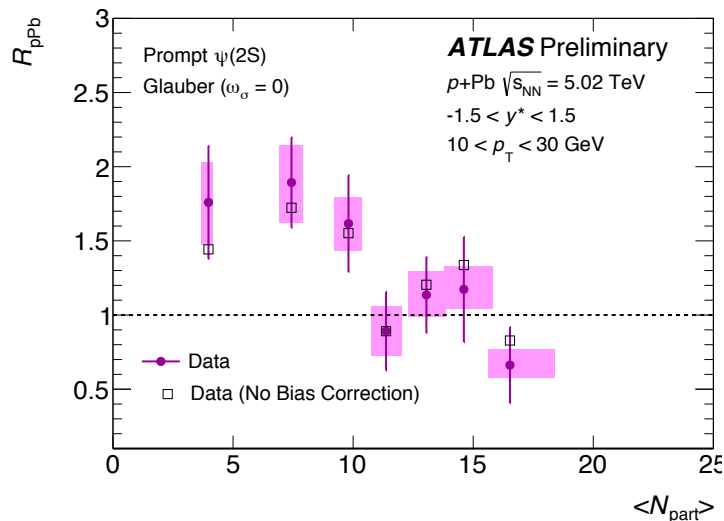
$R_{pPb} \times \langle N_{\text{part}} \rangle$

non-prompt  
 $J/\psi$   
 $R_{pPb} > 1$   
mid cent



Model dependent:  
standard Glauber (left)  
GGCF  $\omega_{\sigma} = 0.11$  (right)

prompt  
 $\psi(2S)$   
 $R_{pPb} > 1$   
low cent

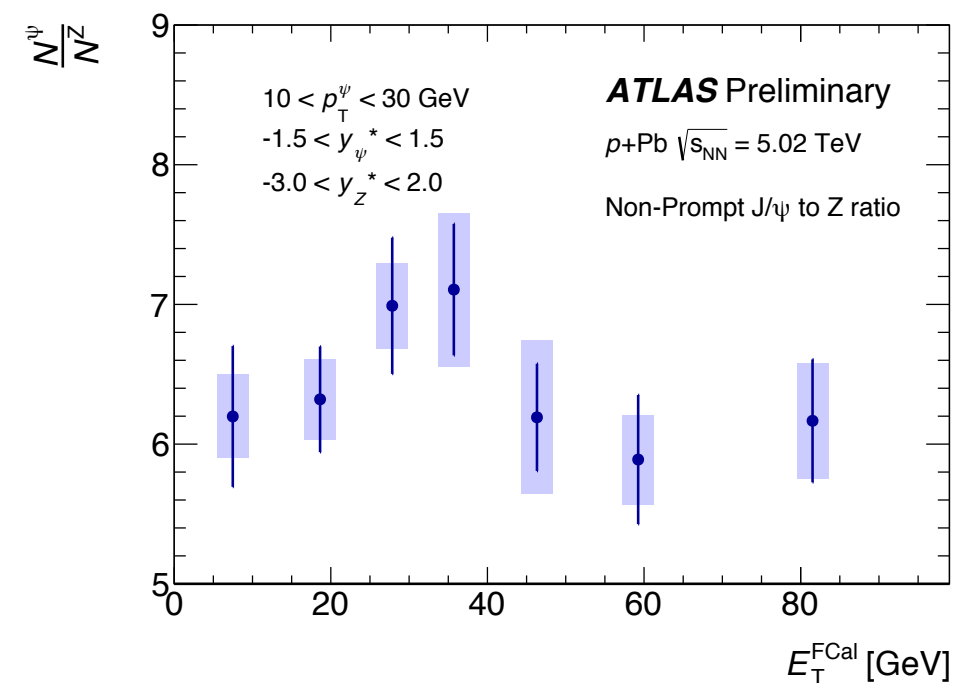
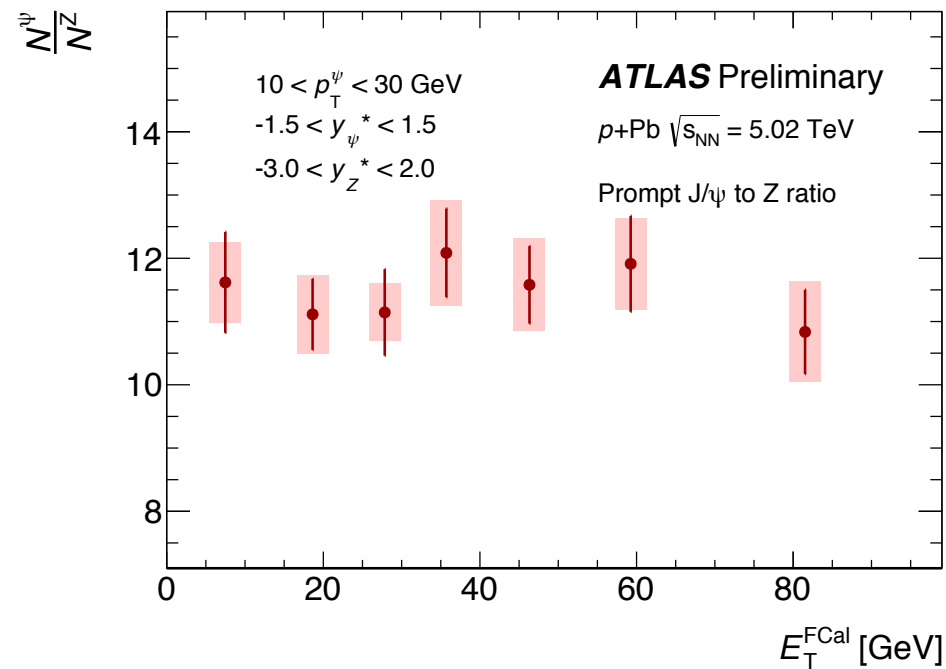


# J/ $\psi$ and $\psi(2S)$ ratios to Z yields @ 5.02 TeV p+Pb

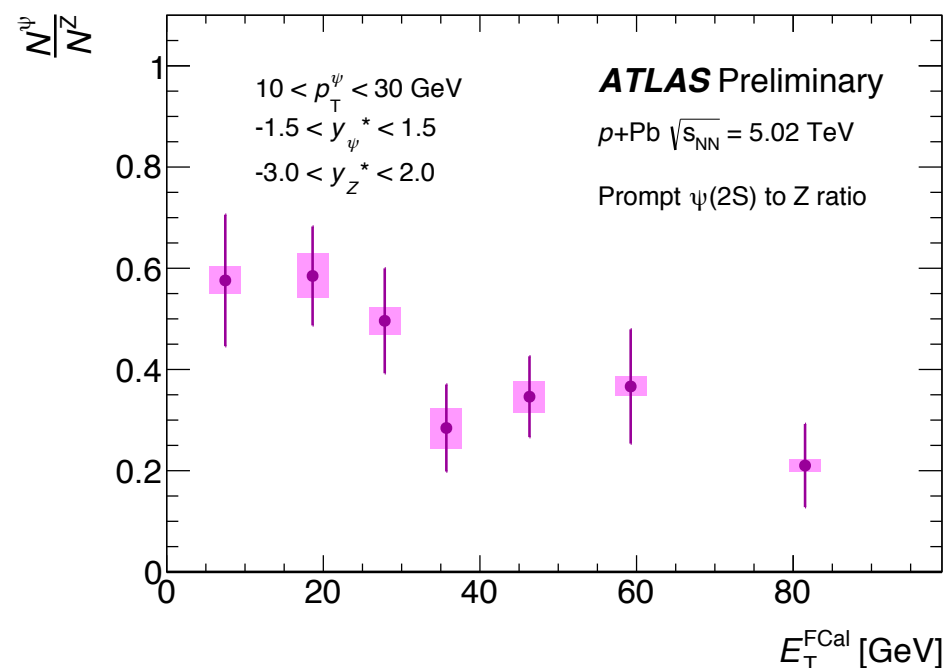
[ATLAS-CONF-2015-023](#)

prompt J/ $\psi$  to Z

non-prompt J/ $\psi$  to Z



prompt  $\psi(2S)$  to Z



Test of  $\psi$  production scaling with the nuclear thickness independently of geometric models

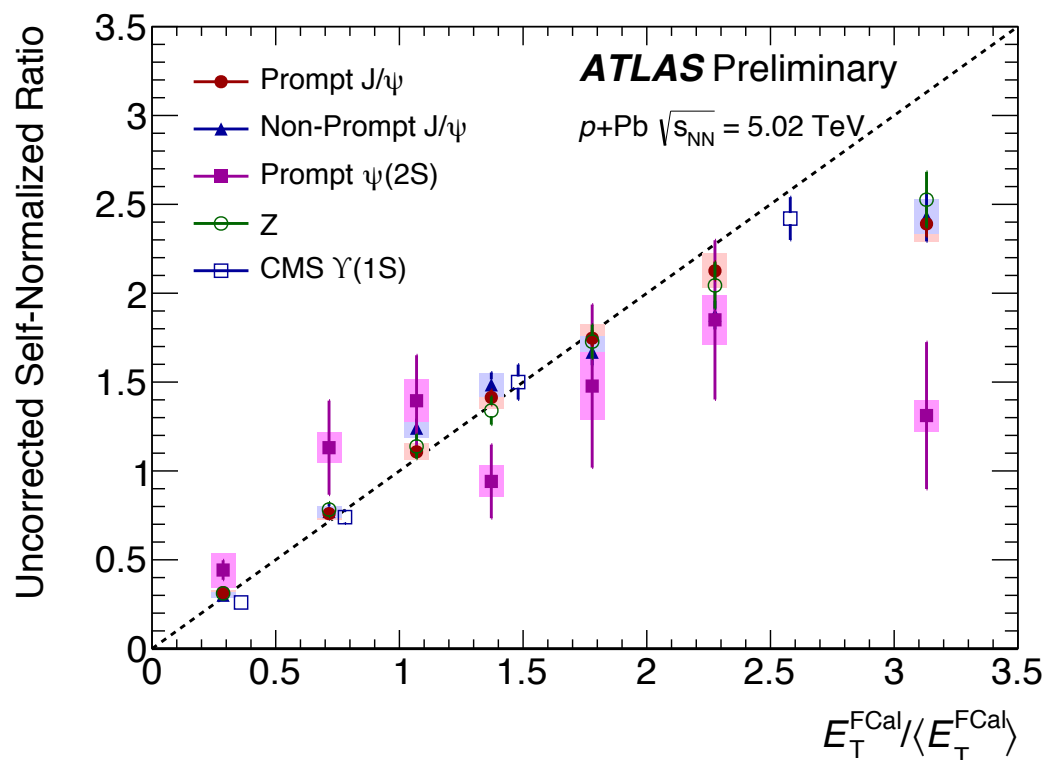
Decreasing trend for  $\psi(2S)$  while J/ $\psi$  appears to be flat



# Self-normalized ratios for $\psi(2S)$ and $J/\psi$ @ 5.02 TeV p+Pb

ATLAS-CONF-2015-023

uncorrected

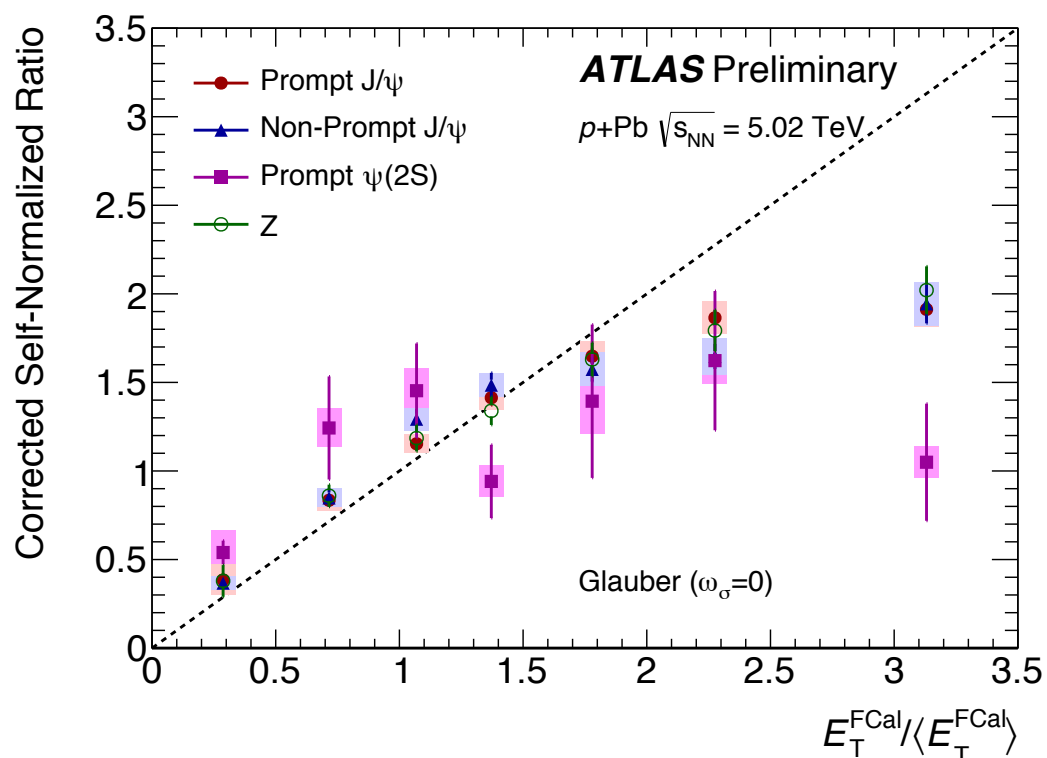


The uncorrected  $J/\psi$  and Z self-normalized ratios show similar trend to CMS results for  $\Upsilon(1S)$ .

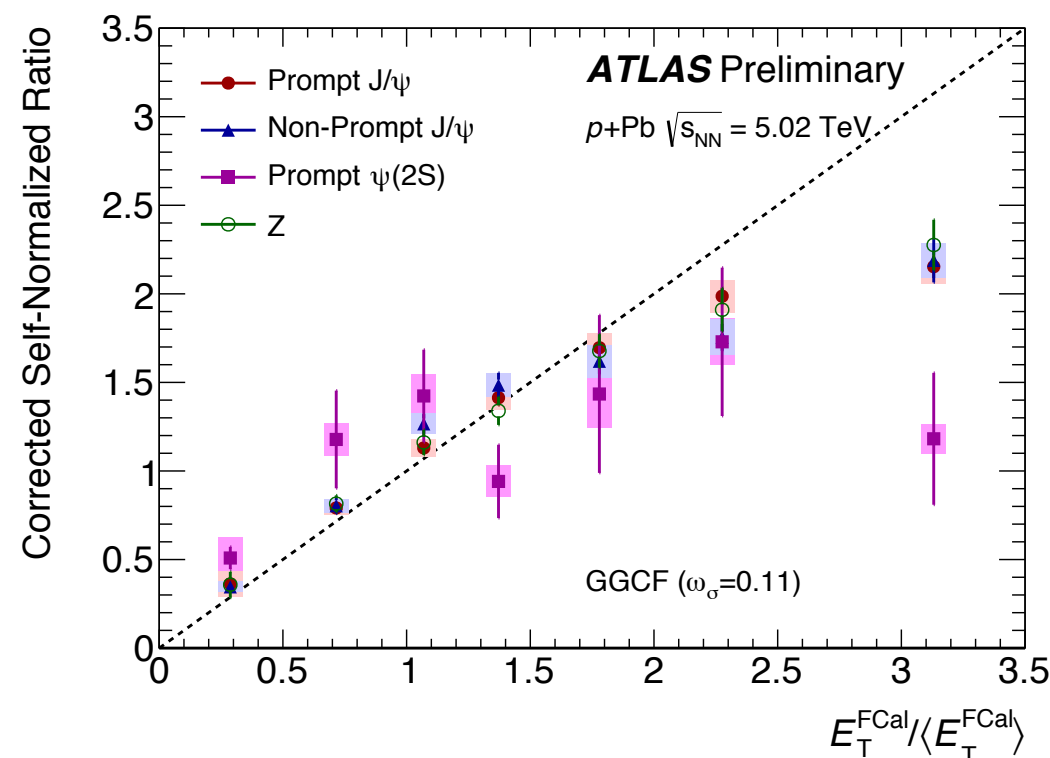
At large  $E_T^{FCal}$ ,  $E_T^{FCal} / \langle E_T^{FCal} \rangle > 3$ , significant deviations from the unity are observed for prompt  $J/\psi$  non-prompt  $J/\psi$  and prompt  $\psi(2S)$ .

The deviations become more significant when the centrality bias correction is applied.

corrected - Glauber



corrected - GGCF



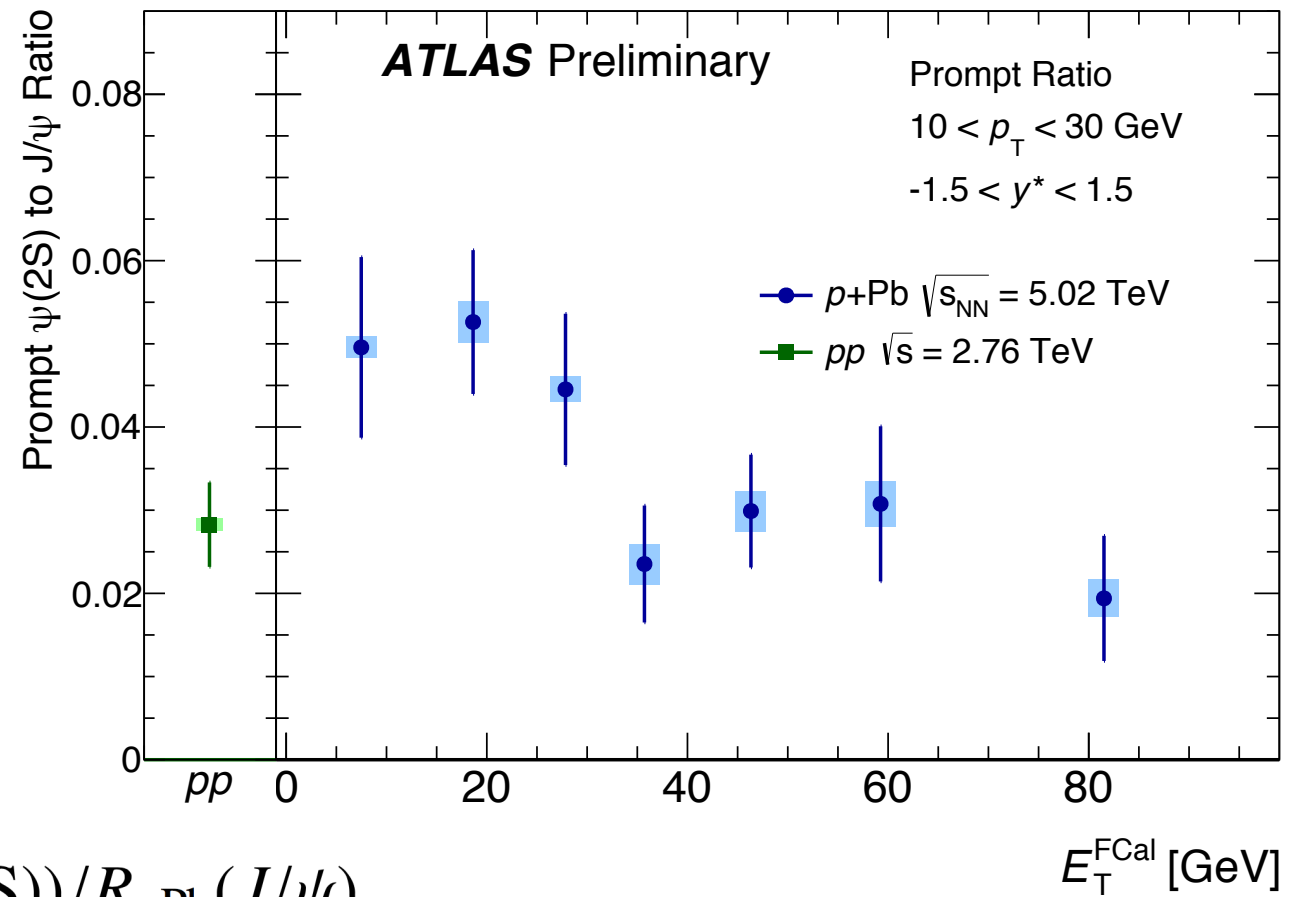
$$\frac{\psi}{\langle \psi \rangle} = \frac{N_\psi / N_{\text{evt}} |_{\text{cent}}}{N_\psi^{0-90\%} / N_{\text{evt}}^{0-90\%}}$$

$$\frac{E_T^{FCal}}{\langle E_T^{FCal} \rangle} = \frac{\langle E_T^{FCal} \rangle |_{\text{cent}}}{\langle E_T^{FCal} \rangle |_{0-90\%}}$$

# Prompt double ratios @ 5.02 TeV p+Pb

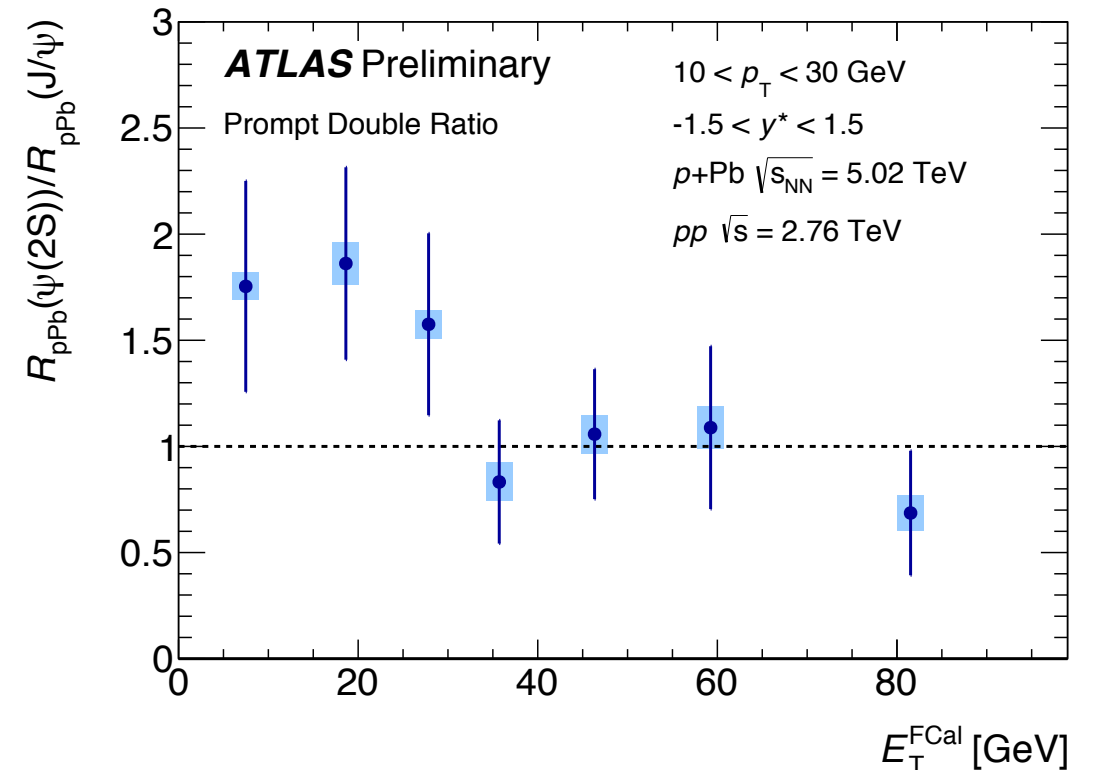
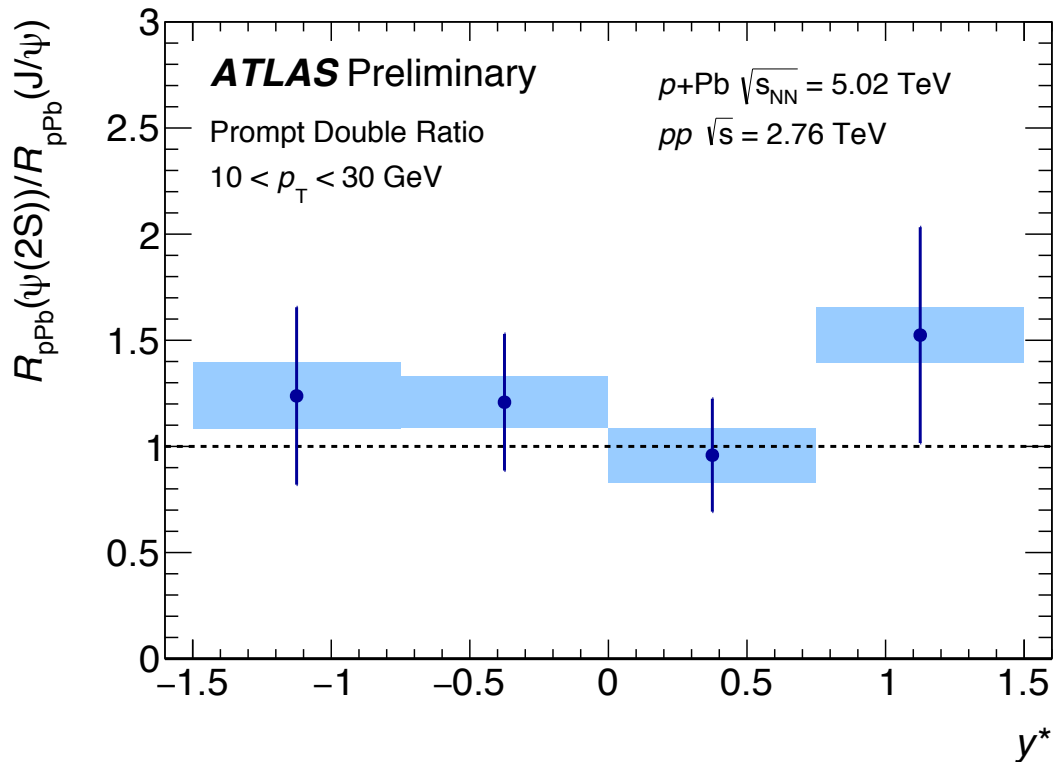
Prompt ratios  
X  
FCal  $E_T$  and  $y^*$

Evidence for centrality dependence  
Similar pattern as Z-normalized  $\psi(2S)$   
Decreasing trend with centrality



ATLAS-CONF-2015-023

$R_{pPb}(\psi(2S))/R_{pPb}(J/\psi)$



## Pb+Pb @ 2.76 TeV Motivations

Measurements of heavy quark production and suppression in ultra-relativistic nuclear collisions probe the interactions of heavy quarks with the hot, dense medium created in the collisions.

Measurement of the suppression of quarkonium yields: experimental signature of the QGP formation.

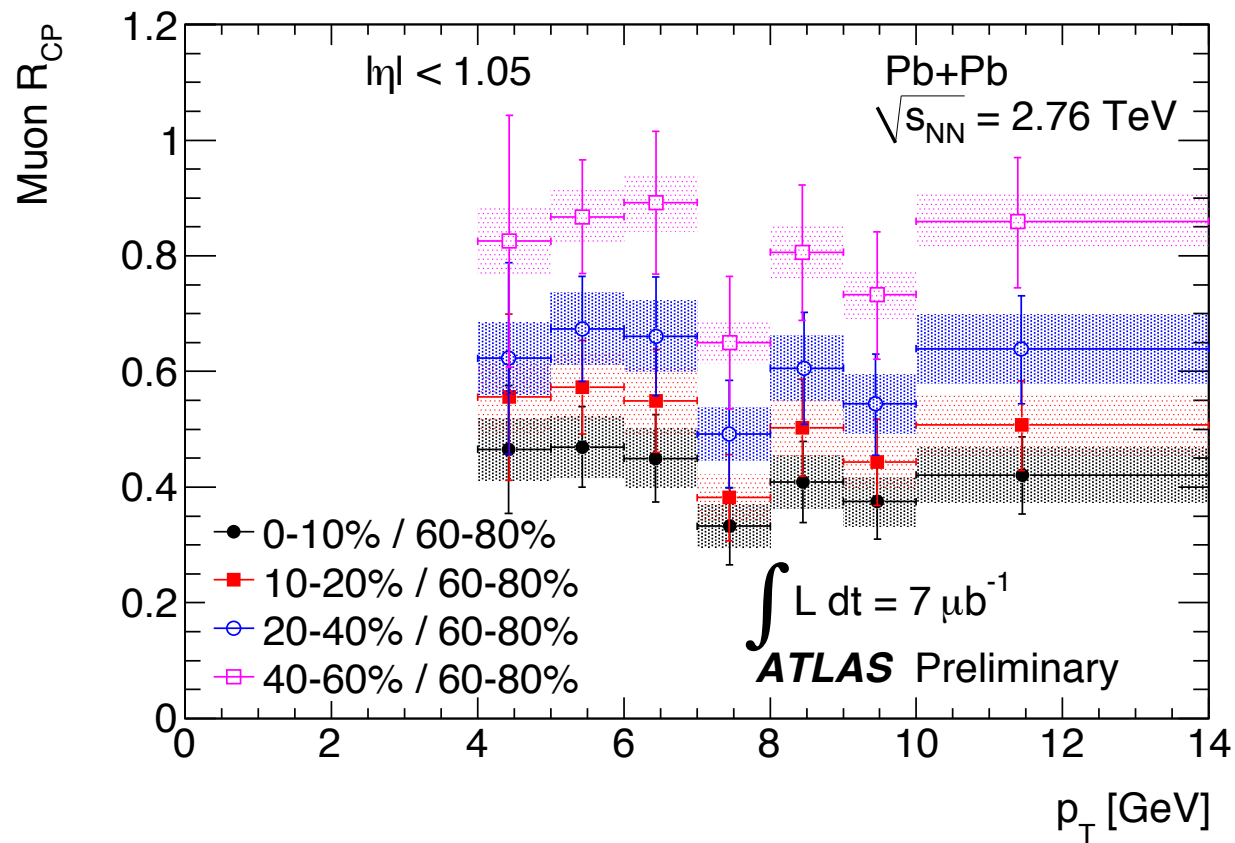
Important complement to studies of light quark and gluon quenching.

# Suppression of heavy flavour muons in Pb+Pb @ 2.76 TeV

60-80% reference

$$R_{CP}(p_T)|_{cent} = \frac{1}{R_{coll}^{cent}} \left( \frac{\frac{1}{N_{evt}^{cent}} \frac{N_S^{cent}}{\epsilon^{cent}}}{\frac{1}{N_{evt}^{60-80}} \frac{N_S^{60-80}}{\epsilon^{60-80}}} \right)$$

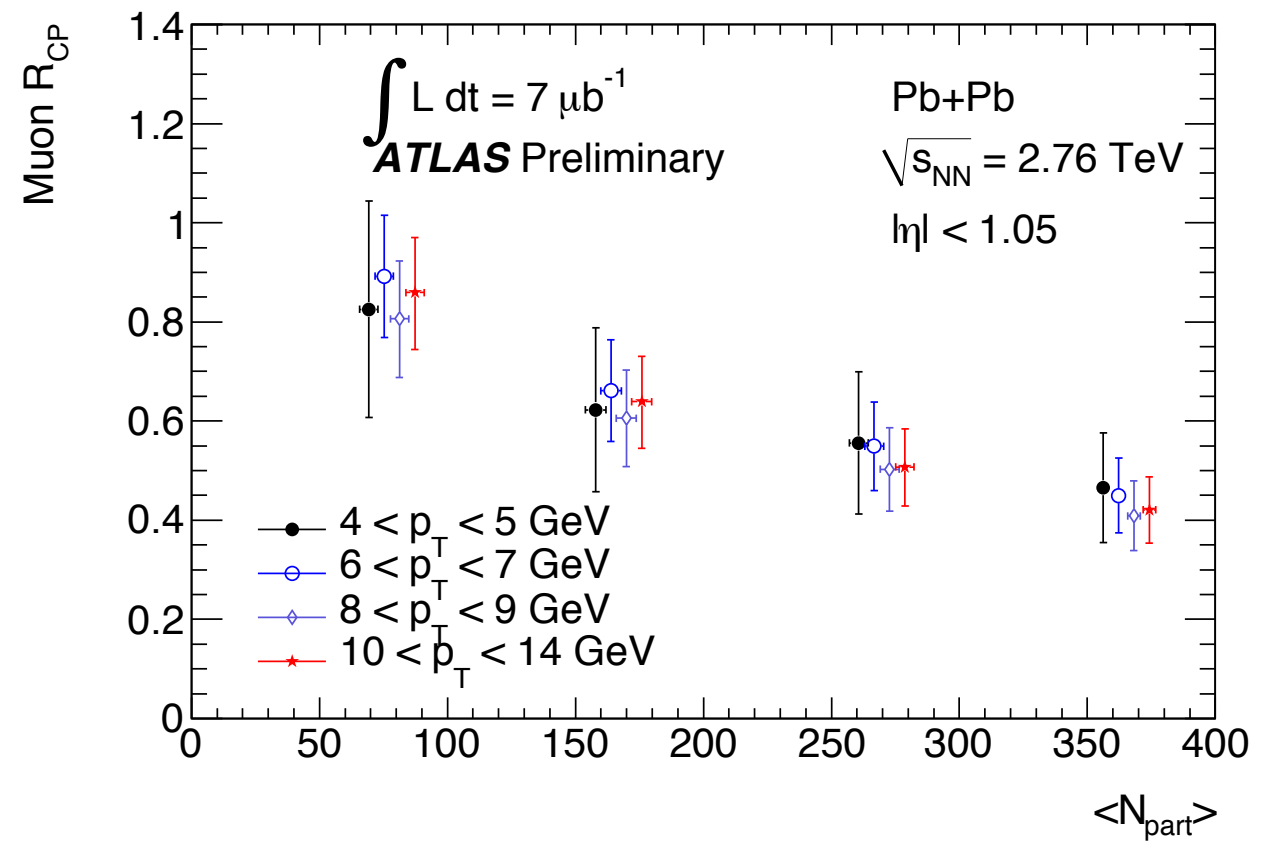
$R_{CP} \times \text{muon } p_T$



No significant variation with muon  $p_T$

[ATLAS-CONF-2012-050](#)

$R_{CP} \times \langle N_{part} \rangle$

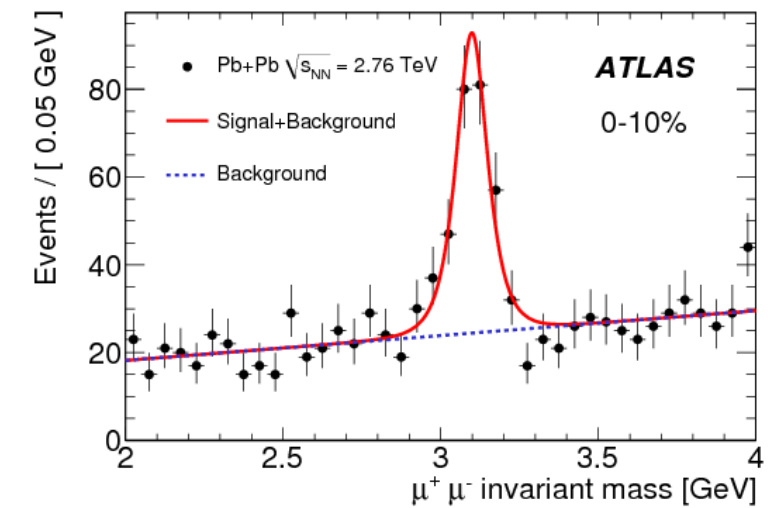
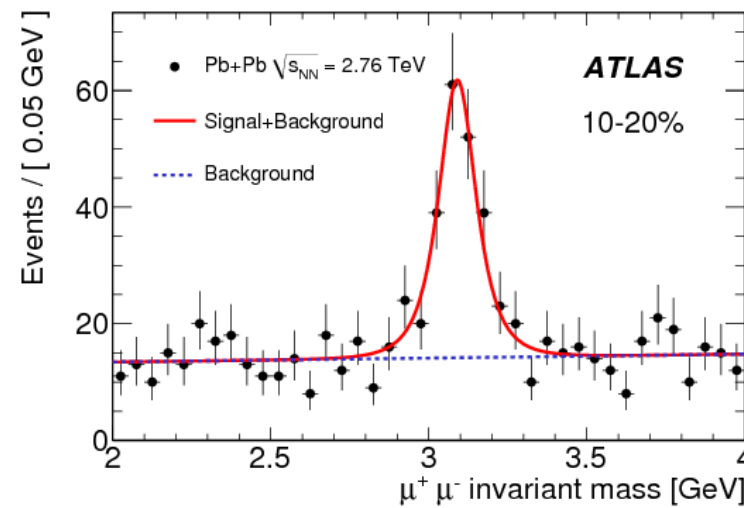
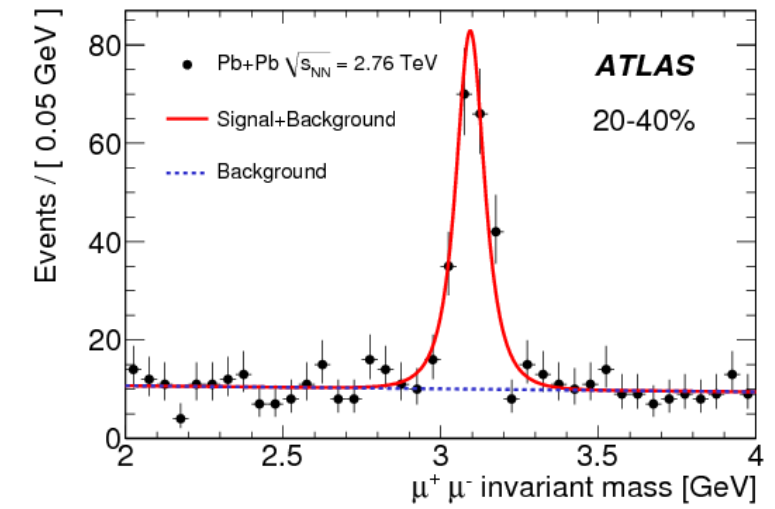
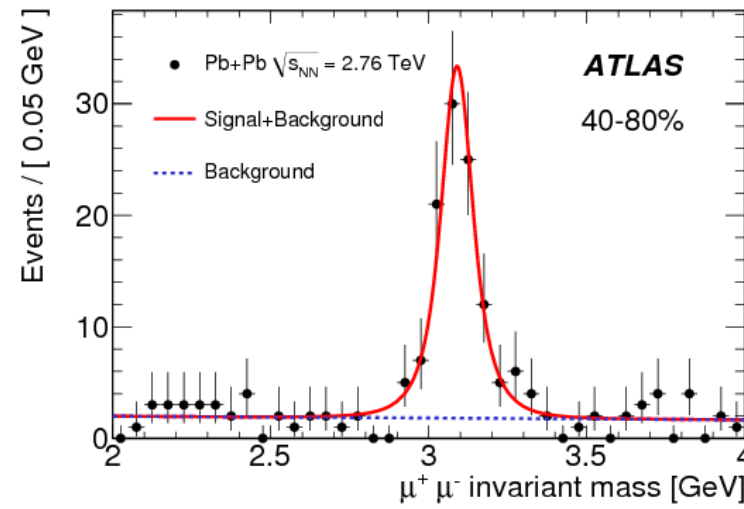
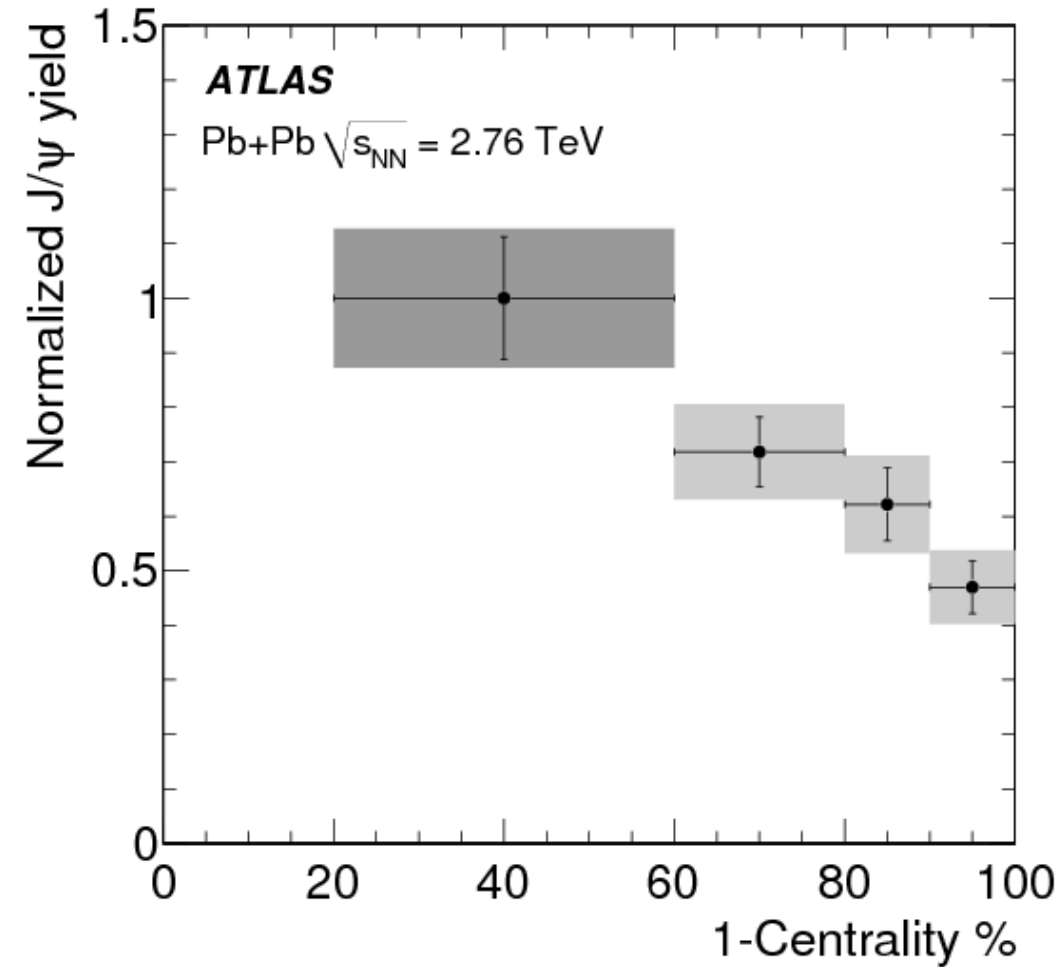


Suppression factor of  $\sim 2.5$  in the yield of muons in the most central compared to most peripheral



# Centrality dependence of $J/\psi$ in Pb+Pb @ 2.76 TeV

[Phys.Lett. B697 \(2011\)](#)



Suppression of  $J/\psi$  yield normalized to the number of binary nucleon-nucleon collisions

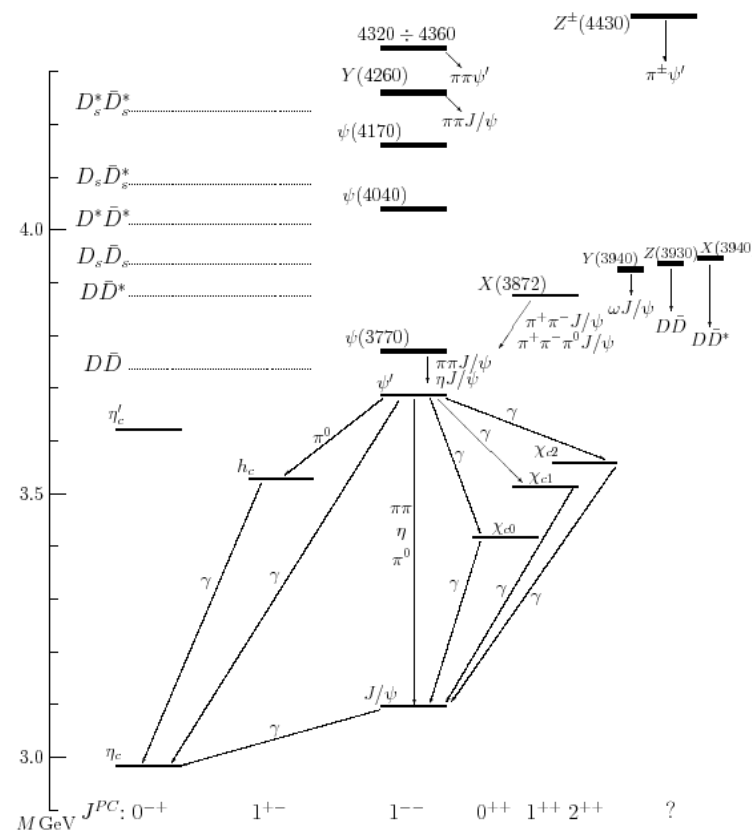
# pp @ 7 and 8 TeV Motivations

At the LHC possibility to explore kinematic regions of high  $p_T \sim 100$  GeV:

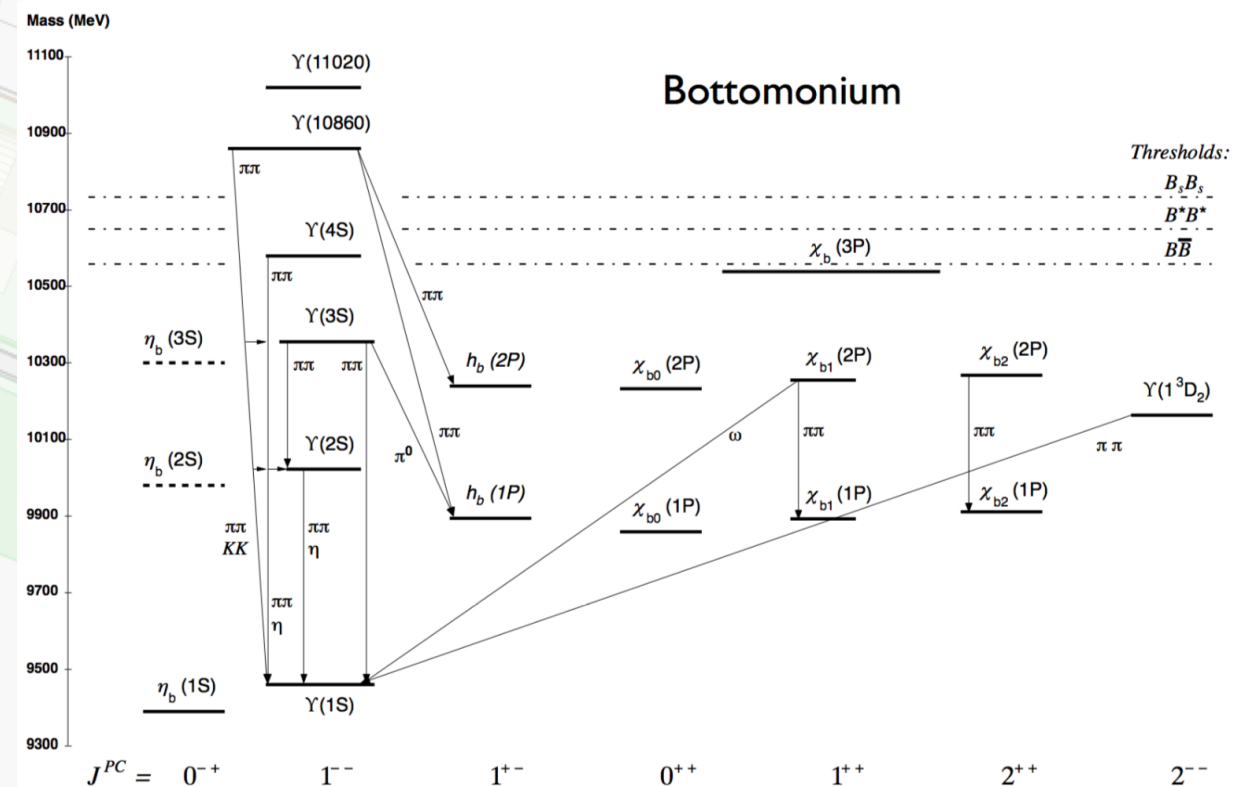
- test predictions of various theoretical models for both quarkonium and open state production;
- corrections over the LO (NLO, and NLL) + accurate quantitative comparison of data with QCD predictions can be performed to discriminate among various quarkonium production models (color singlet (CS), color octet (CO or NRQCD), color evaporation (CE), kT factorization).

Understanding of quarkonium production requires discrimination and understanding of the various modes of production :

## Charmonium



## Bottomonium



$J/\psi \rightarrow \mu\mu$  candidate in 7 TeV collisions

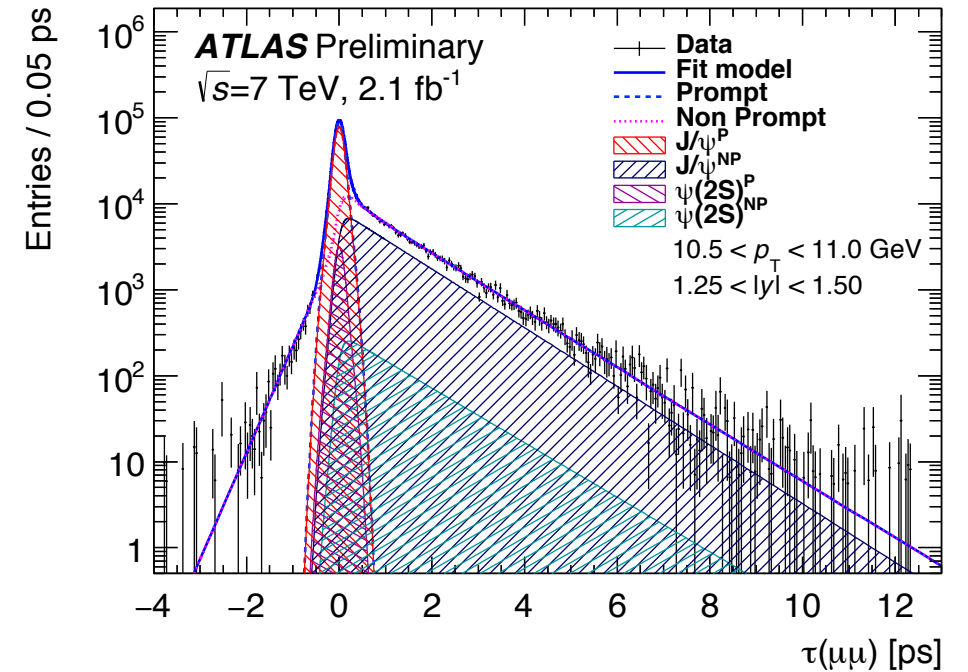
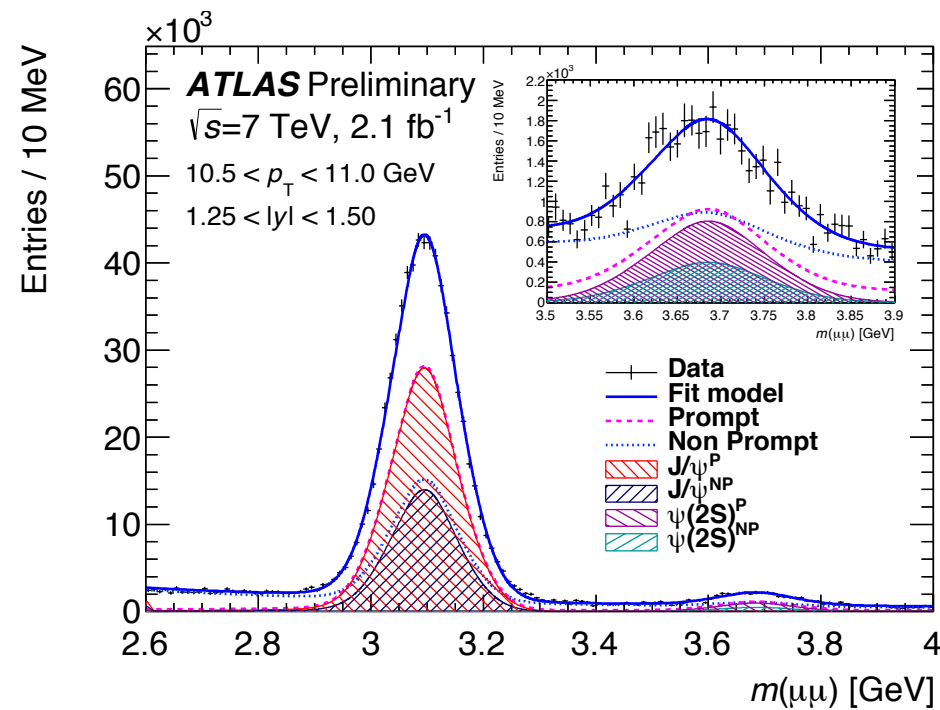
run #: 152409, evt #: 2452006  
Inv. Mass=3.1GeV  
 $P(\mu^+) = 28$  GeV,  $\eta=0.93$   
 $P(\mu^-) = 15$  GeV,  $\eta=0.95$

# Brand new high-statistics measurement of $J/\psi$ and $\psi(2S)$ @ 7 and 8 TeV pp!!!

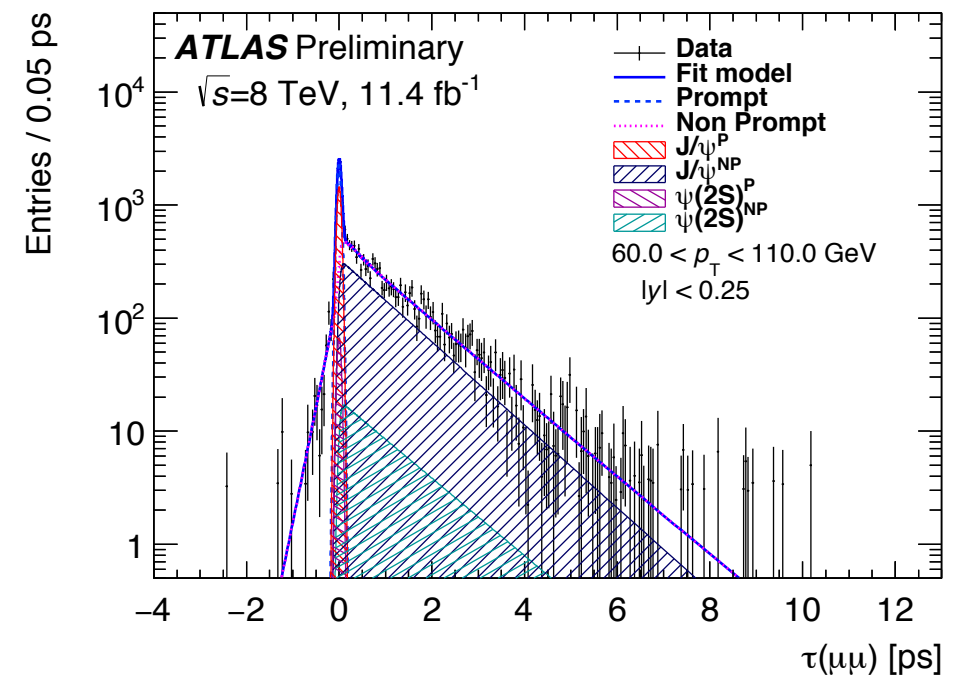
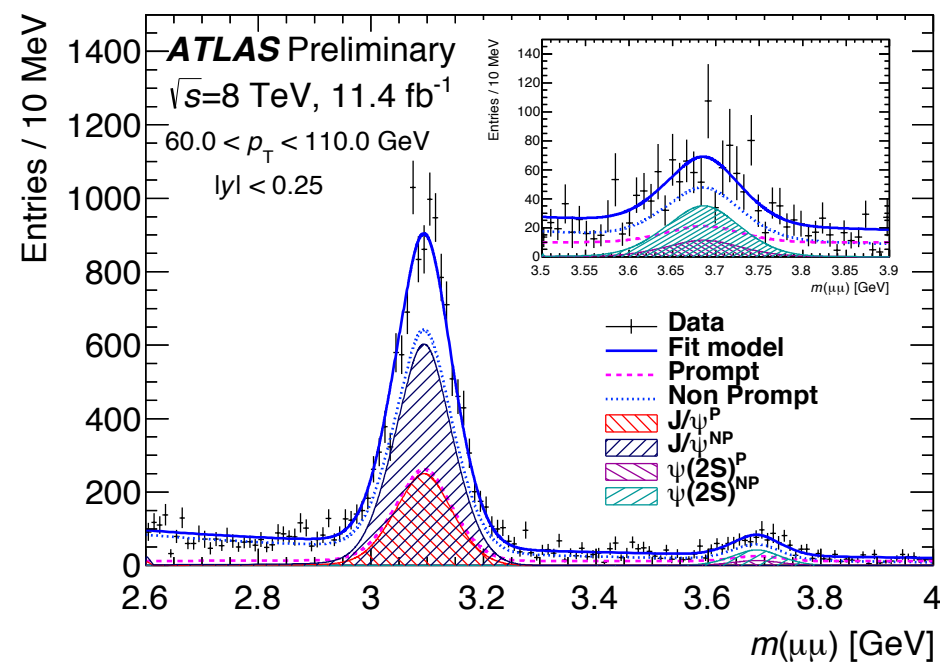
$8 < |y| \leq 110 \text{ GeV}, |y| < 2.0$

ATLAS-CONF-2015-024

7 TeV



8 TeV





# Differential cross-sections of $J/\psi$ and $\psi(2S)$ @ 7 and 8 TeV pp

ATLAS-CONF-2015-024

prompt

$J/\psi$

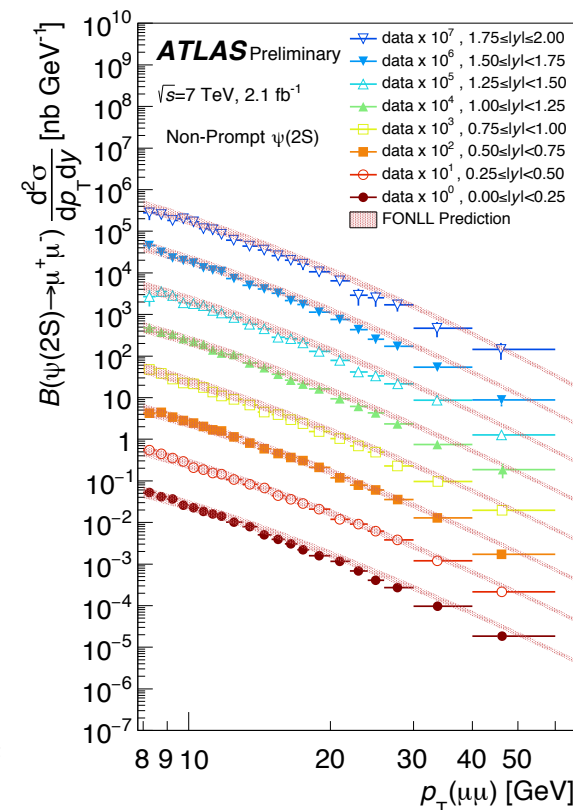
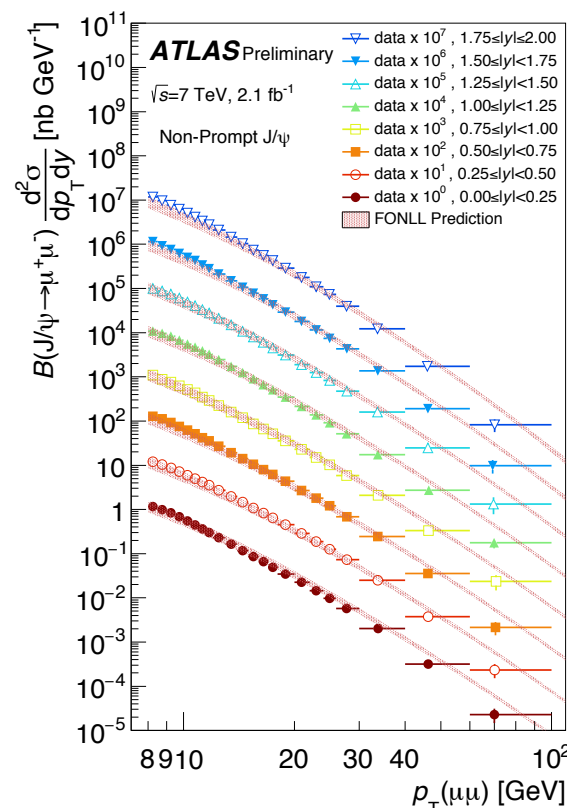
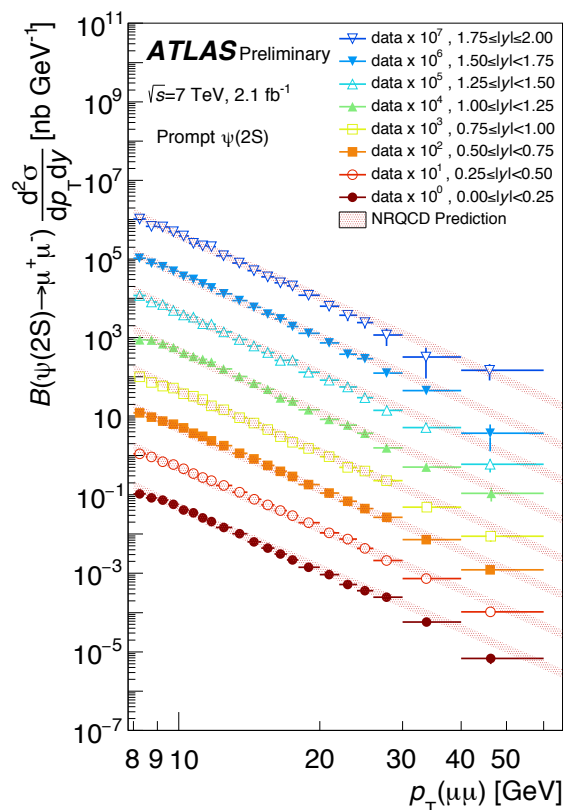
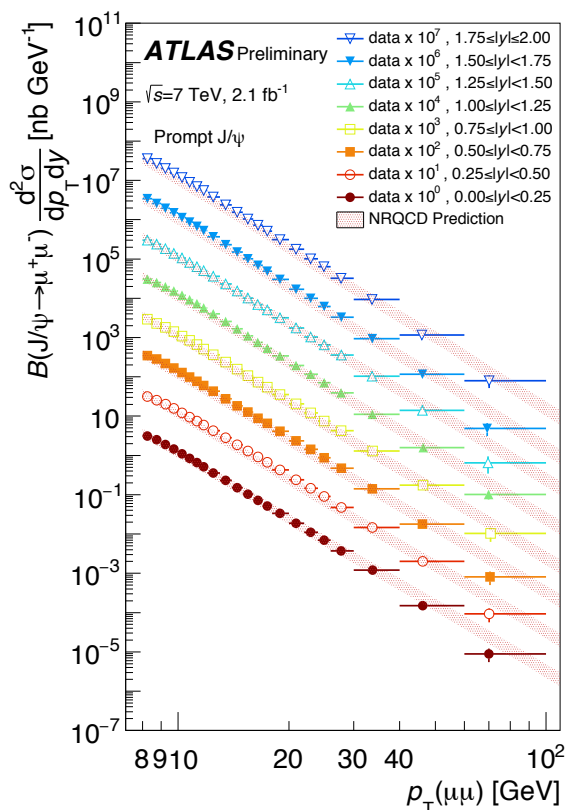
$\psi(2S)$

non-prompt

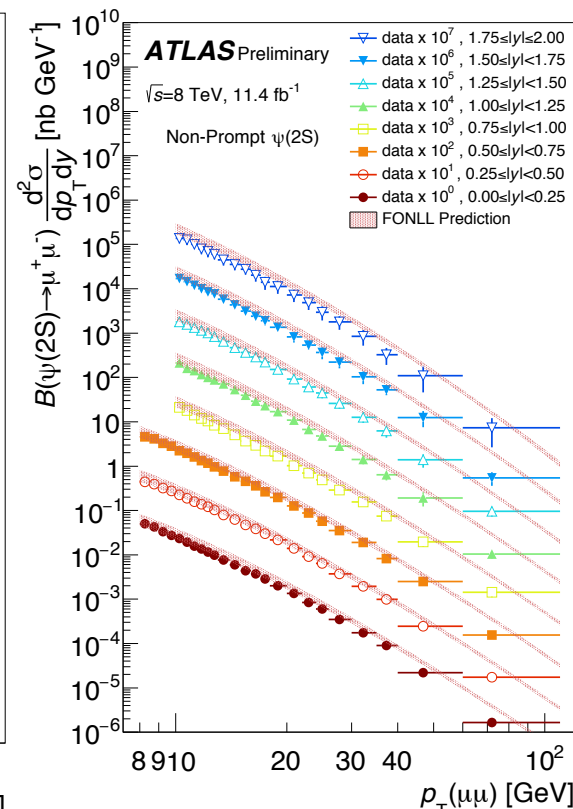
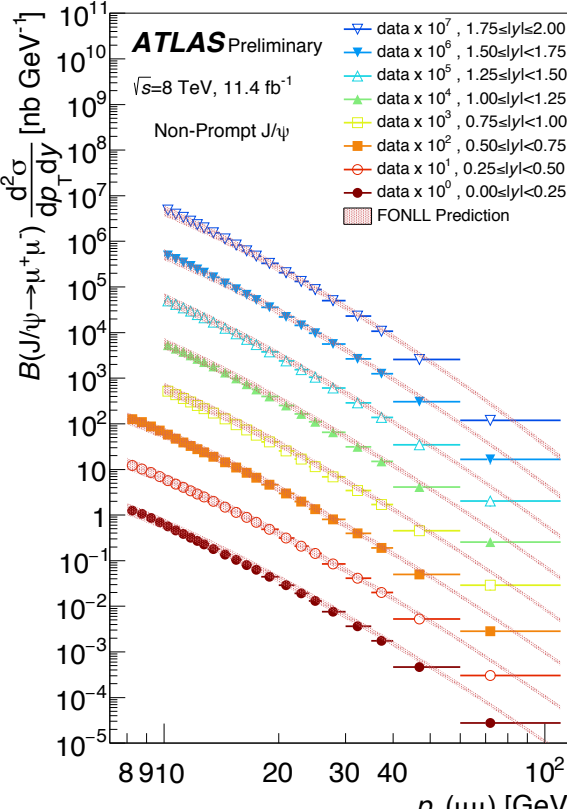
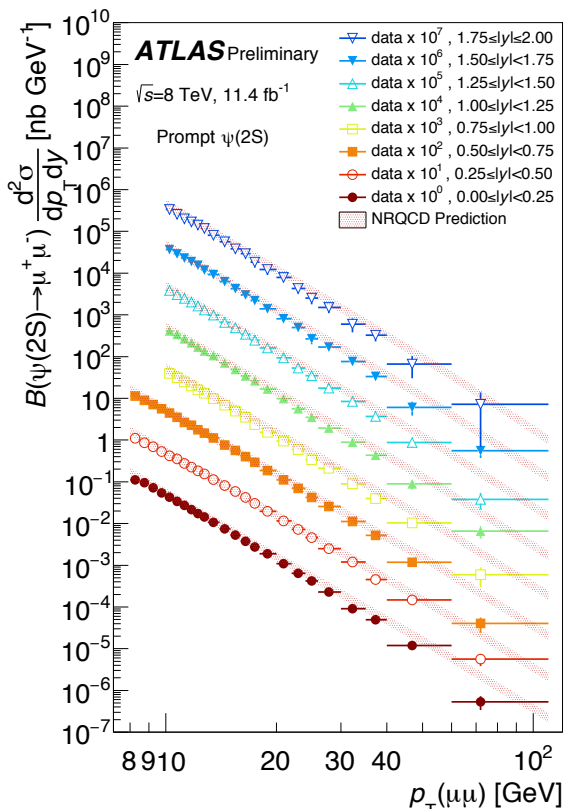
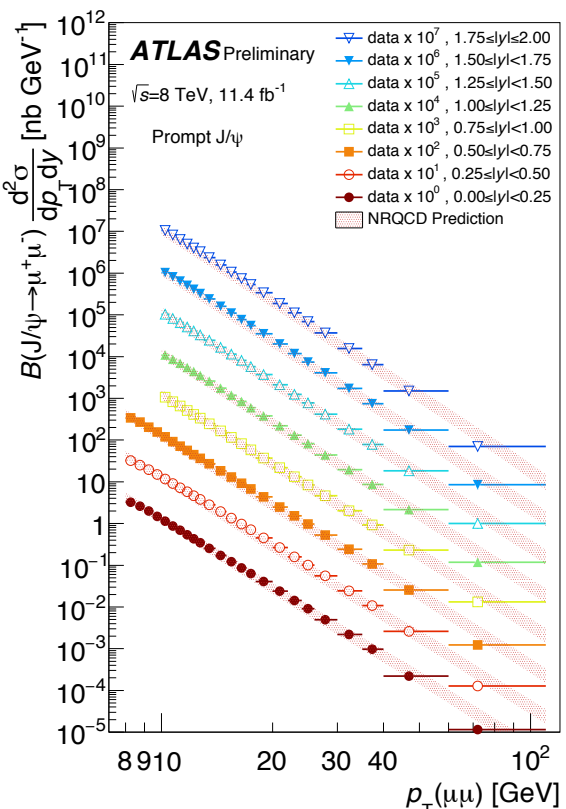
$J/\psi$

$\psi(2S)$

7 TeV



8 TeV

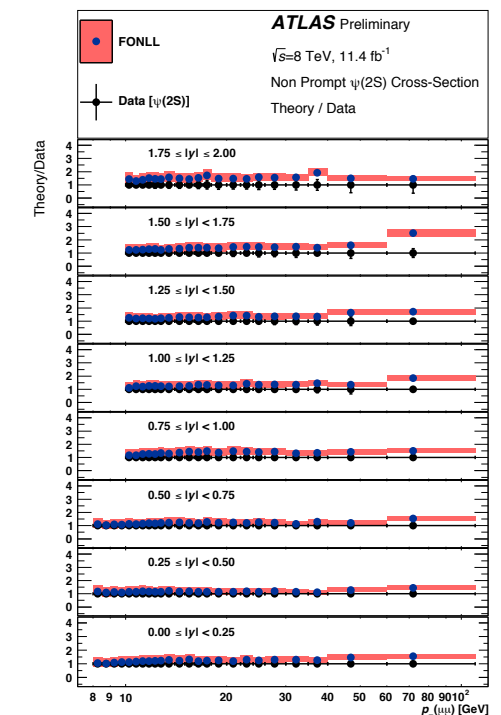
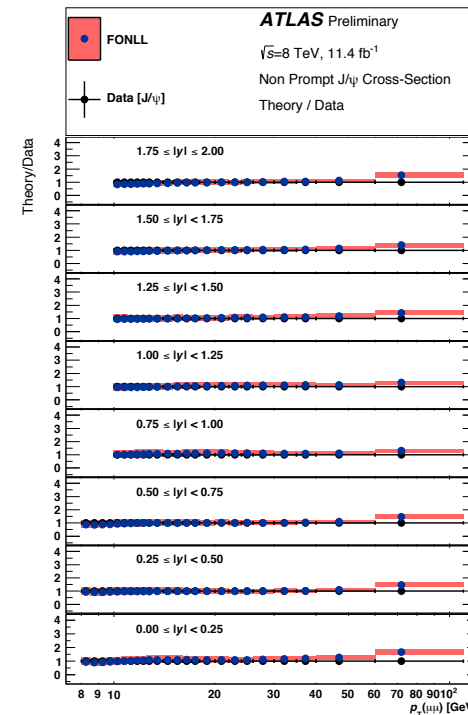
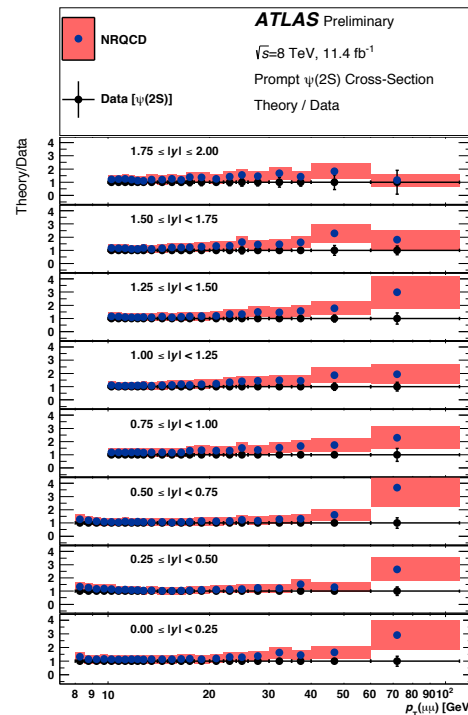
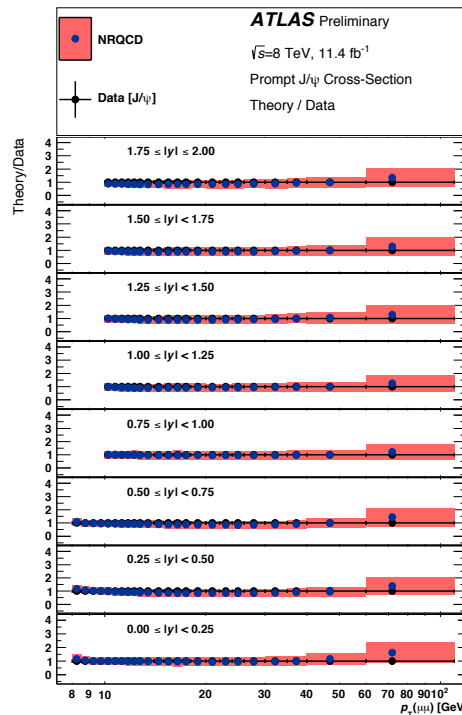
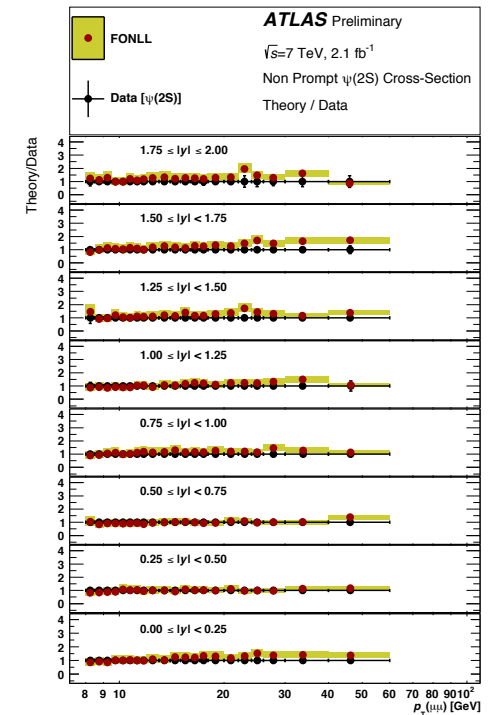
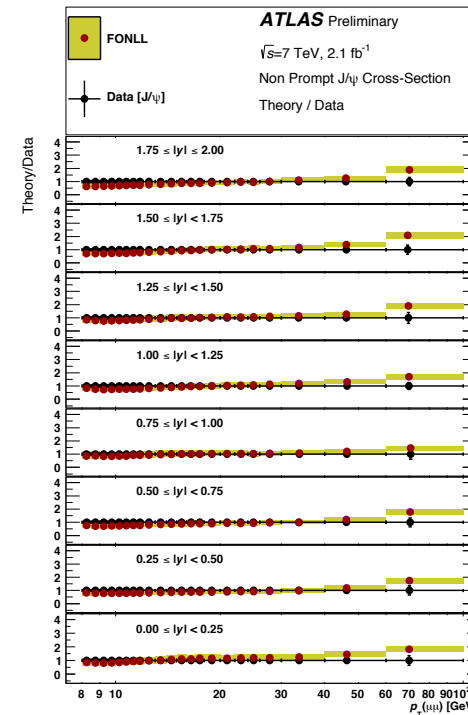
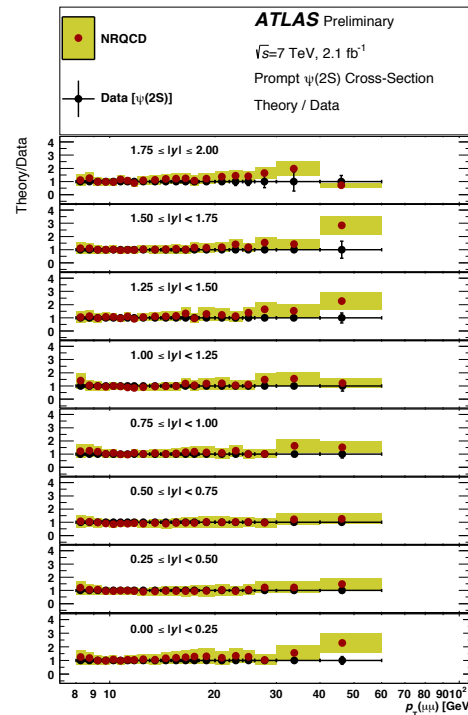
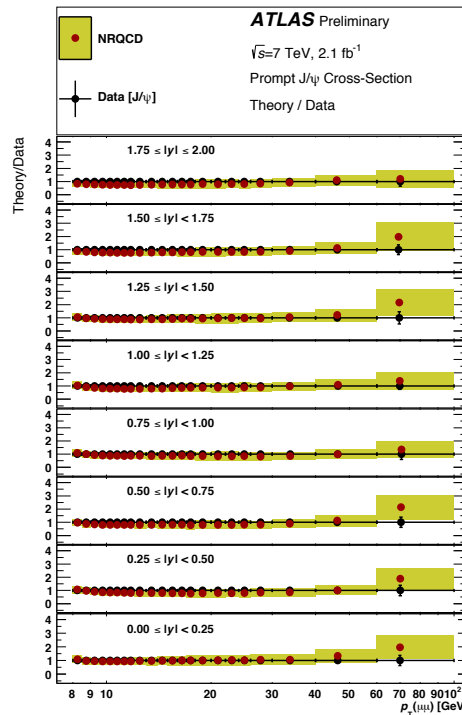


# Ratios of theoretical predictions to data

$J/\psi$  NRQCD  $\psi(2S)$

$J/\psi$  FONLL  $\psi(2S)$

7 TeV



8 TeV

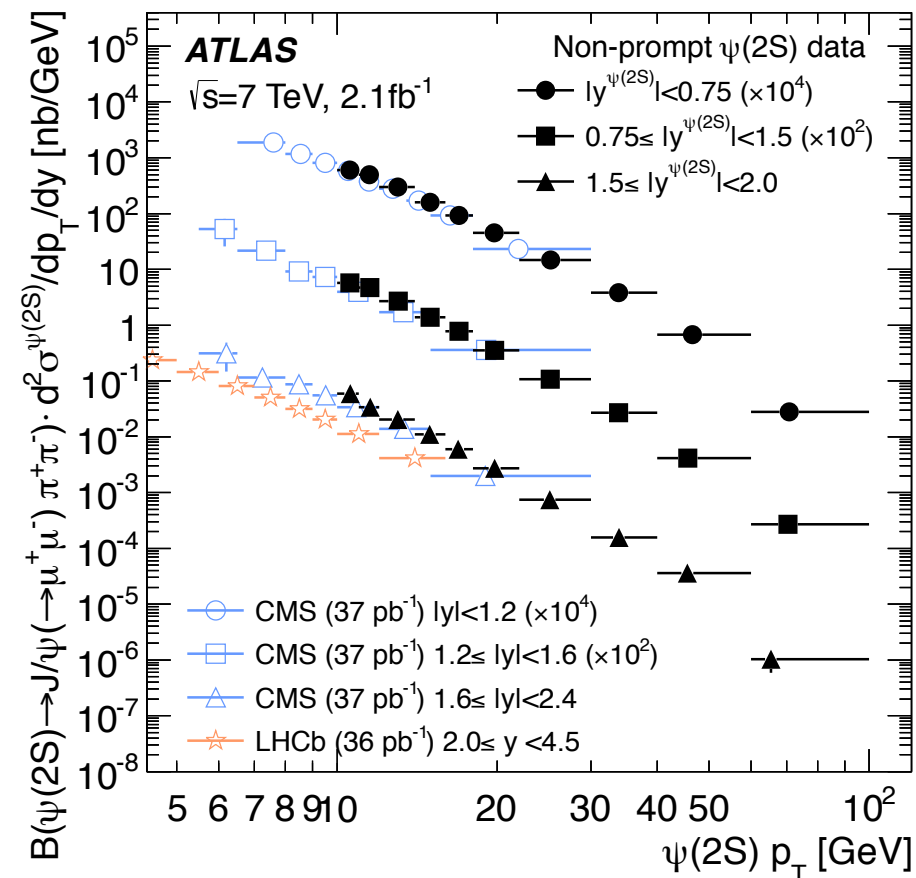
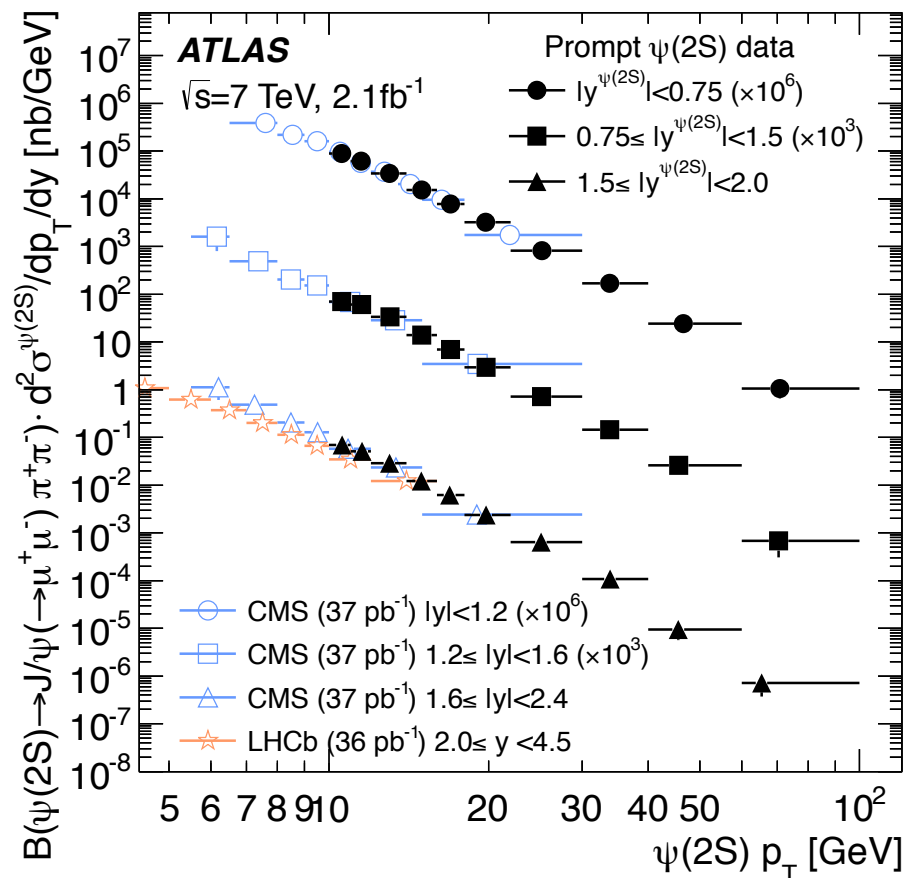
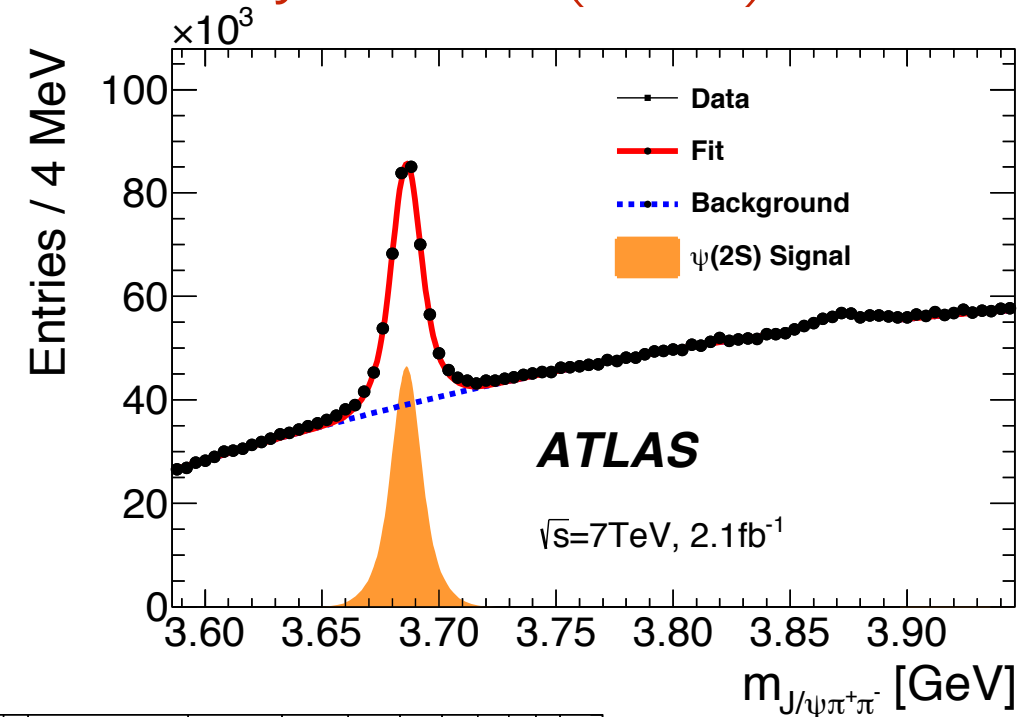
Fair agreement in the whole  $p_T$  range,  
 no ratio dependence in  $\eta$

Agreement generally good, albeit theory predicts  
 slightly harder  $p_T$  spectra for  $J/\psi$  and higher yields  
 for  $\psi(2S)$  than observed

# $\psi(2S) \rightarrow J/\psi (\rightarrow \mu^+ \mu^-) \pi^+ \pi^-$ production cross section @ 7 TeV pp

[JHEP 09 \(2014\) 079](#)

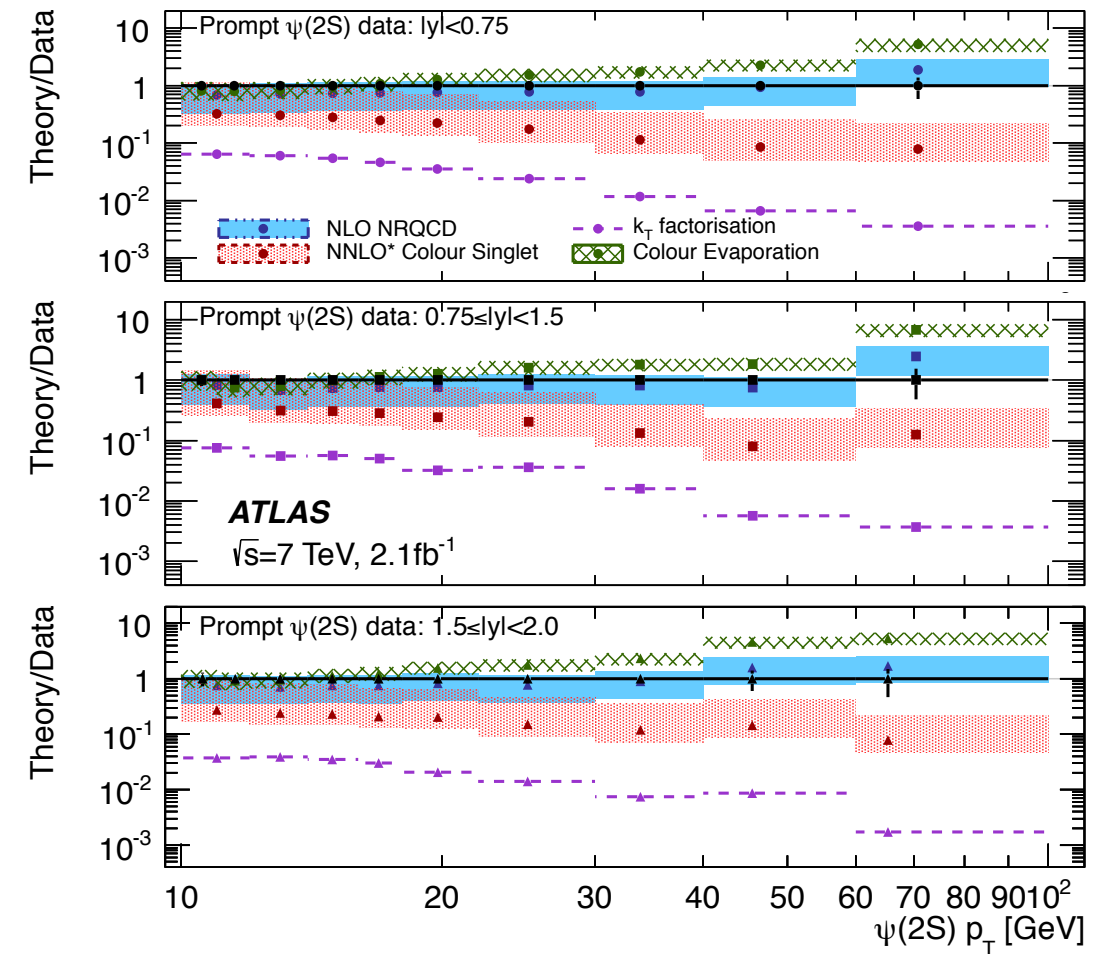
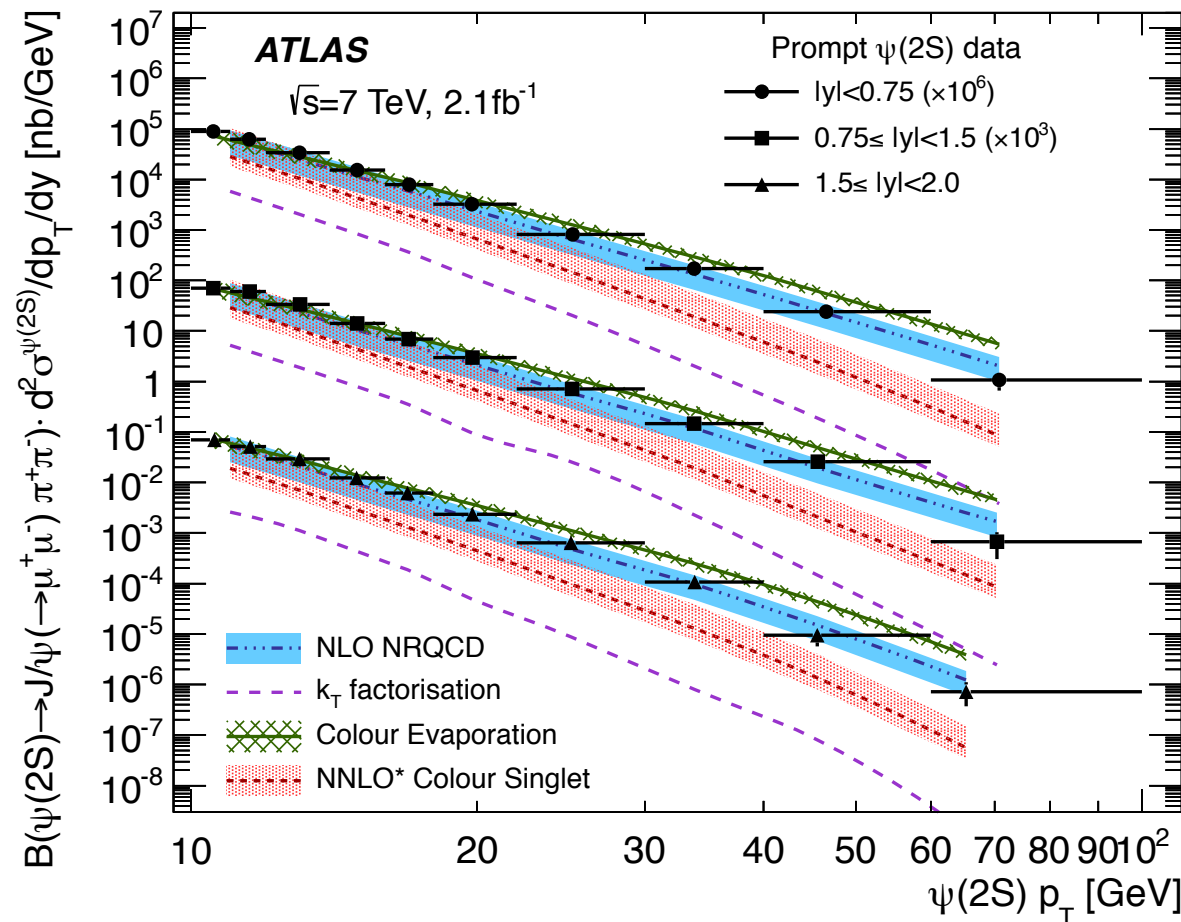
- muon  $p_T > 4$  GeV
- pion candidate tracks  $p_T > 0.5$  GeV
- unbinned mass-lifetime maximum likelihood fit to separate prompt and non prompt production components
- extend  $p_T$  range probed to 100 GeV





# Prompt $\psi(2S) \rightarrow J/\psi(\rightarrow \mu^+\mu^-)\pi^+\pi^-$ production @ 7 TeV pp

JHEP 09 (2014) 079



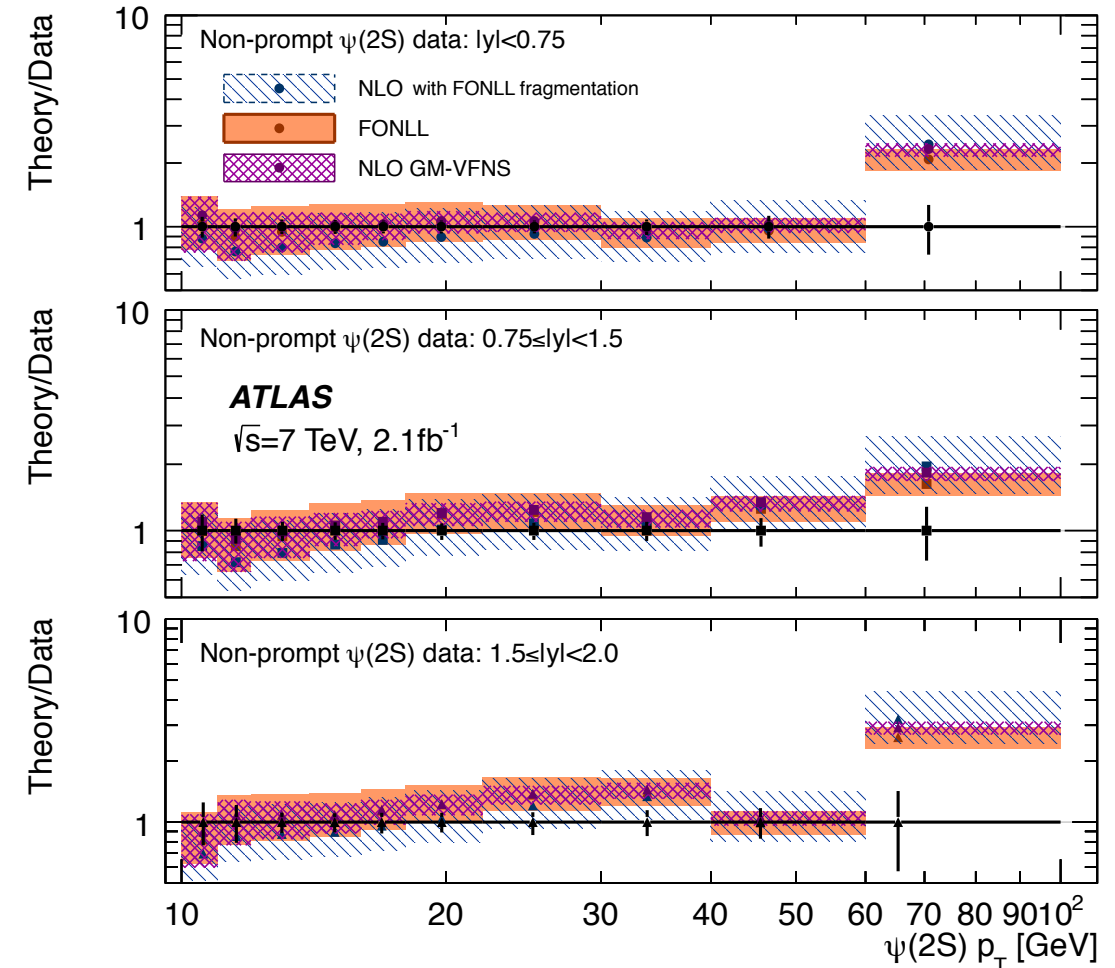
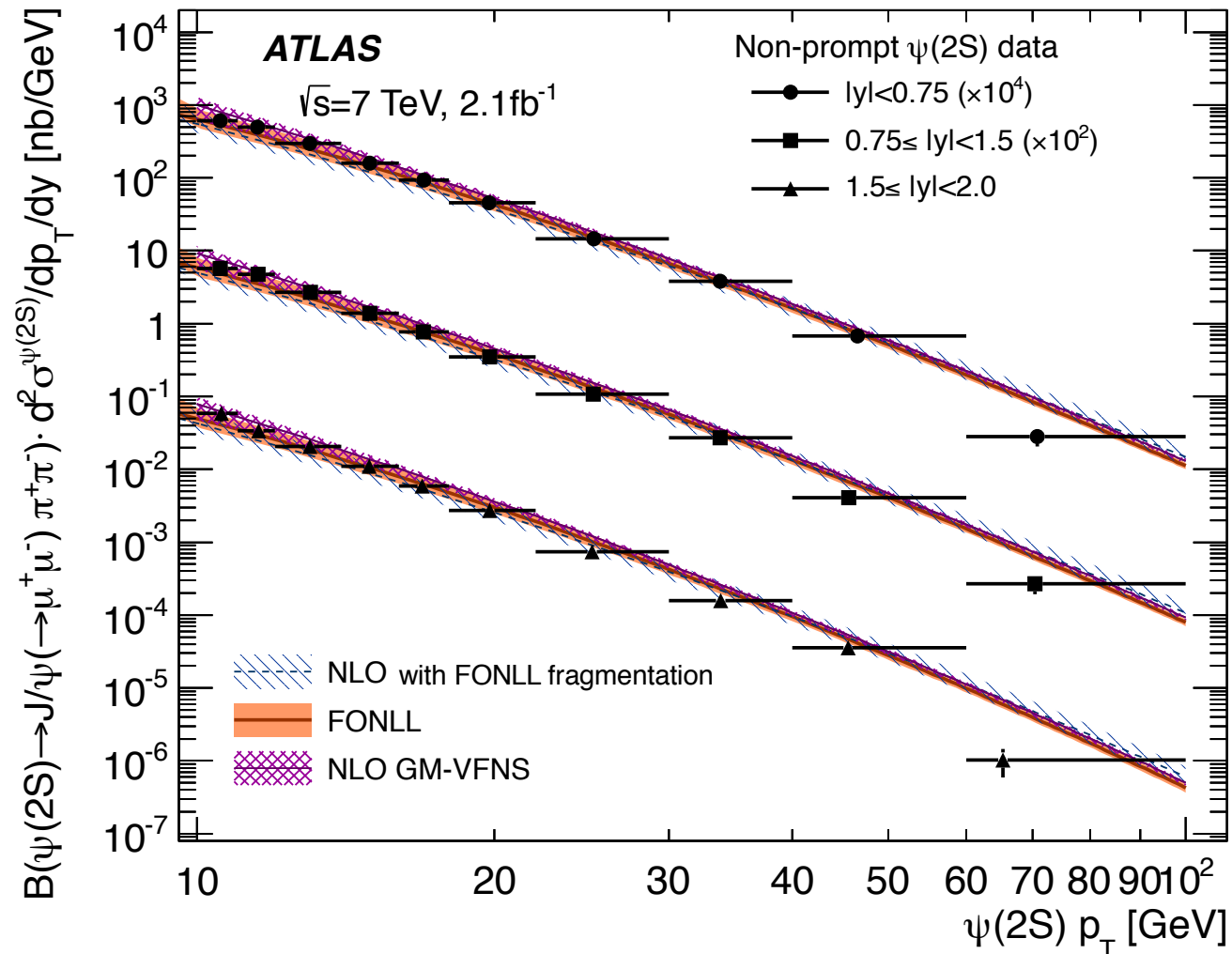
Agreement with NRQCD, overestimate at highest  $p_T$  never before explored

$k_T$ -factorisation model does not describe data well

Colour Singlet NNLO\* predictions fall short at highest scales

# Non-prompt $\psi(2S) \rightarrow J/\psi(\rightarrow \mu^+\mu^-)\pi^+\pi^-$ production @ 7 TeV pp

[JHEP 09 \(2014\) 079](#)



Good agreement with NLO and FONLL predictions at low  $p_T$ , but discrepancies observed in both at larger  $p_T$

# $\chi_c \rightarrow J/\psi(\rightarrow \mu\mu)\gamma(\rightarrow ee)$ production @ 7 TeV pp

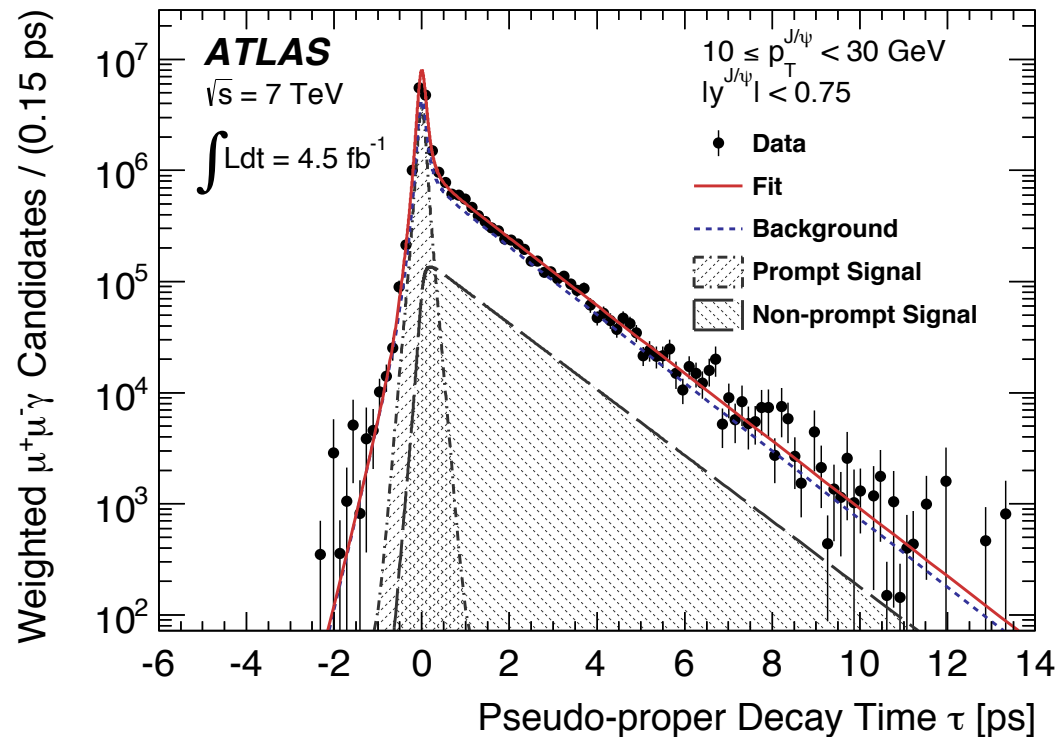
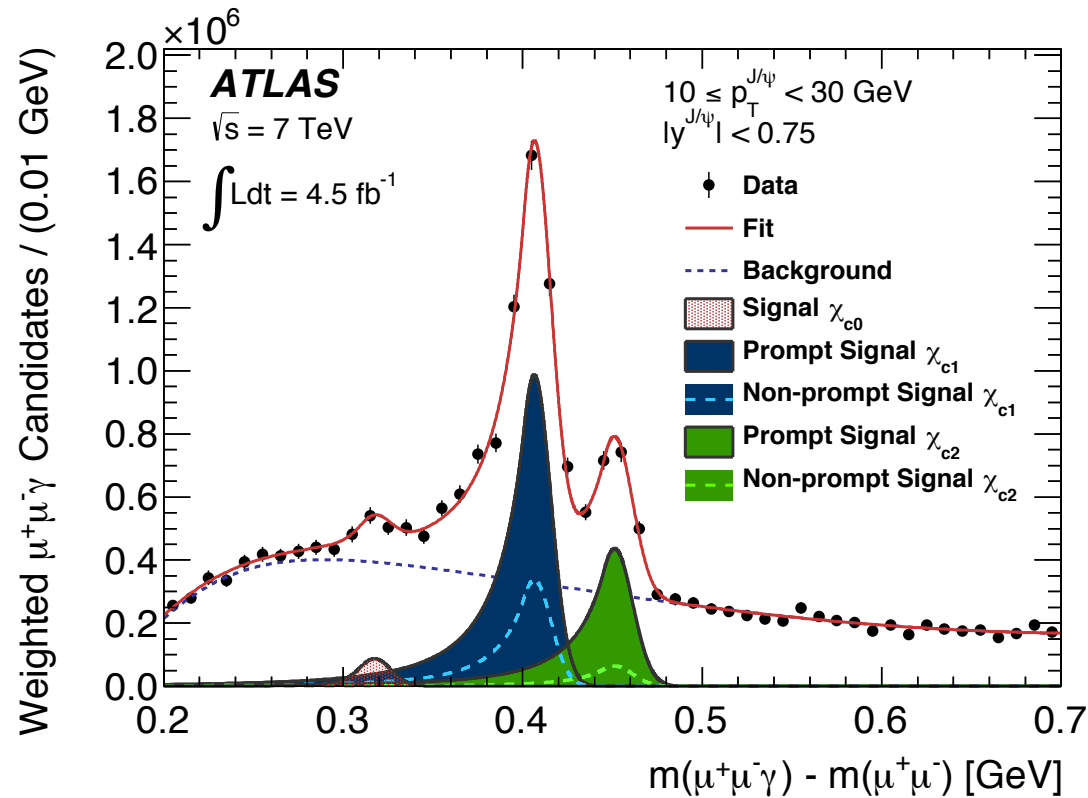
[JHEP 07 \(2014\) 154](#)

P-wave charmonium production!

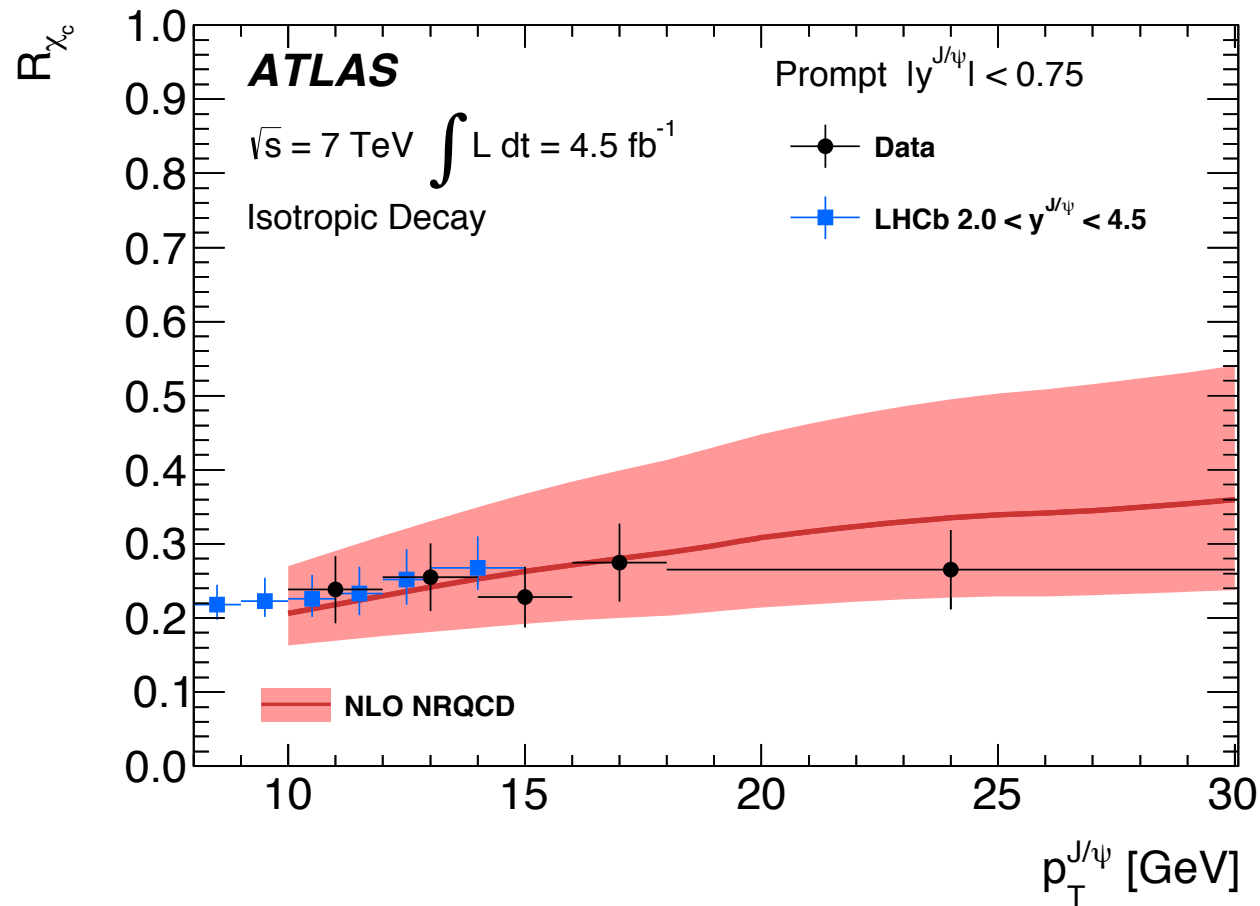
Important to understand this production channel to get a complete picture of quarkonium production.

Experimentally challenging:

- low  $p_T$  muons;
- precise reconstruction of soft ( $p_T \sim 5$  GeV) photon through conversions: low efficiencies
- unbinned maximum likelihood fit on corrected mass and lifetime
- extract the production of the  $\chi_c$  states



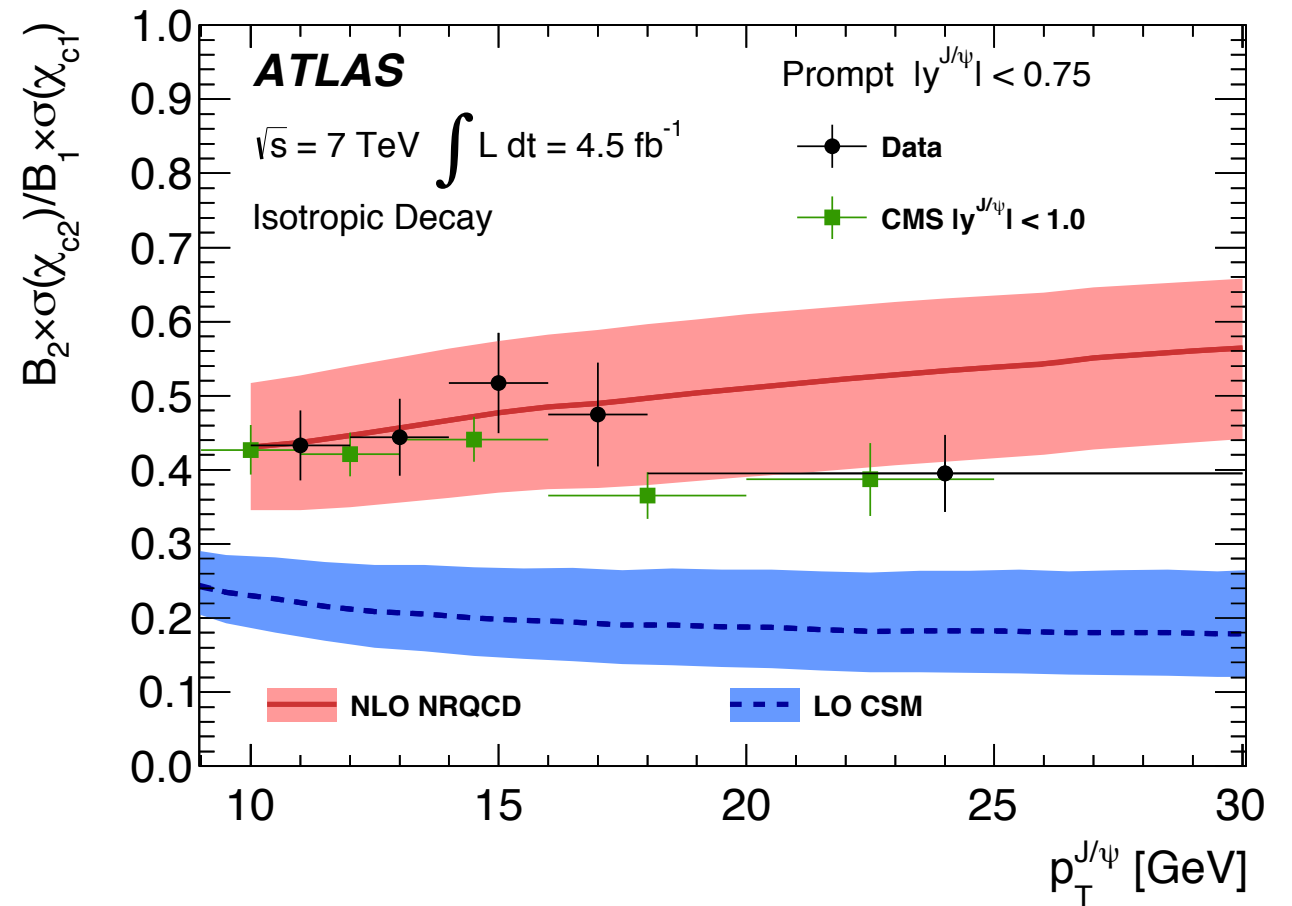
# Prompt $\chi_c \rightarrow J/\psi\gamma$ and $\sigma(\chi_{c2})/\sigma(\chi_{c1})$ ratio @ 7 TeV pp



Fraction of prompt  $J/\psi$  produced in  $\chi_c$  feed down

20-30% of prompt  $J/\psi$  are produced in  $\chi_c$  decays

[JHEP 07 \(2014\) 154](#)



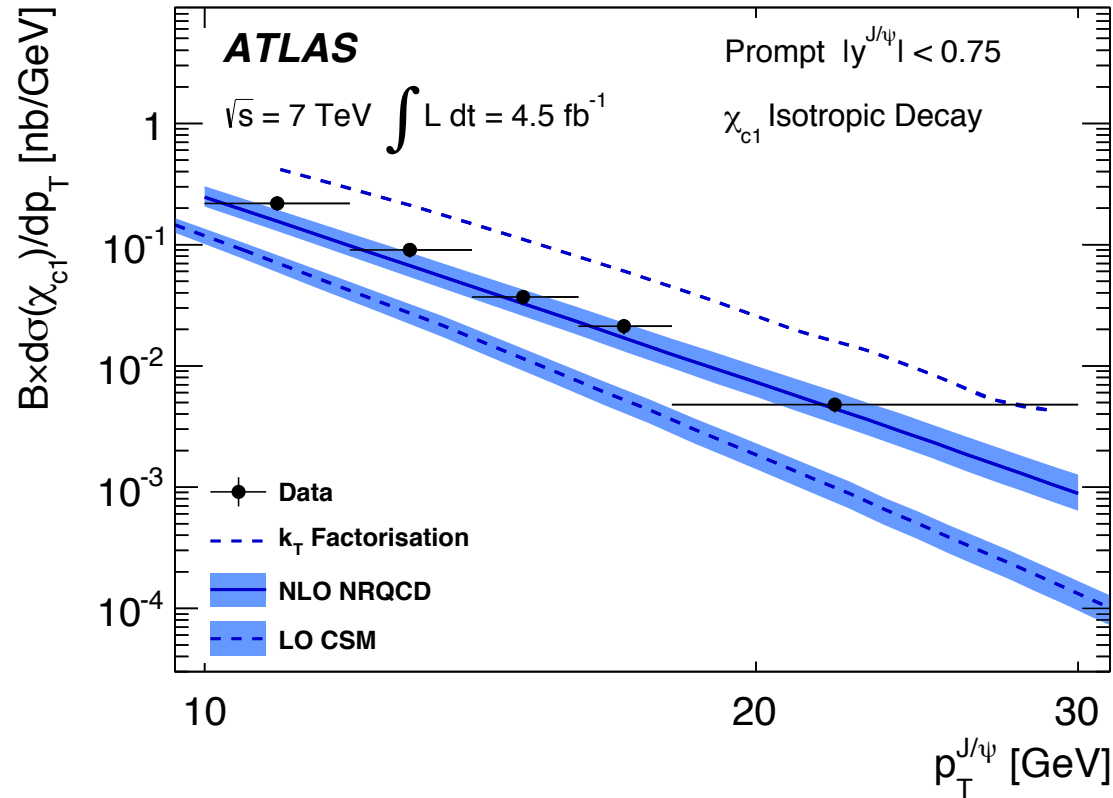
**Prompt  $\chi_c$  cross-section ratio**

more  $\chi_{c1}$  than  $\chi_{c2}$

ratio sensitive to presence of possible colour octet contributions in NRQCD

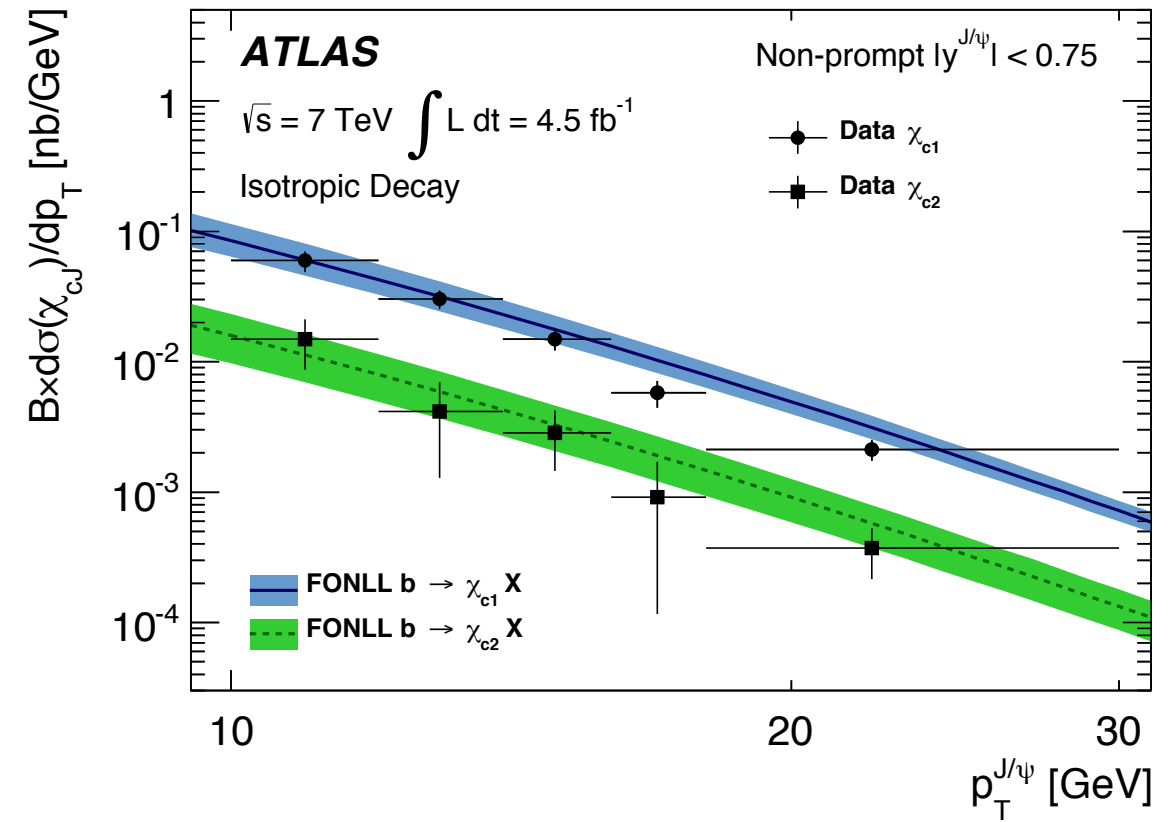
# $\chi_c$ production rates @ 7 TeV pp

## Absolute prompt $\chi_{c1}$

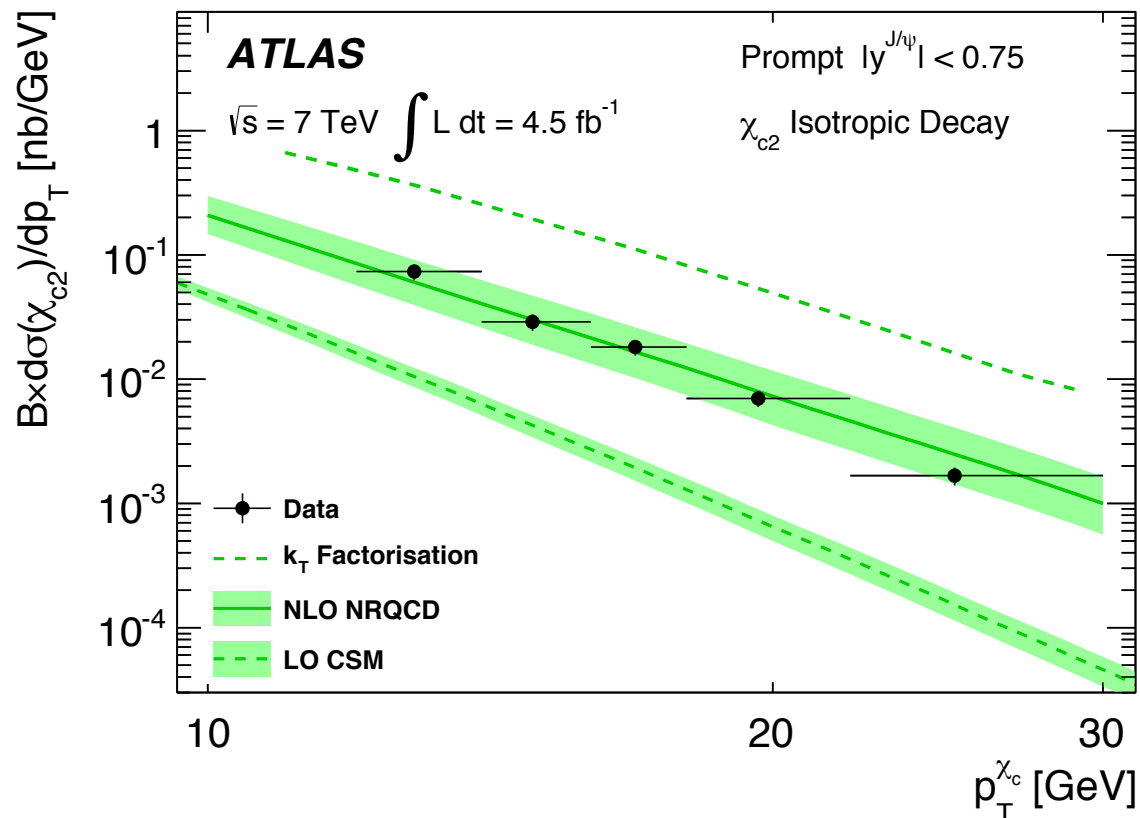


JHEP 07 (2014) 154

## Absolute non-prompt



## Absolute prompt $\chi_{c2}$



# Summary

## p+Pb @ 5.02 TeV and pp @ 2.76 TeV :

- Measured differential cross sections,  $R_{FB}$  for  $J/\psi$ ,  $R_{pPb}$  for  $J/\psi$  and  $\psi(2S)$  via pp interpolation; non-prompt component for  $J/\psi$  and  $\psi(2S)$ .
- $R_{FB}$  agrees with theoretical predictions that include shadowing effects based on EPS09.
- **Non-prompt  $J/\psi$  and  $\psi(2S)$  cross sections in pp:** good agreement with FONLL predictions.
- **$R_{pPb}$  of prompt and non-prompt  $J/\psi$ :** independent of centrality with centrality bias corrections.
- **$R_{pPb}$  of prompt and non-prompt  $J/\psi$ :** above unity showing no significant dependence on  $p_T$  and  $y^*$ .
- **$p_T$ ,  $y^*$  dependence of prompt  $\psi(2S)$   $R_{pPb}$ :** not clear, but there is an overall enhancement integrated over the whole kinematic region.
- **Prompt  $\psi(2S)$   $R_{pPb}$ :** decreasing trend from peripheral to central collisions, confirmed by the  $\psi(2S)$  to Z ratio.
- **Prompt  $\psi(2S)$  to  $J/\psi$  double ratio:** no obvious rapidity dependence, but decreases with increasing event activity.

## Pb+Pb @ 2.76 TeV:

- **Muons  $R_{CP}$ :** factor of  $\sim 2.5$  suppression in the yield for most central compared to most peripheral collisions.
- **Normalized  $J/\psi$  yield:** centrality dependent suppression.

## pp @ 7 and 8 TeV:

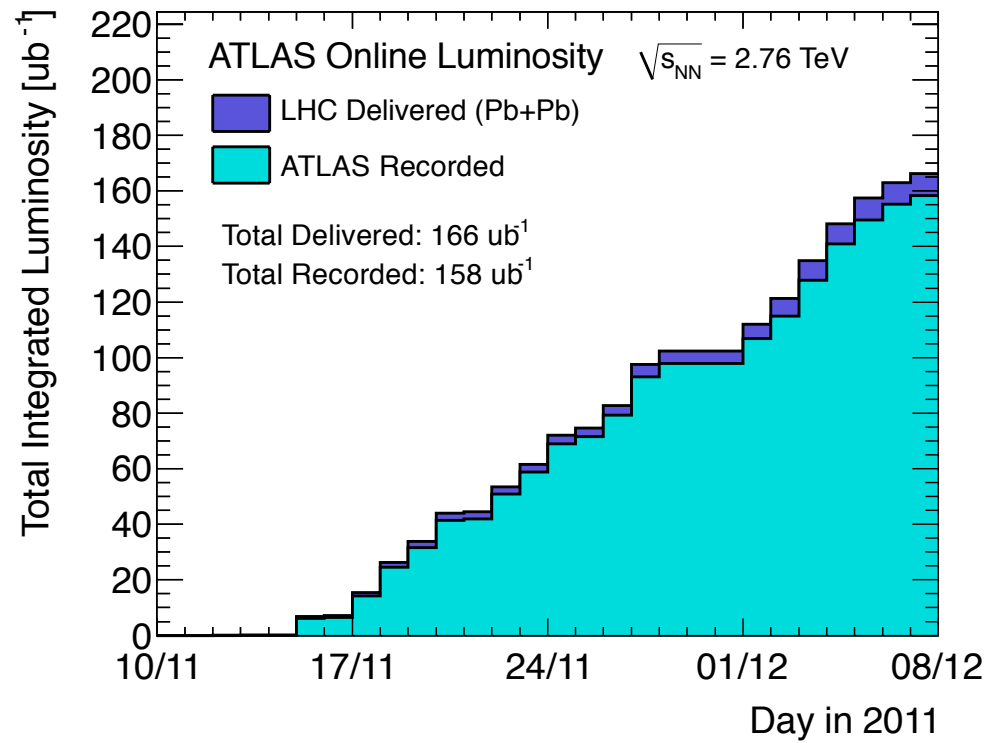
- $J/\psi$ ,  $\psi(2S)$  brand new differential cross-sections of prompt and non-prompt production:  $8 < |y| \leq 110$  GeV,  $|y| < 2.0$ .
  - **Prompt production and NRQCD predictions (including colour-octet contributions with various matrix elements tuned to earlier collider data):** good agreement.
  - **Non prompt production and FNOLL predictions:** reasonable agreement across  $p_T$  and  $y$ .
- **$\psi(2S)$  (S-wave) and  $\chi_c$  (P-wave):** study production just below the open charm threshold to undertake feed-down uncertainties.

Additional slides

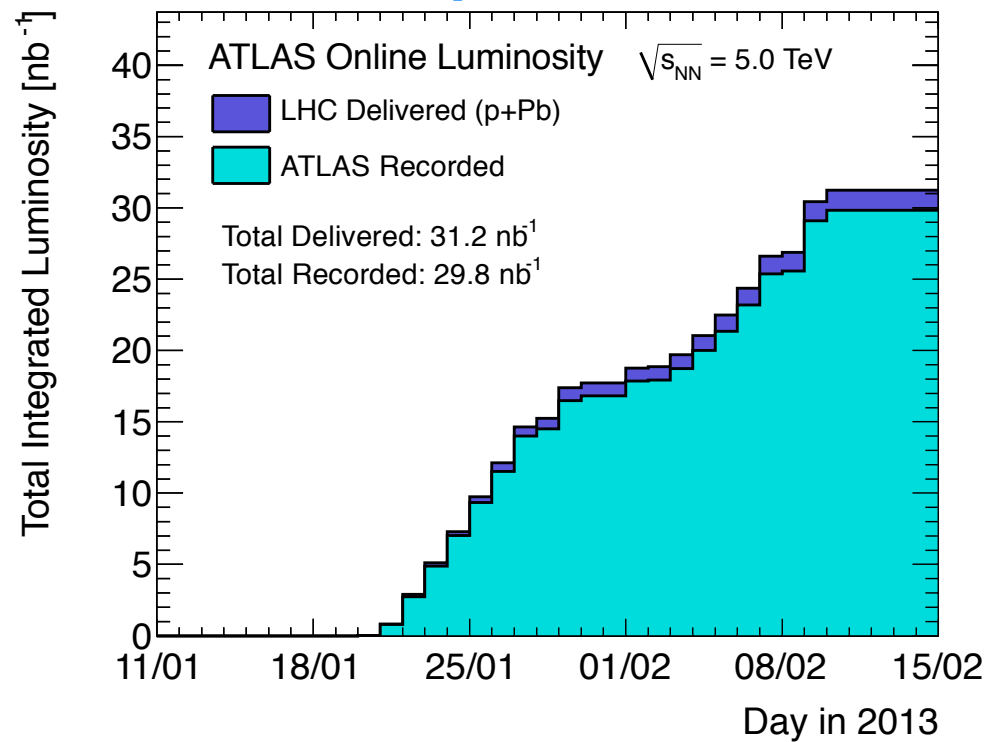


# Extraordinary Run I!!!

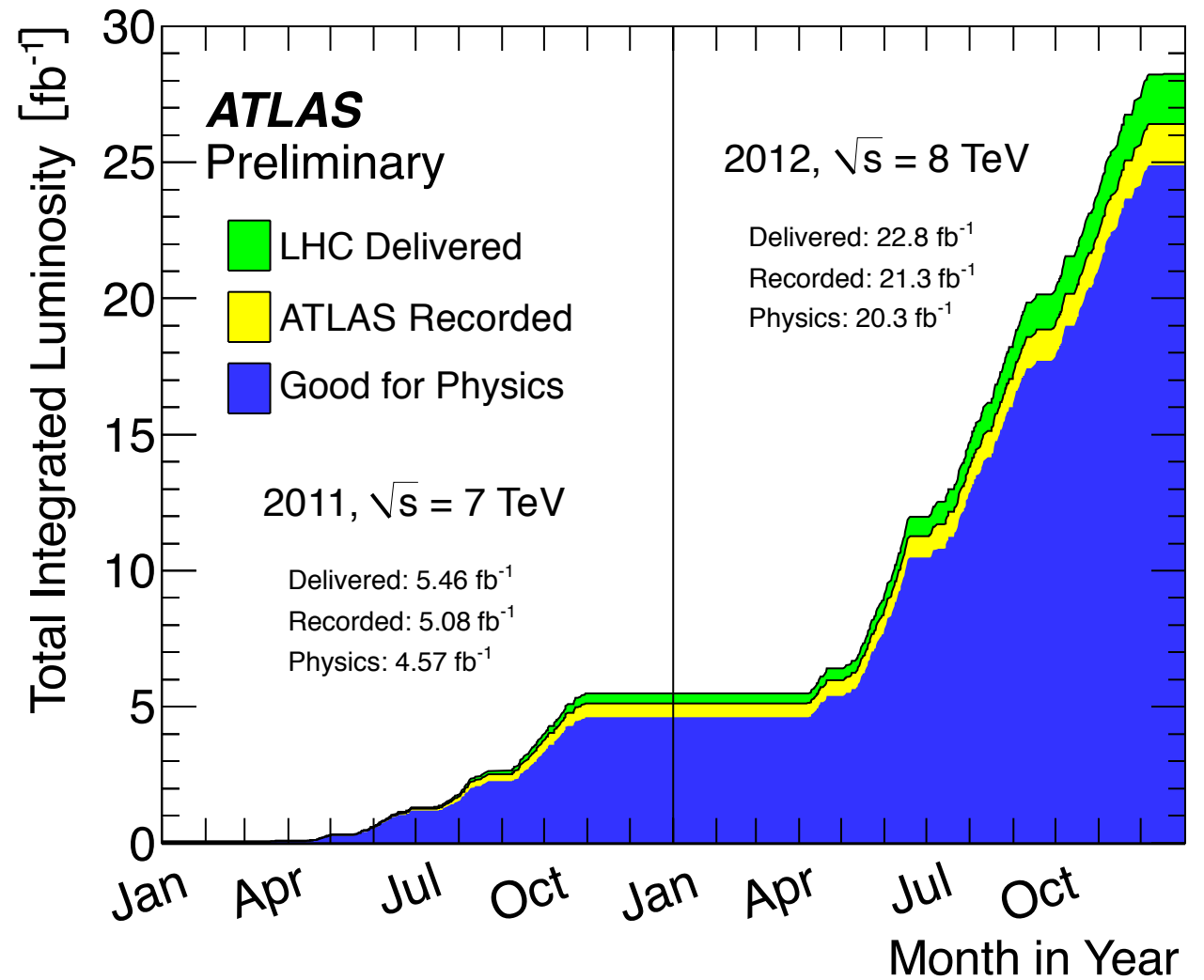
Pb+Pb



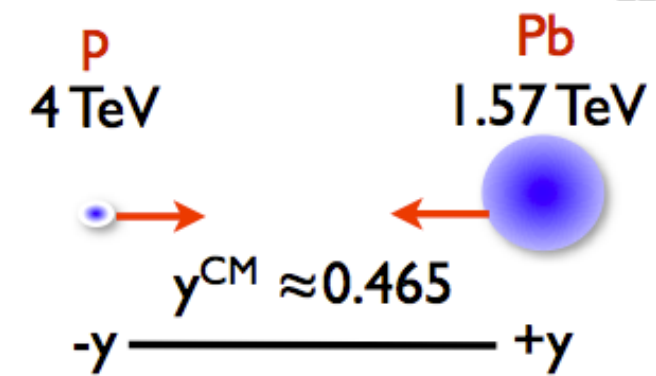
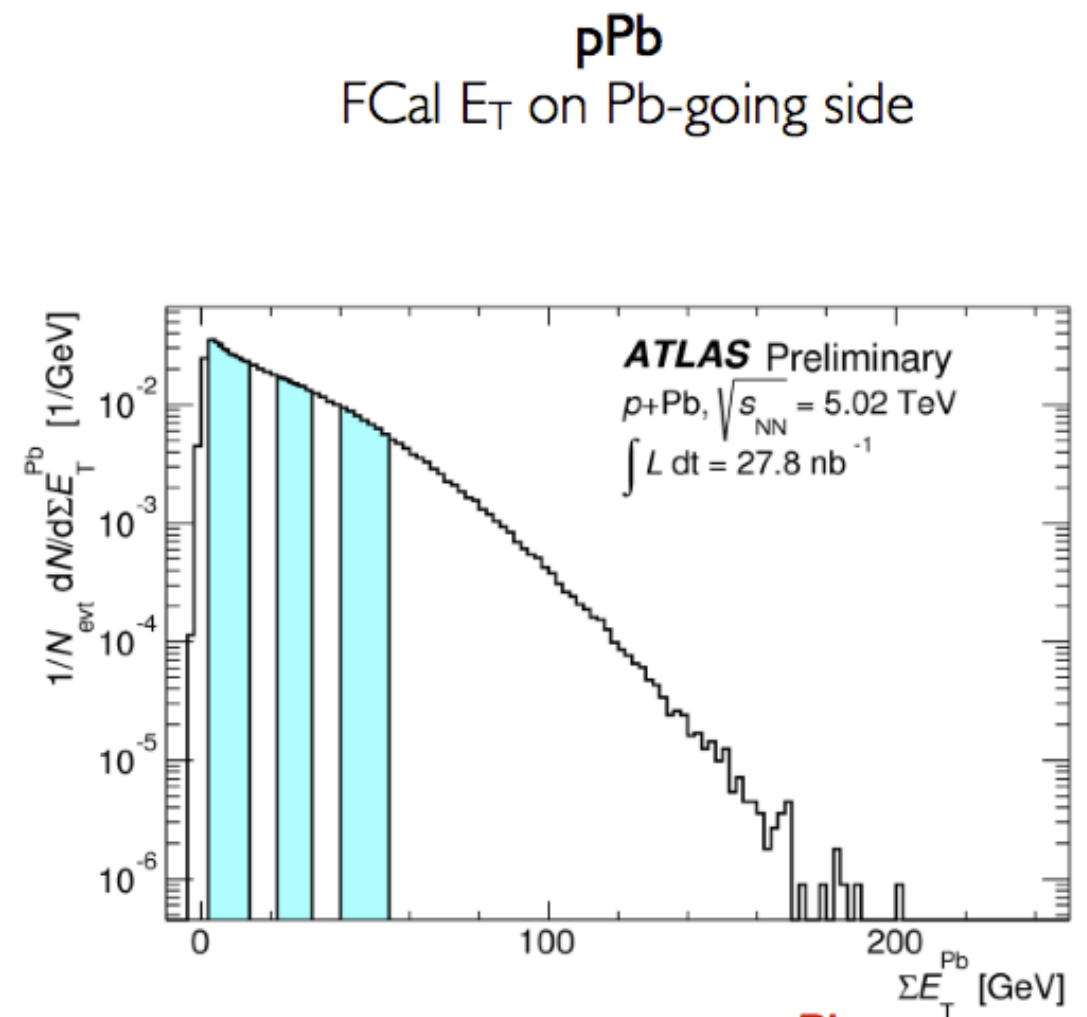
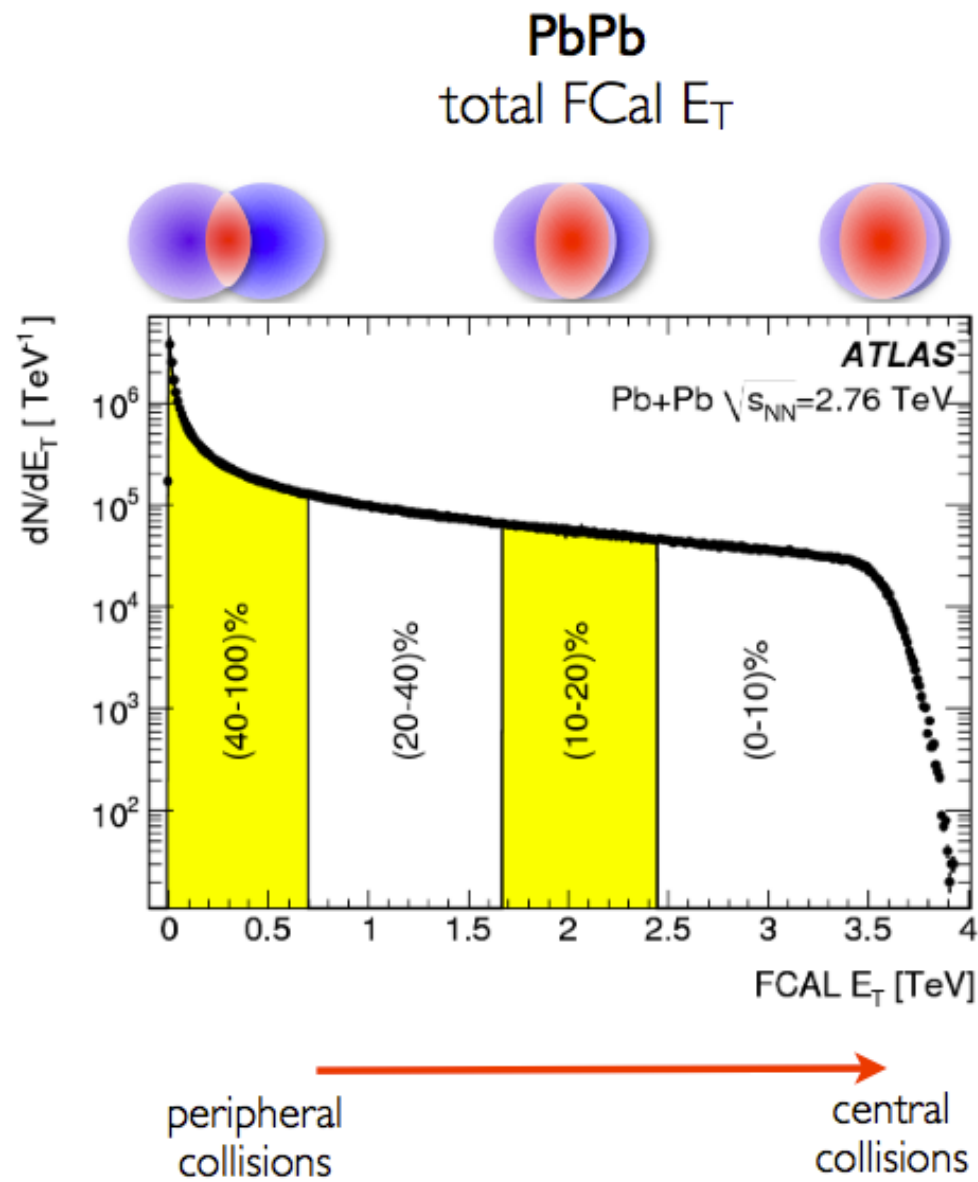
p+Pb



pp



# Centrality



# Interpolation of pp data

$$\sigma(\sqrt{s}) = \begin{cases} p_0 + \sqrt{s}p_1 & \text{linear} \\ (\sqrt{s}/p_0)^{p_1} & \text{power law} \\ p_0(1 - \exp(-\sqrt{s}/p_1)) & \text{exponential} \end{cases}$$

Interpolation between pp data @ 2.76 TeV with 7 and 8 TeV

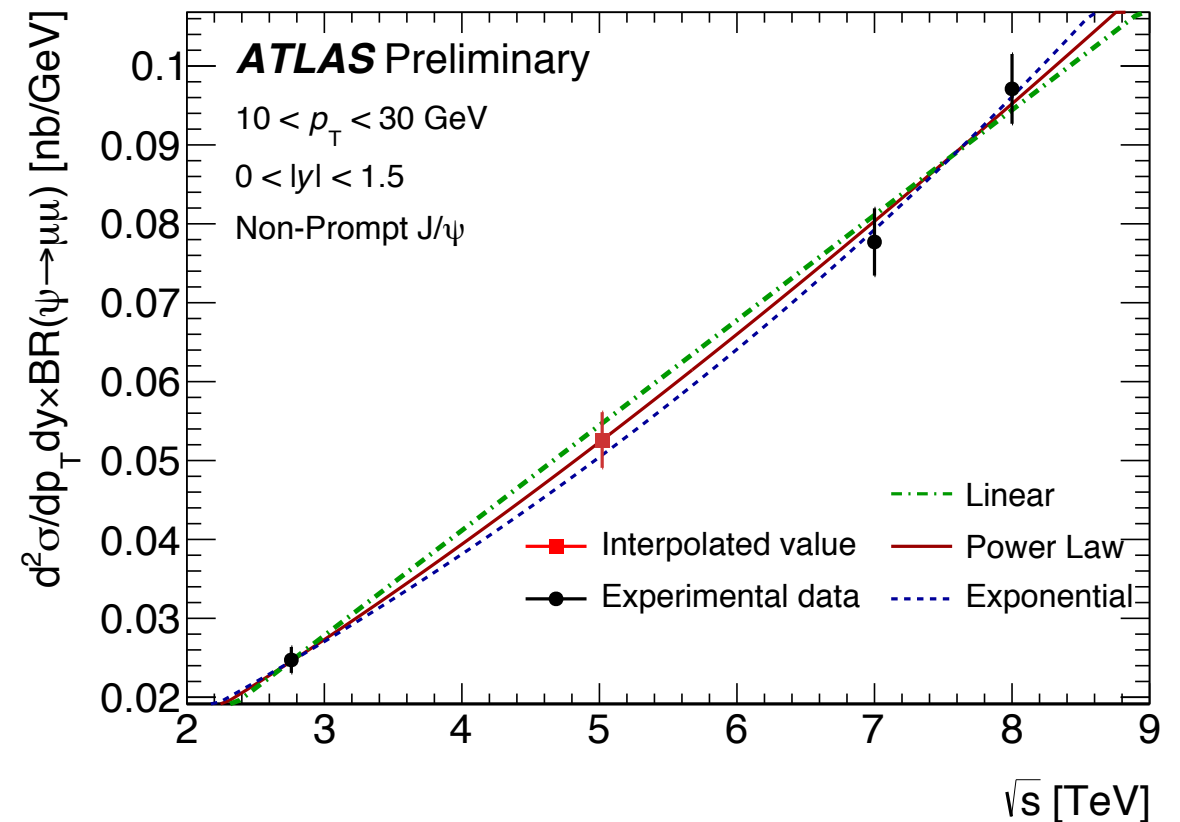
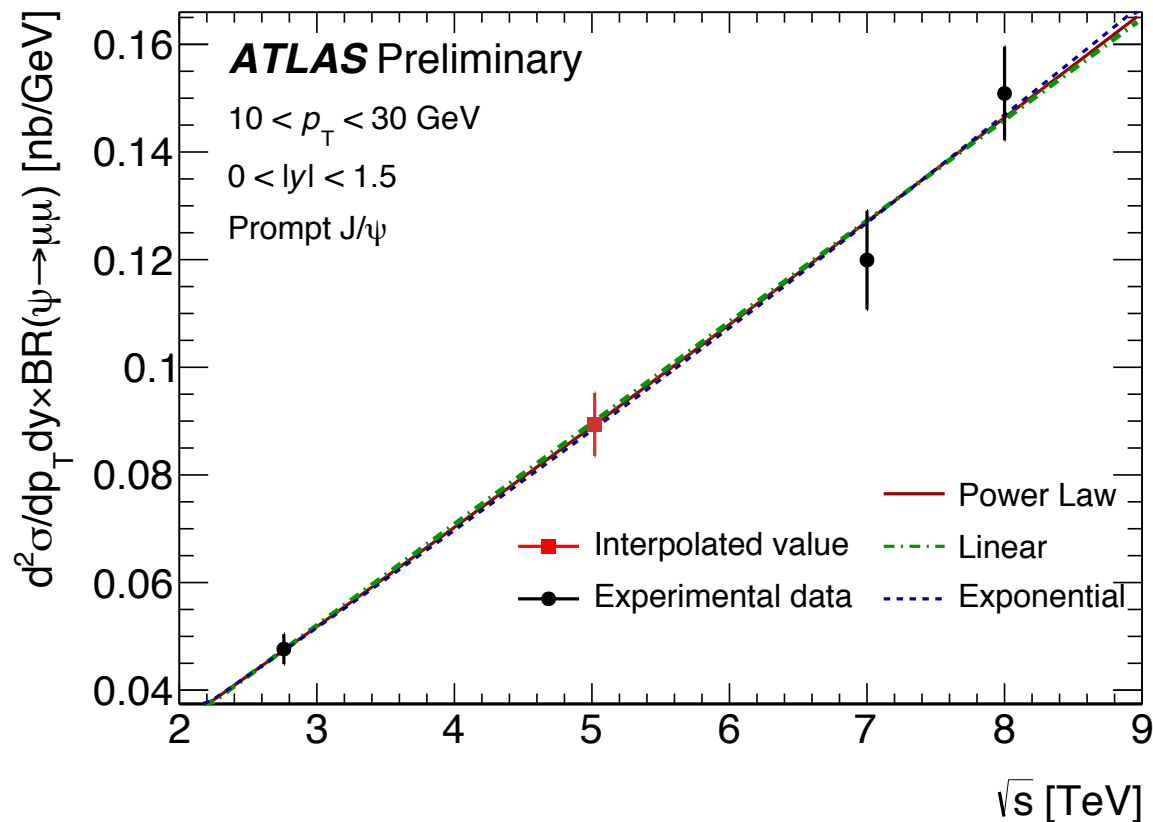
8.5-10 GeV in pT, only 2.76 and 7 TeV

10-30 GeV in pT: 2.76, 7 and 8 TeV

[ATLAS-CONF-2015-023](#)

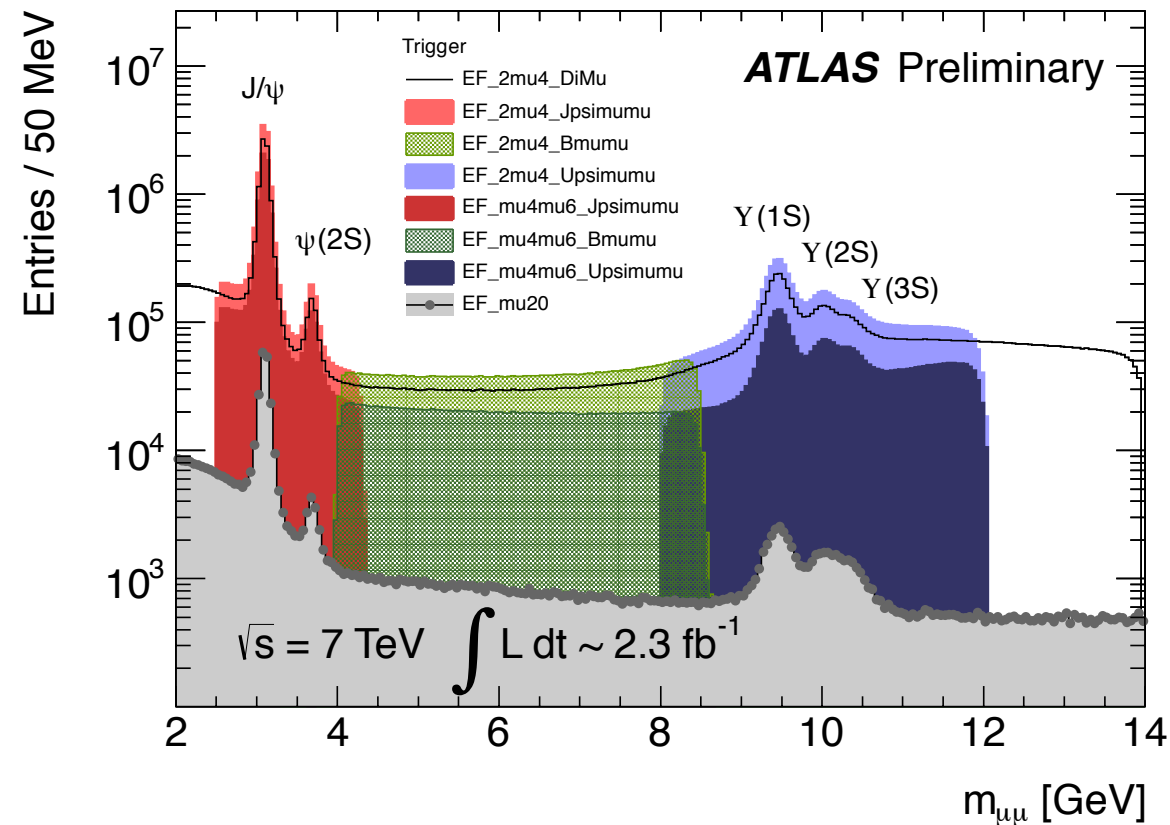
prompt J/ψ

non-prompt J/ψ



# Quarkonium/Heavy Flavour trigger @ 7 and 8 TeV pp

Mainly based on dimuon signatures with some analyses using single-muon triggers



## Level-1:

HW based, fast muon detectors, coarse resolution "region-of-interest" (RoI), dimuons with  $p_T > 4$  GeV

## Level- 2 / Event Filter (EF):

SW based, precise confirmation of the muons with Inner Detector track reconstruction, dimuon vertex construction (inv. mass cut)

# Cross section evaluation for quarkonium analyses @ 7 and 8 TeV pp

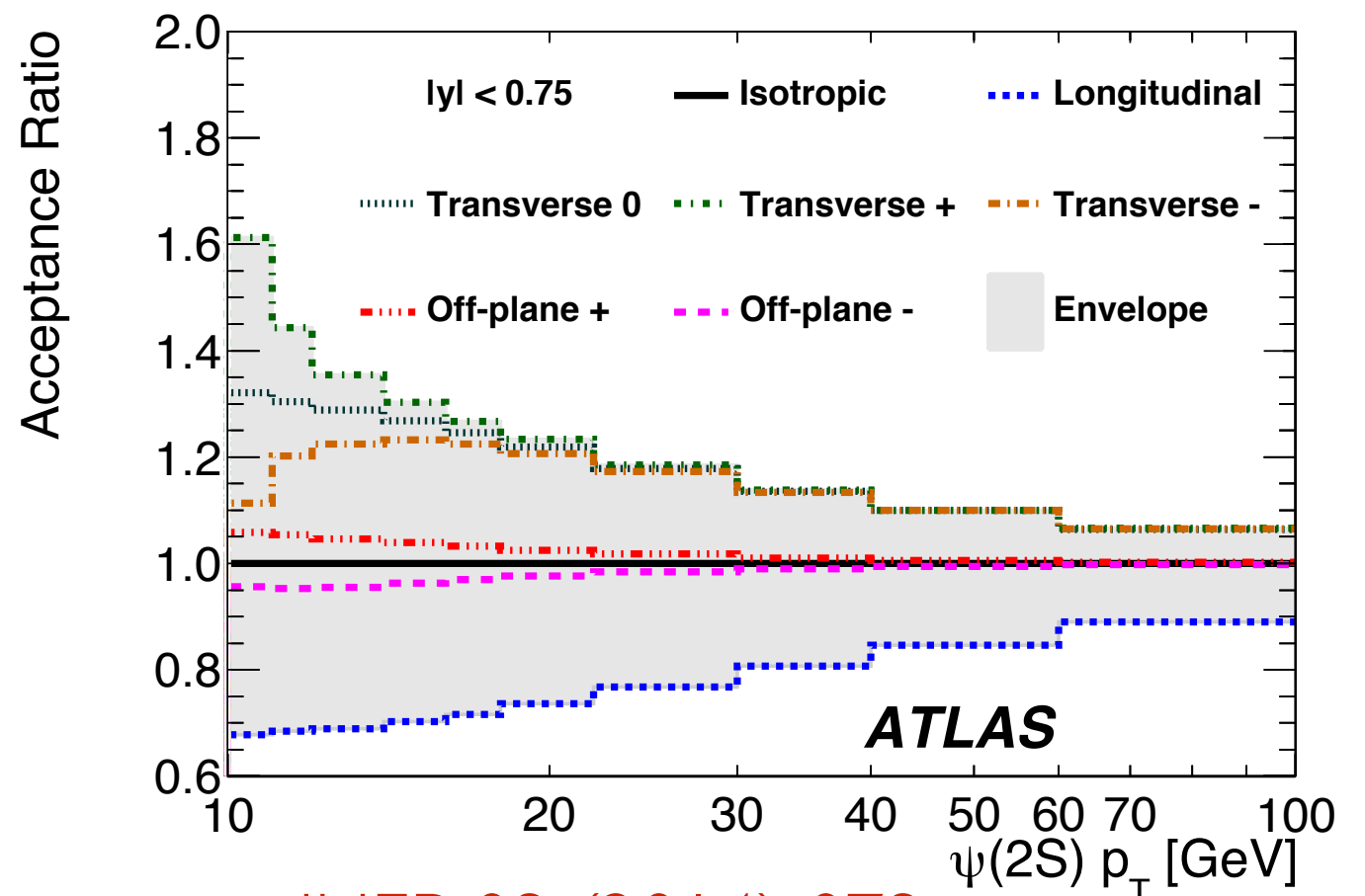
For each channel  $Q \rightarrow \text{final}$ :

$$\frac{d^2\sigma_Q}{dp_T dy} \cdot BR(Q \rightarrow \text{final}) = \frac{N_{corr}^{Q \rightarrow \text{final}}}{\mathcal{L} \cdot \Delta p_T \cdot \Delta y},$$

- extraction of the signals is obtained with unbinned maximum likelihood methods;
- efficiency corrections for tracking, reconstruction and triggering are obtained with data driven methods (e.g., tag and probe for the trigger);
- acceptance corrections, to recover the visible phase space in  $p_T$  and  $y$  for comparison with QCD predictions, are obtained with simulation;

- they depend on the unknown polarization status of  $Q$  (spin alignment);
- the correction is evaluated for the isotropic case and an envelope of variations is computed for the various polarizations. Example:

$\Psi(2S) \rightarrow J/\psi \pi\pi\pi$

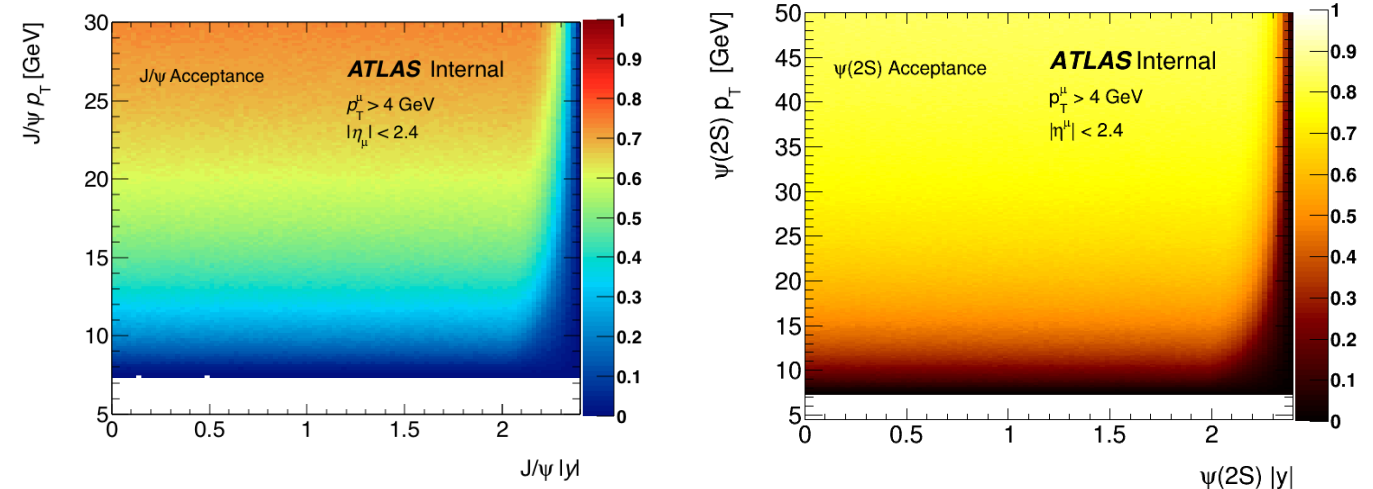


[JHEP 09 \(2014\) 079](#)

# Charmonia analyses @ 5.02 TeV p+Pb and @ 2.76 TeV pp

- muon candidates:
  - combination of charged-particle tracks reconstructed in the ID and MS

- acceptance



- muon pairs:
  - opposite sign charges and originating from a common vertex
  - prompt and non-prompt processes distinguished by “pseudo-proper time”

- trigger efficiency:

$$\epsilon_{\text{trigger}} = \epsilon_{\text{L1}} \cdot \epsilon_{\text{EF}}$$

$$\epsilon_{\text{L1}} = 1 - [1 - \epsilon_{\text{L1}}^\mu(p_{\text{T1}}^\mu, q_1^\mu \cdot \eta_1^\mu)] \cdot [1 - \epsilon_{\text{L1}}^\mu(p_{\text{T2}}^\mu, q_2^\mu \cdot \eta_2^\mu)]$$

$$\epsilon_{\text{EF}} = \epsilon_{\text{EF}}^\mu(p_{\text{T1}}^\mu, q_1^\mu \cdot \eta_1^\mu) \cdot \epsilon_{\text{EF}}^\mu(p_{\text{T2}}^\mu, q_2^\mu \cdot \eta_2^\mu)$$

- weight applied:

$$w_{\text{total}}^{-1} = A \cdot \epsilon_{\text{reco}} \cdot \epsilon_{\text{trig}}$$

- unbinned mass-lifetime maximum likelihood fit to separate prompt and non prompt production components



# Charmonia analyses @ 5.02 TeV p+Pb

Elements in common:

- Same pPb data sample, same triggers, secondary dimuon vertex refitting
- Same muon selection criteria and reconstruction efficiency corrections
- Same version of  $J/\psi$  acceptance map

Elements that are different:

- Included  $\psi(2S)$  in fit model; fit model was kept as similar as possible to 7 and 8 TeV analyses to reduce interpolation uncertainties
- Included 2.76 TeV pp data for calculation of  $R_{pPb}$
- Updated efficiency map from 8 TeV pp was used for LI trigger correction
- Finer-binned Event Filter efficiency map was used
- Centrality dependence was studied using several centrality estimators

# Open heavy flavour in Pb+Pb

## Muon signal extraction

1) Separate muons (heavy flavour decays) from **pion** and **kaon** decays

2) Momentum balance

$$\frac{\Delta p_{\text{loss}}}{p_{\text{ID}}} = \frac{p_{\text{ID}} - p_{\text{MS}} - \Delta p_{\text{calo}}(p, \eta, \phi)}{p_{\text{ID}}}$$

Muon Spectrometer  
Inner Detector  
momentum and  
angle-dependent  
average energy loss  
of muons in the  
calorimeter (from  
MC simulations)

3) Scattering angle significance:

$$S(k) = \frac{1}{\sqrt{n}} \left( \sum_{i=1}^k s_i - \sum_{j=k+1}^n s_j \right)$$

deflections in the trajectory resulting from decays in flight

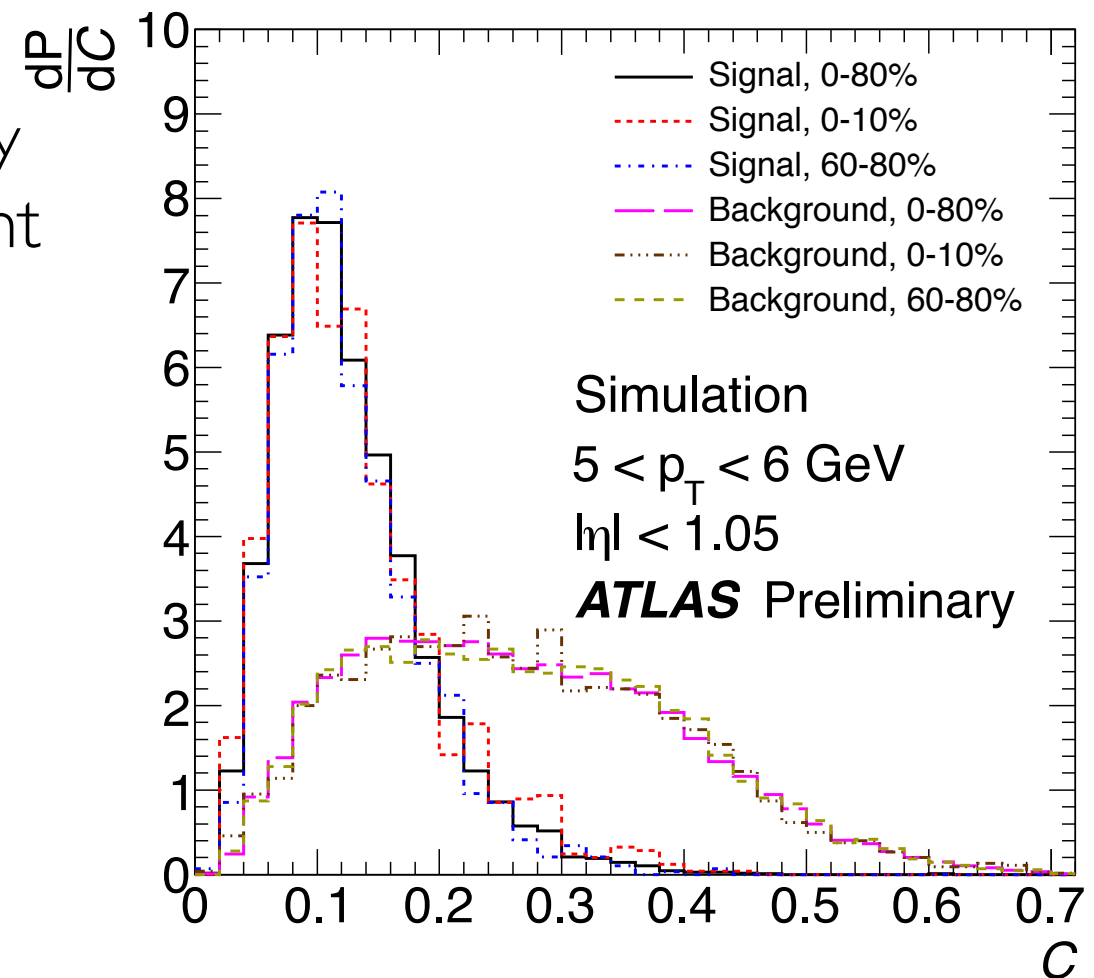
4) Take the maximum:

$$S = \max \{|S(k)|, k = 1, 2, \dots\}$$

C Distributions  
PYTHIA+HIJING

5) Composite discriminant ( $r = 0.07$ ):

$$C = \left| \frac{\Delta p_{\text{loss}}}{p_{\text{ID}}} \right| + rS$$

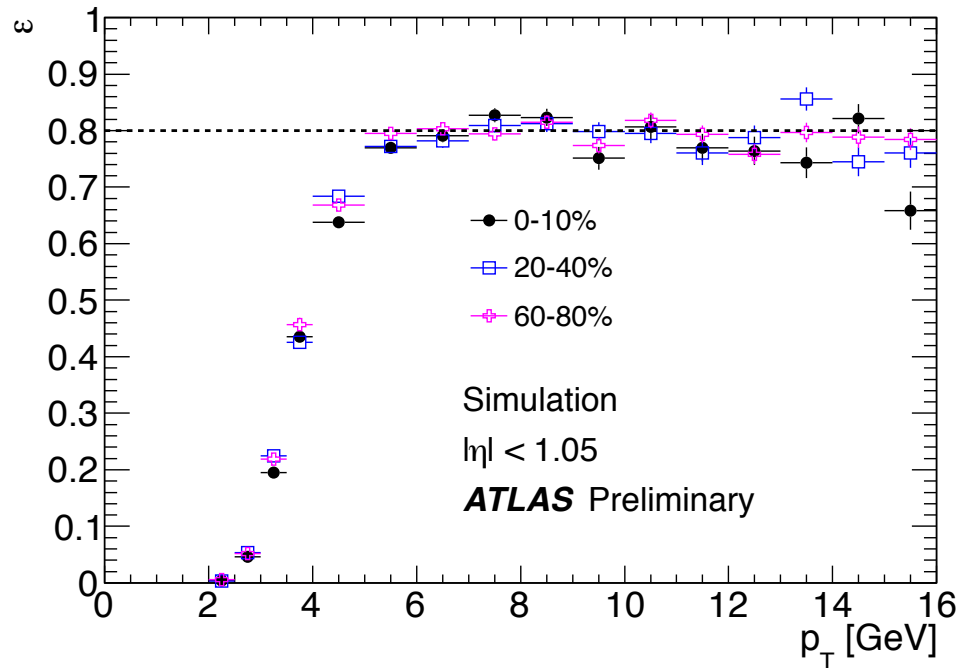


[ATLAS-CONF-2012-050](#)

# Open heavy flavour in Pb+Pb @ 2.76 TeV

Signal extracted from a template fit

Efficiency for reconstructing muons associated with HF decays



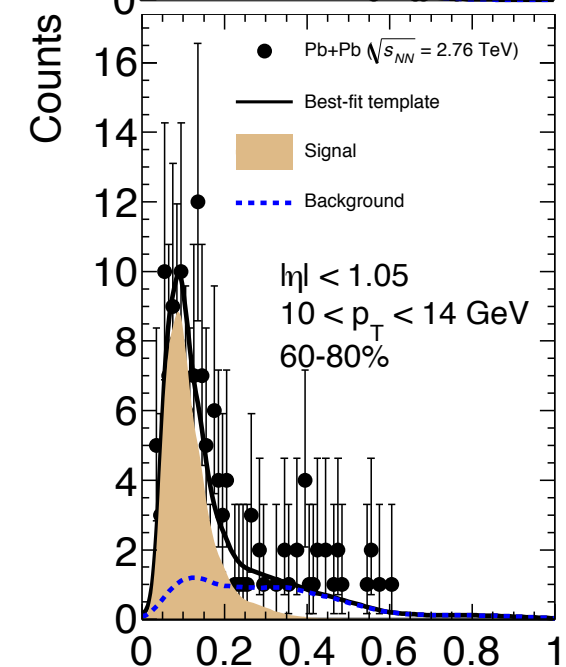
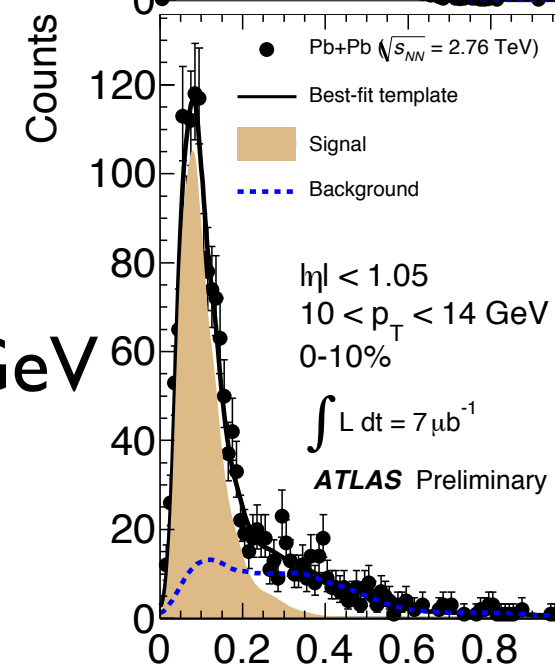
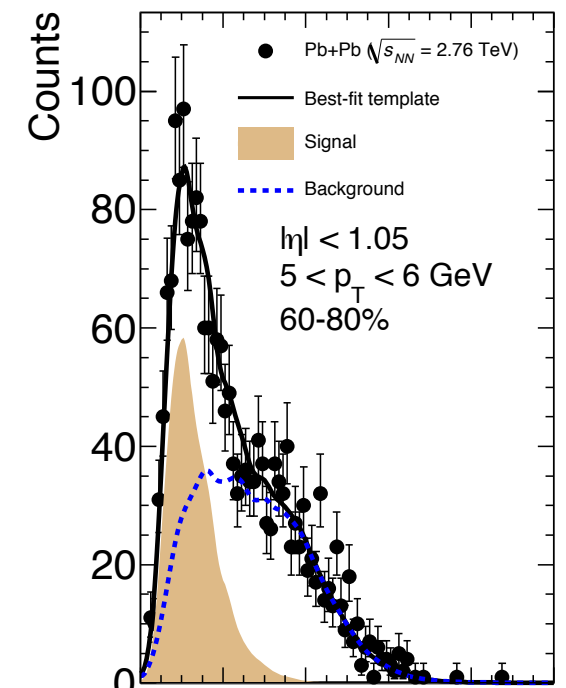
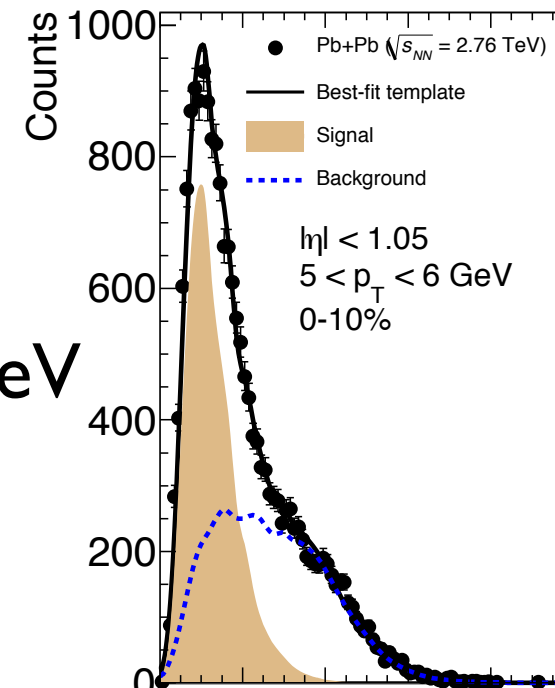
$5 < p_T < 6 \text{ GeV}$

$10 < p_T < 14 \text{ GeV}$

[ATLAS-CONF-2012-050](#)

0-10%

60-80%

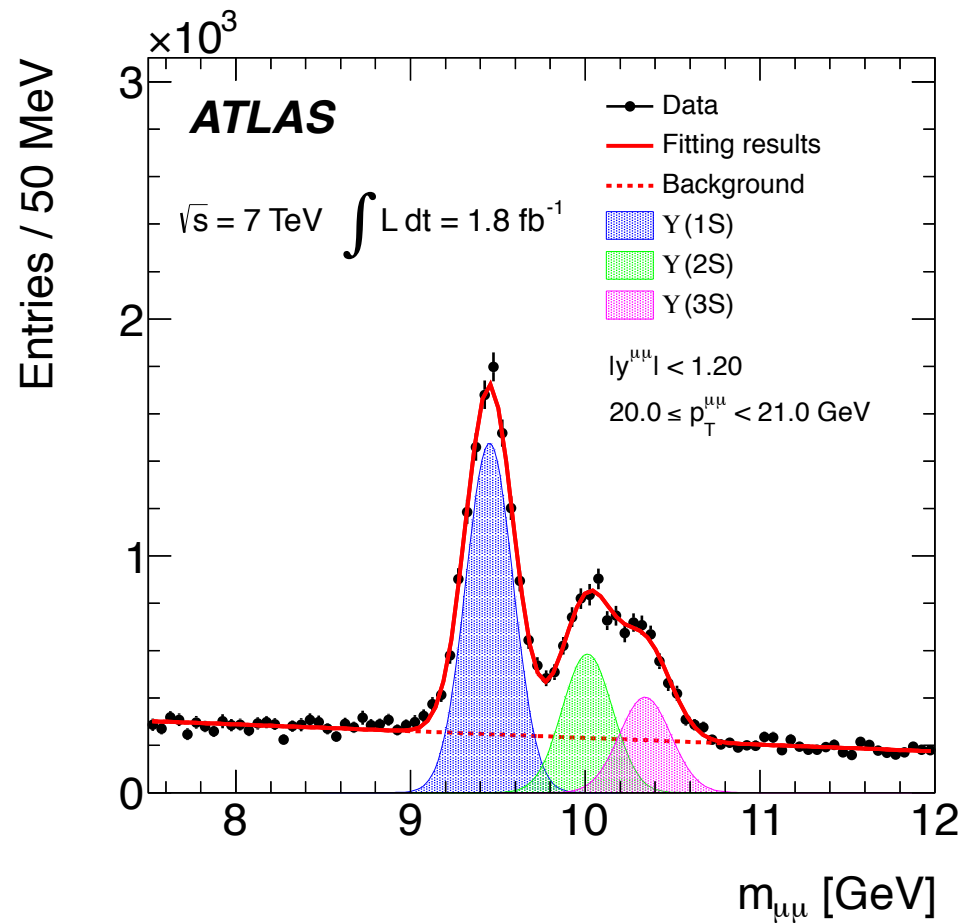


C

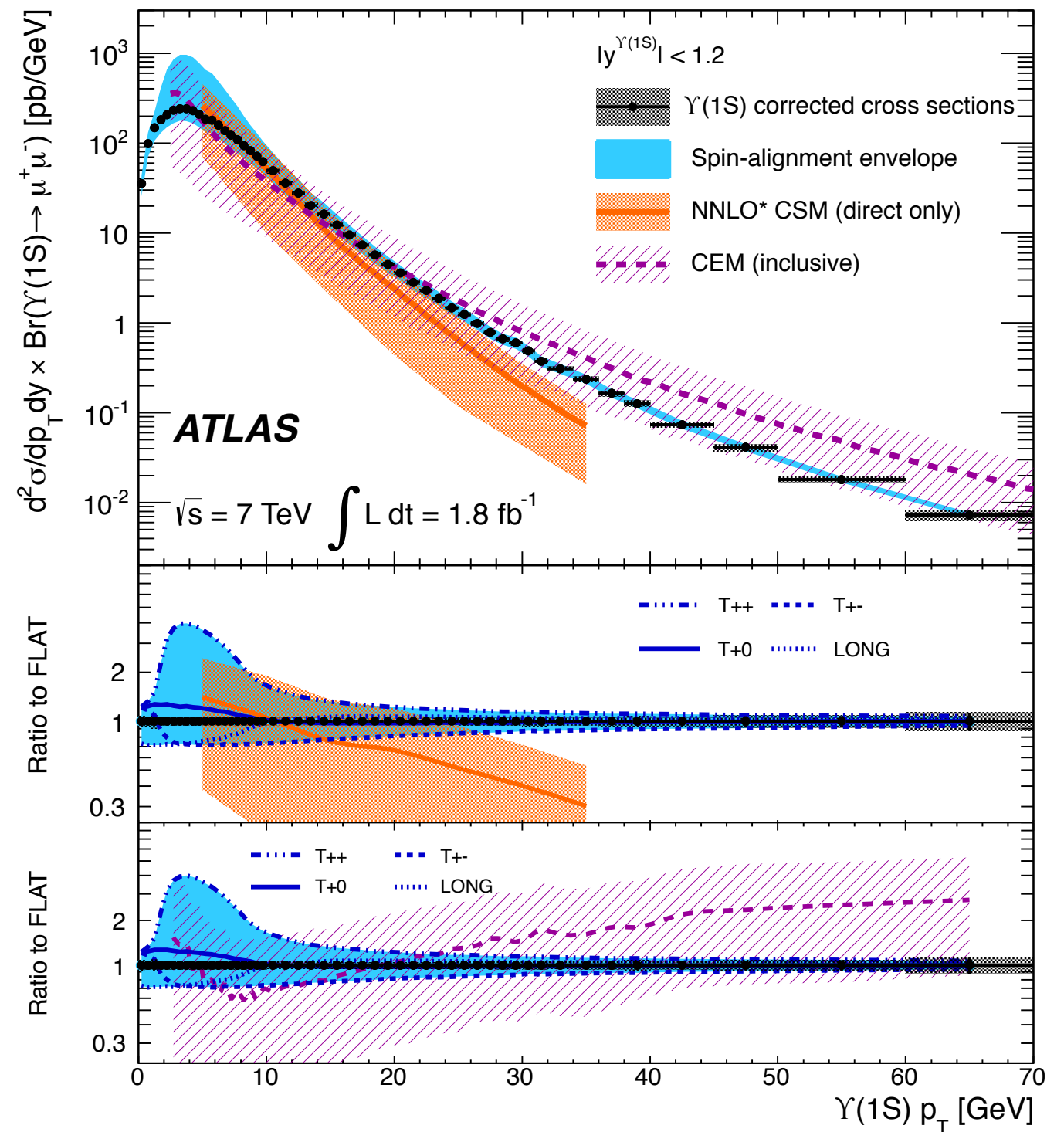
C

# Upsilon ( $\Upsilon_n \rightarrow \mu\mu$ ) production @ 7 TeV pp

[Phys. Rev. D 87, 052004 \(2013\)](#)



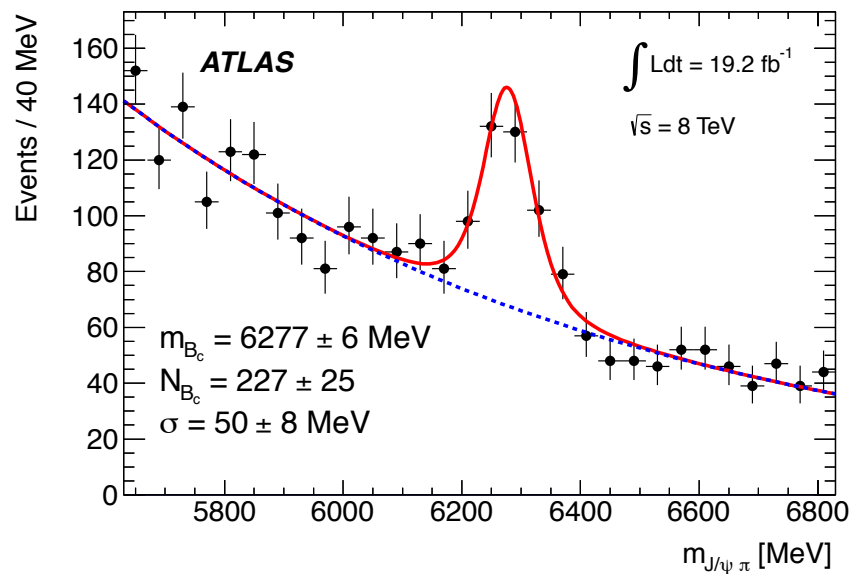
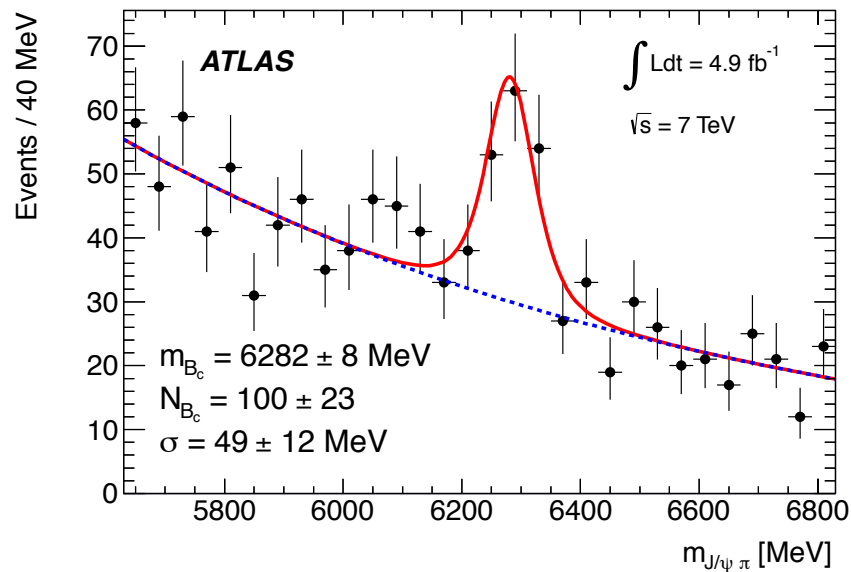
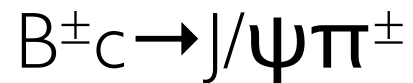
Predictions of direct production with the NNLO\* Color Singlet Mechanism (CSM) and inclusive predictions from the Color Evaporation Model (CEM).



# Observation an excited of $B_c^\pm$ meson state @ 7 TeV and 8 TeV pp

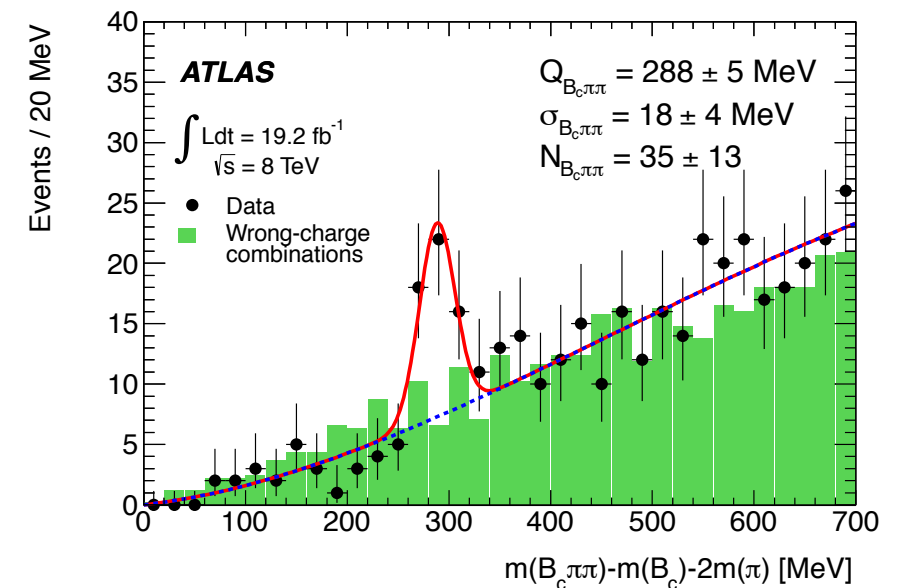
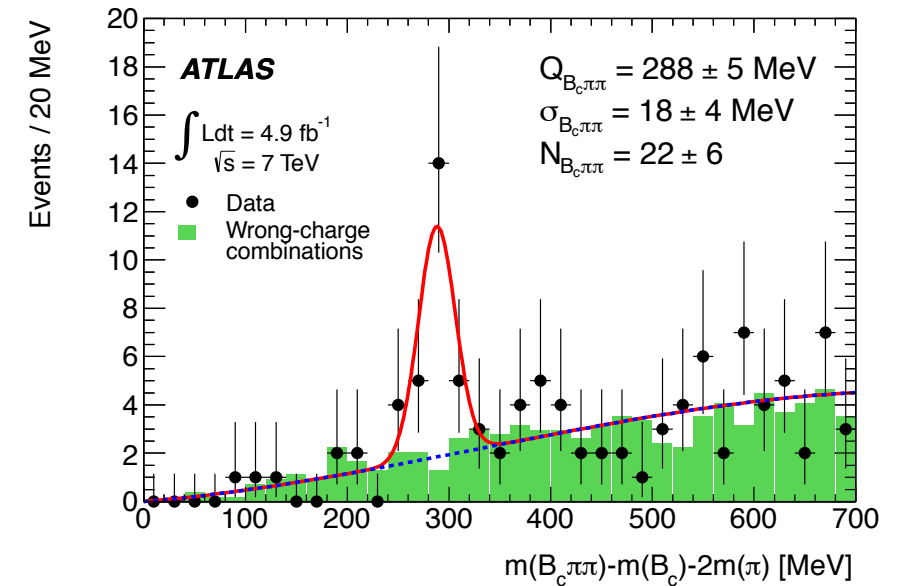
[Phys. Rev. Lett. 113, 212004 \(2014\)](#)

invariant mass distributions of



distributions of the right charge combinations

$$Q = m(B_c^\pm \pi \pi) - m(B_c^\pm) - 2m(\pi^\pm)$$

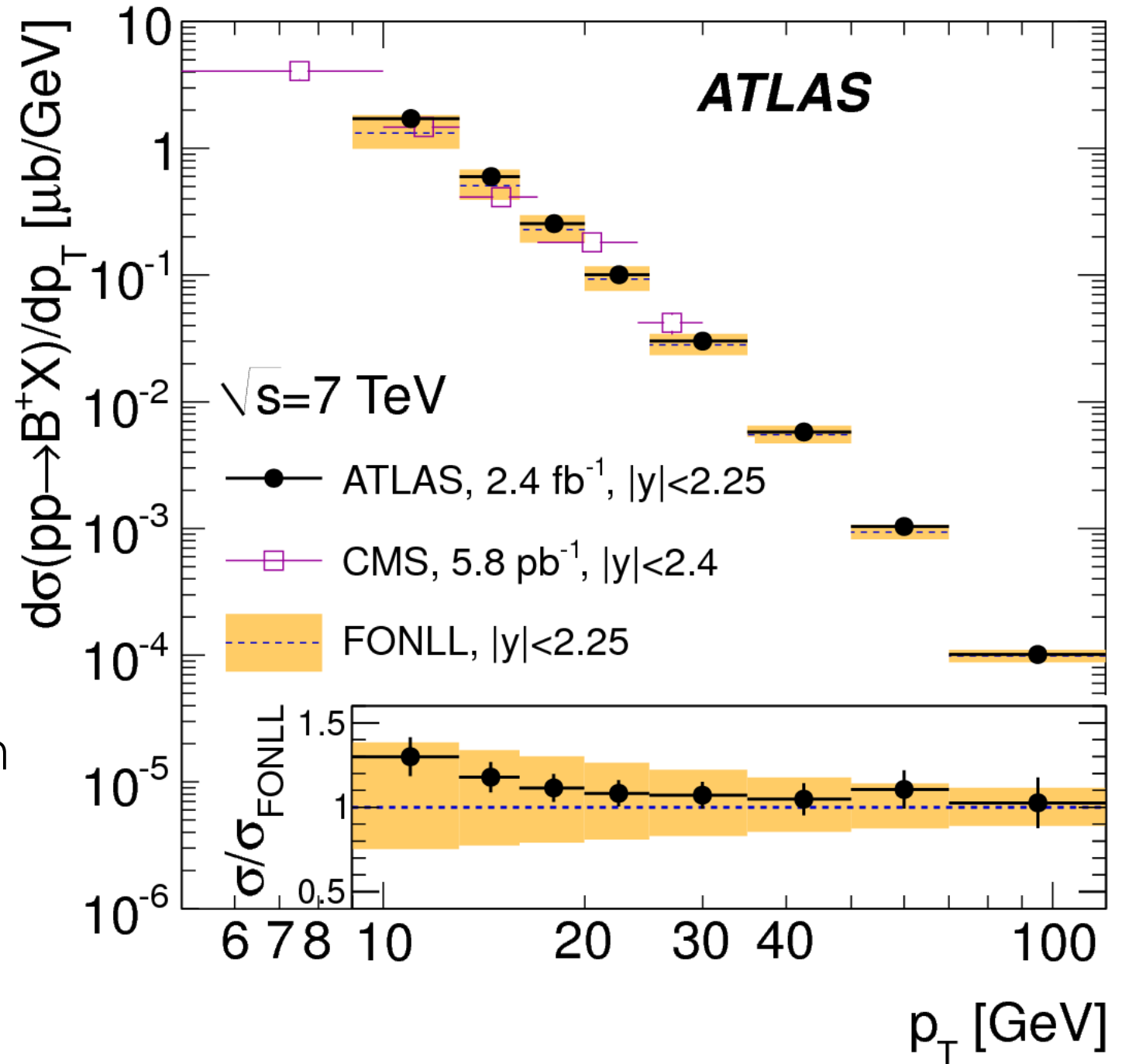
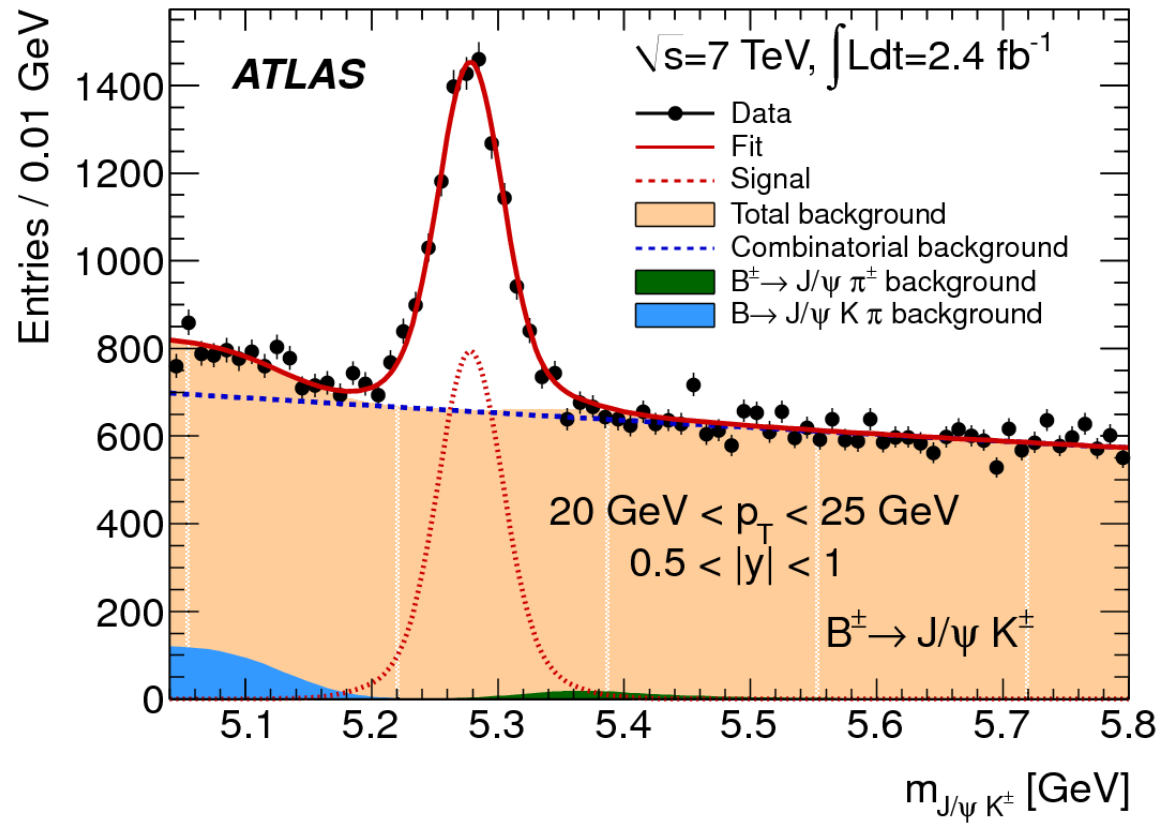


The mass and decay of this state are consistent with expectations for the second S-wave state of the  $B_c^\pm$  meson,  $B_c^\pm(2S)$



# $B^+ \rightarrow J/\psi(\rightarrow \mu\mu) K^+$ production @ 7 TeV pp

[JHEP10\(2013\)042](#)



Predictions of the FONLL calculation for b-quark production compared with the data, assuming a hadronisation fraction of  $f_{b \rightarrow B^+}$  of  $(40.1 \pm 0.8)\%$

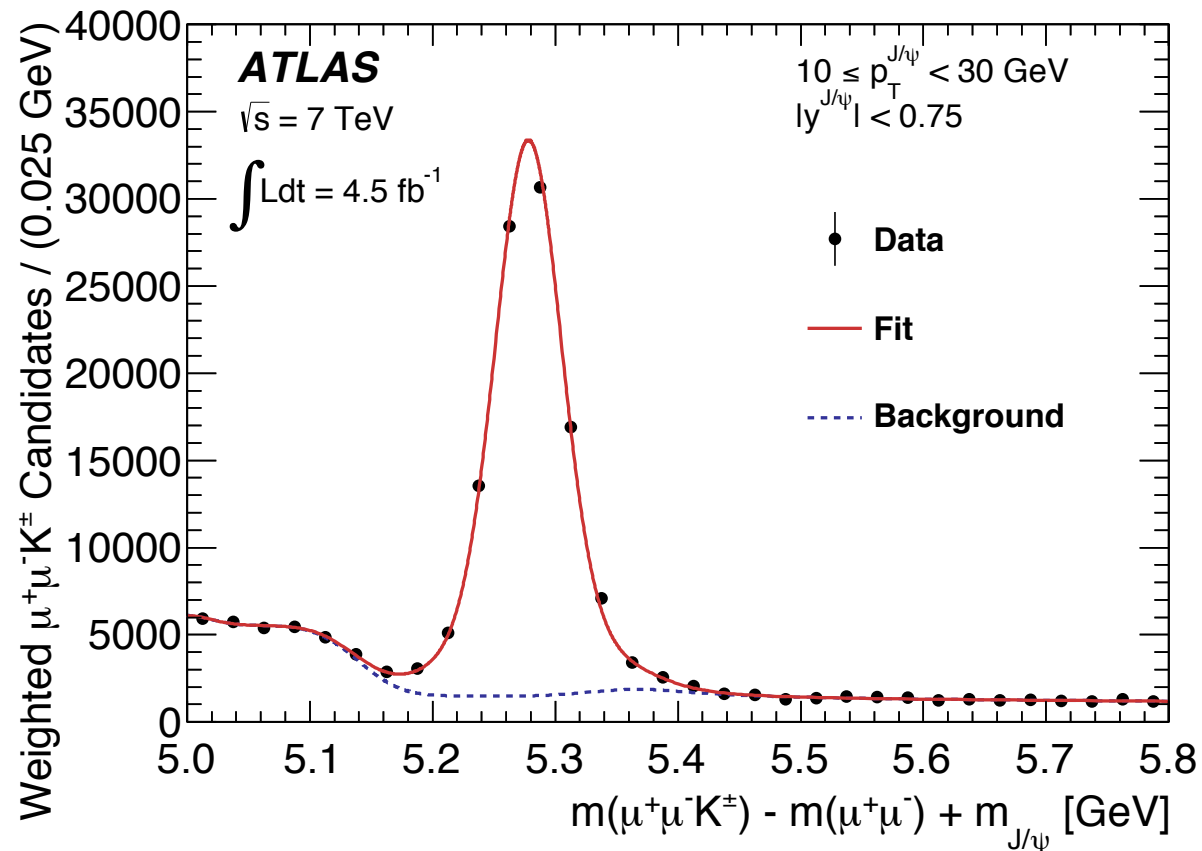
# Measurement of $\text{Br}(B^\pm \rightarrow \chi_{c1} K^\pm)$ @ 7 TeV pp

[JHEP 07 \(2014\) 154](#)

Branching fraction measurement from the  $\chi_c \rightarrow J/\psi \gamma$  sample and the reference  $B^+ \rightarrow J/\psi K^+$

$$\text{BR}(B^+ \rightarrow \chi_c K^+) = \mathcal{A}_B \cdot \frac{N_{\chi_c}^B}{N_{J/\psi}^B} \cdot \frac{\text{BR}(B^+ \rightarrow J/\psi K^+)}{\text{BR}(\chi_c \rightarrow J/\psi \gamma)}$$

## $B^\pm \rightarrow J/\psi K^\pm$



## $B^\pm \rightarrow \chi_{c1} K^\pm$

